DYNAMIC COMPOSITION OF MEMBRANE MICRODOMAINS

by

Yu Zi Zheng

B.Sc., Concordia University, 2006

A THESIS SUBMITTED IN PARTIAL FULFILLMENT OF

THE REQUIREMENTS FOR THE DEGREE OF

DOCTOR OF PHILOSOPHY

in

The Faculty of Graduate Studies

(Biochemistry and Molecular Biology)

THE UNIVERSITY OF BRITISH COLUMBIA

(Vancouver)

May 2012

Abstract

Lipid rafts are cholesterol enriched membrane microdomains involved in many cellular functions. Caveolae are a sub-type of lipid rafts that are smooth invaginations of the plasma membrane (PM) whose formation requires caveolin-1 (Cav1). Here, we determined the lipid rafts and caveolae proteome from various cells in an unbiased manner and examined the dynamic raft proteome change during *Salmonella* infection using quantitative proteomics. In chapter 2, we approach the status of mitochondrial proteins in detergent-resistant membrane (DRM) preparations by employing Stable Isotope Labeling by Amino acids in Cell culture (SILAC) to evaluate the composition of differentially purified subcellular fractions. Our data demonstrate that mitochondrial proteins that were previously identified as raft components are partially copurifying contaminants of raft preparations. In tumor cells deficient for Golgi β-1,6N-acetylglucosaminyltransferase V (Mgat5), reduced Cav1 expression is associated not with caveolae but with oligomerized Cav1 domains, or scaffolds. These cell lines displaying differing Cav1/caveolae phenotypes are effective tools for probing the composition of caveolae. Using SILAC in chapter 3, we are able to quantitatively distinguish the composition of caveolae from the background of DRM proteins and show that the presence of caveolae enriches protein composition of DRM, including the recruitment of multiple heterotrimeric G-protein subunits. Furthermore in chapter 4, we explored the dynamic change of membrane protein composition according to an external signal. *Salmonella* are Gram-negative intracellular bacteria believed to attack lipid rafts as the site of entry. We applied SILAC examined the change of host raft proteome at a couple of time points during *Salmonella* infection. Dozens of proteins have shown to be highly regulated, one of them – Cav1 is shown to be required by *Salmonella* entrance. We also developed a high-content

screening assay that is able to estimate the number of bacteria entered or survived inside the host for future functional studies of the novel proteins identified. This research gives us a better understanding of the raft proteome and how rafts are localized, as well as it can be changed. The *Salmonella* infection work leads to a global raft proteome dynamic analysis and identifies several proteins that may be novel bacterial host targets.

Preface

Part of sections 1.1, 1.3 and 1.4 has been published in a review. Zheng YZ, Foster LJ; Contributions of quantitative proteomics to understanding membrane microdomains. J Lipid Res. 2009 Oct;50(10):1976-85. © the American Society for Biochemistry and Molecular Biology. Zheng YZ, Foster LJ; Biochemical and proteomic approaches for the study of membrane microdomains. J Proteomics. 2009 Feb 15;72(1):12-22. The two reviews were written by me and edited by my supervisor LJF.

Data in chapter 2 has been published. Zheng YZ, Berg KB, Foster LJ; Mitochondria do not contain lipid rafts, and lipid rafts do not contain mitochondrial proteins. J Lipid Res. 2009 May;50(5):988-98. © the American Society for Biochemistry and Molecular Biology. I planned and conducted most of the experiments with some help from my supervisor LJF. The exception is the linear density gradient section, where the data was collected by KBB who was a summer research student under my supervision. The manuscript was primary written by me with some writing from KBB and editing by LJF.

The work in chapter 3 has been published. Zheng YZ, Boscher C, Inder KL, Fairbank M, Loo D, Hill MM, Nabi IR, Foster LJ; Differential impact of caveolae and caveolin-1 scaffolds on the membrane raft proteome. Mol Cell Proteomics. 2011 Oct;10(10):M110.007146. © the American Society for Biochemistry and Molecular Biology. I performed all the proteomics experiments (comparative, co-IP, MβCD treatment and label-free). IRN conducted the STED work, CB conducted the microscopy experiments and MF did the isoproterenol treatment work. KLN helped with one replicate of the label-free proteomics work with assistant from DL, MMH helped with the planning and setting up of

the label-free proteomics experiment. I was the primary writer of the manuscript with help from CB, IRN and LJF. IRN and LJF helped with the editing. Section 3.2.2 and 3.3.3 has been submitted for publication. Boscher C, Zheng YZ, Lakshminarayan R, Johannes L, Dennis JW, Foster LJ, Nabi IR; Galectin-3 regulates mobility of N-cadherin and GM1 ganglioside at cell-cell junctions of mammary carcinoma cells. J Biol Chem. I planned and performed the proteomics experiment with data analysis. The manuscript was written by CB and IRN with some input from myself and LJF.

Data in chapter 4 will be published. The project was planned by me and my supervisor LJF. I designed and conducted most of the experiments, including the proteomics, microscopy, knocking-down and high-content screening assay except the MRM work that was done by Joost Gouw and Anders Kristensen helped with making Figure 4.4. I wrote the chapter with corrections and input from LJF.

Table of Contents

List of Tables

List of Figures

List of Abbreviations

APC	Antigen presenting cells
BCR	B cell receptor
CSD	Caveolin scaffolding domains
Cav1, 2, 3	Caveolin-1, -2 and -3
CT-b	Cholera toxin b-subunit
CEMMs	Cholesterol-enriched membrane microdomains
CEMs	Cholesterol-enriched membranes
CID	Collision-induced dissociation
DIGs	Detergent-insoluble glycolipid-enriched complexes
DRM	Detergent-resistant membrane
DIGE	Difference gel electrophoresis
DTT	Dithiothreitol
DN	Dominant-negative
ESI	Electrospray ionization
ER	Endoplasmic reticulum
EGFR	Epidermal growth factor receptor
FDR	False discovery rate
FT	Fourier transform
FCM	Fuzzy c-means
GPCR	G protein coupled receptor
Gal3	Galectin-3
GM1	Ganglioside
GC	Gas chromatography
GEMs	Glycosphingolipid-enriched membranes

GPI-APs	Glycosylphosphatidylinositol-anchored proteins
Mgat5	Golgi β-1,6N-acetylglucosaminyltransferase V
HPLC	High-performance liquid chromatography
HIV	Human immunodeficiency virus
IPA	Ingenuity Pathways Analysis
IAA	Iodoacetamide
iTRAQ	Isobaric tags for relative and absolute quantitation
ISO	Isoproterenol
ICAT	Isotope-coded affinity tagging
LPS	Lipopolysaccharide
LC-MS/MS	Liquid chromatography-tandem mass spectrometry
MS	Mass spectrometry
m/z	Mass-to-charge
MALDI	Matrix-assisted laser desorption/ionization
MβCD	Methyl-β-cyclodextrin
MEFs	Mouse embryonic fibroblasts
MRM	Multiple reaction monitoring
MOI	Multiplicity of infection
MURC/Cavin4	Muscle-restricted coiled-coil protein
NGS	Normal goat serum
NMR	Nuclear magnetic resonance
PFA	Paraformaldehyde
ppm	Parts-per-million
SPI-1	Pathogenicity island 1
SPI-2	Pathogenicity island 2

PM	Plasma membrane
PDGF	Platelet-derived growth factor
PTRF/Cavin1	Polymerase 1 and transcript release factor
PTM	Post-translational modification
PCA	Principal Component Analysis
PCP	Protein Correlation Profiling
Q	Quadrupole
rcf	Relative centrifugal force
RT	Retention time
SCV	*Salmonella* containing vesicle
SIFs	*Salmonella*-induced filaments
SRBC/Cavin3	SDR-related gene product that binds to C kinase
SDR/Cavin2	Serum deprivation response
SV 40	Simian virus 40
SDC	Sodium deoxycholate
SDS-PAGE	Sodium dodecyl sulfate polyacrylamide gel electrophoresis
SILAC	Stable Isotope Labeling of Amino acids in Cell culture
STED	Stimulated Emission Depletion microscopy
SCX	Strong cation exchange chromatography
SELDI	Surface-enhanced laser desorption/ionization
TCR	T cell receptor
MS/MS	Tandem mass spectrometry
TEMs	Tetraspanin-enriched microdomains
TOF	Time-of-flight
Tx-100	Triton X-100

2D	Two-dimensional
2DGE	Two-dimensional gel electrophoresis
T3SSs	Type III secretion systems

Acknowledgements

I would like to thank my supervisor Dr. Leonard J. Foster for all the help he gave to me during my graduate study, especially all those cares I have received from you as an international student. Thank you for supporting me going for internship and study aboard. And thank you very much for all the things I have learned from you not only scientifically but also personally.

I would like to thank to my lab fellows especially Nick Stoynov, Queenie Chan, Lindsay Rogers and Dale Robinson for all the help and assistance. Thanks to my committee members: Dr. Juergen Kast and Dr. Masa Numata. I would like to thank Dr. Masa Numata for his advises on caveolae research and help with my fellowship application and Dr. Juergen Kast for his advises on proteomics, mass spectrometry and data analysis.

At the end, I would like to thank my parents for sending me study aboard and continuous supporting me for the past years and even now; especially thank to my dad who gave me lots of confidence to peruse a Ph.D. degree and many other dreams. Also thank my husband Michael for being a good friend for all these years and accompany me through this journey.

To my family and coming baby

1 Introduction

1.1 Membrane microdomain

1.1.1 Biological membranes

Biological membranes are flexible, selectively permeable lipid bilayers. In addition to their paramount role in maintaining cell or organelle structures, they are also involved in many essential cellular processes, such as cell signaling and trafficking, due to their unique interaction with both the inside and the outside of cells or organelles (see review [1]). The bilayers are constructed of two monolayers of lipids 5 to 8 nm thick in which the hydrophobic portions of each lipid in the two monolayers interact with each other, leaving the hydrophilic head of the lipids exploring to the outside aqueous environment. The three major types of lipids in eukaryotic membranes are phospholipids, glycolipids and cholesterols. The specific lipid composition of membranes varies between organelles and between cells, reflecting functional differences; for example, cholesterol is prominent in plasma membranes (PM) but barely detectable in mitochondrial membranes. Apart from this kind of segregation, membrane lipids are also asymmetrically distributed between the two monolayers and under goes constant changes in distribution that can have biological consequences [2, 3].

Proteins are the other major membrane component beside lipids and carbohydrates; lipid and protein ratios ranging from 1:4 to 4:1 by mass depend on the specific function of the membranes. The protein composition of biological membranes is even more diverse and transient than the lipid compositions since they have to carry out a wider variety of membrane-associated processes. Furthermore, the different protein compositions reflect specific functions of cells and organelles, e.g. mitochondria, the cell's energy generating

organelle are enriched with ATP synthase on its inner membrane. Whole genome analysis predicts that integral membrane proteins comprise one-third of all the proteins encoded by the human genome [4]. Generally, membrane-associated proteins include not only proteins that are physically embedded in lipid bilayers, such as ion channels and pumps, but also proteins covalently anchored to the membrane (e.g., glycosylphosphatidylinositol (GPI)-anchored proteins (GPI-APs) in the outer leaflet of the PM, acylated proteins in the inner leaflet of the PM), as well as otherwise soluble proteins that interact with the above two classes of proteins or membrane lipids; thus, the number of proteins that should actually be considered as 'membrane proteins' is even much larger than the one-third of the proteome that is integral to the membrane. [5].

1.1.1.1 Fluid mosaic model

The fluid mosaic model proposed in 1972 by Singer and Nicolson was the first model of biological membranes that stated that they are two-dimensional (2D) solutions of lipids and proteins. The lipids bilayers are fluid and arranged in an amphipathic structure with globular proteins integral to the non-polar core of the bilayer and polar groups protruding from the membrane into the aqueous phase. Moreover, lipids and proteins are free to diffuse laterally in the plane but not rotate through the membrane, so that the membrane structural and functional asymmetry is preserved. Importantly, this model implies that membrane lipids and proteins are evenly distributed in the 2D surface [6].

1.1.1.2 Compartmental model and membrane microdomain theory

Recent experimental evidence has led to the old fluid mosaic model being replaced by the membrane compartmentalization model [7] in which membranes are compartmentalized, or non-uniform, as a result of an uneven distribution of specific lipids and/or proteins into various microdomains. Membrane microdomains are cellular functional units of biological membranes that are different from other protein complexes in several ways: 1) Their localization on the cell surface puts them precisely in the interface between cells and external environments, including other cells. Many receptors, enzymes, substrates and cell signaling proteins, as well as adaptor/scaffold proteins, are located on membrane microdomains [8]; the membranes are thought to provide a platform for the initiation and coordination of several cell signaling and trafficking events [9-11]. 2) Unlike other cytosolic protein complexes, membrane microdomains are formed not only on the basis of protein-protein interactions but also through lipid-lipid and lipid-protein interactions. 3) The size of these microdomains is generally larger than other protein complexes, ranging up to several microns in diameter [12, 13], and they can be very abundant, occupying up to 30% of the total membrane area in certain cells [14]. 4) They are highly dynamic, constantly recruiting and displacing proteins as demands require [15, 16].

1.1.2 Lipid rafts and caveolae

1.1.2.1 Cholesterol enriched membrane rafts

Lipid rafts are perhaps the best-studied and thus most well-understood membrane microdomain, although our understanding of them is still far from complete. They are viewed as platforms for many cell signaling factors to integrate and to interact and the lipid raft

theory [17] proposes that certain proteins preferentially cluster into this unique environment, forming membrane reaction centers essential for many cellular processes, such as cell signaling and trafficking [9, 18, 17]. In fact, lipid rafts are one class of membrane microdomains that were originally defined biochemically as the low-buoyant density detergent-resistant membrane (DRM) fraction of cells but that are now recognized as a subset of DRMs enriched in cholesterol and sphingolipids [19-23]. Cholesterol is thought to intercalate between the rigid hydrophobic tails of sphingolipids and saturated phospholipids, allowing a very tightly packed structure with unique biophysical characteristics compared with surrounding membranes (Figure 1.1).

Figure 1.1 Cartoon representation of the five membrane microdomains described in this thesis: lipid rafts, caveolae and tetraspanin-enriched microdomains, as well as Galectin lattices and GPI-anchored proteins

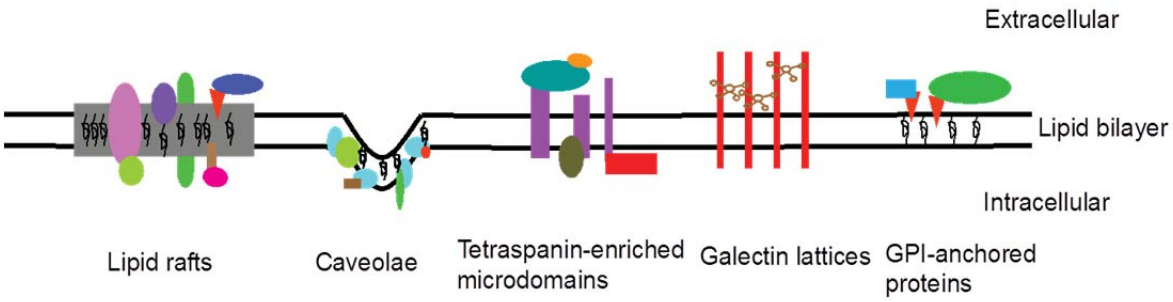

Lipid rafts are depicted as cholesterol and sphingolipid-dependent complexes in the plane of the membrane. Caveolae are formed by protein interactions with caveolins and are invaginations, coming out of the plane of the membrane. Tetraspanin-enriched microdomains have a less well-envisioned structure, with the requirement for tetraspanin the only commonality. Galectin lattices are formed by glycoprotein oligomerization through galectin binding. Finally, GPI-anchored proteins are soluble proteins anchored to the PM by a glycosylphosphatidylinositol (GPI) moiety.

Lipid–lipid and lipid–protein interactions are the likely biophysical basis behind the formation of rafts as cholesterol inserts into the lipid bilayer, clustering together and then recruiting proteins with a high likelihood to partition into an environment rich in cholesterol and/or sphingolipids. The tight lipid interactions create a lipid ordered phase which is more rigid than a typical membrane and less subject to phase transitions that then allows for phase separation by certain nonionic detergents at low temperature, followed by subsequent floating on density gradient centrifugation. Protein–protein interactions are also an important aspect of raft biology, as more proteins come to rafts either in the plane of the membrane (i.e., membrane proteins diffusing into rafts) or from the cytosol or lumen of the cell to form, in some cases, very large protein complexes [24, 25]. Flotillins, caveolins, some type of tyrosine kinases and GPI-anchored proteins are among the most well studied protein markers of rafts. The raft field has been dogged by biophysical arguments that rafts are only an artifact of detergent extraction [26-28] but recent direct observations of rafts in synthetic vesicles and their visualization by immunofluorescence microscopy and scanning atomic force microscopy [29-34] has finally laid such uncertainties to rest.

Lipid rafts are relatively small, ranging in size from 10 to 200 nm; their size depends on the cell types and biological states they occur in since they are dynamic structures that change their protein compositions according to external signals or stimulus. Most lipid rafts are localized on the plasma membrane of cells but rafts are found in some internal organelles. Endoplasmic reticulum (ER) proteins are found in rafts [35, 36], although this has been questioned by recent studies [37, 38] (also see chapter 2). Moreover, lipid rafts are believed to be present in the Golgi complex due to the increase in sphingolipids and

cholesterol along the secretory pathway [39]. Raft domains also have been identified in organelles in the endocytosis pathways like the endosomes and phagosomes [40-42].

1.1.2.2 Detergent-resistant membranes (DRMs) and lipid rafts

Due to the insolubility of rafts in non-ionic detergents and the enrichment of cholesterol and sphingolipids in the preparation, lipid rafts have a low buoyant density. Lipid rafts in many studies and papers have been commonly referred to as DRMs (detergent-resistant membranes), DIGs (detergent-insoluble glycolipid-enriched complexes), CEMs (cholesterol-enriched membranes), CEMMs (cholesterol-enriched membrane microdomains) or GEMs (glycosphingolipid-enriched membranes) [43]; these names were used interchangeably with lipid rafts but we now know that rafts are only a sub-domain of DRMs. Biochemically isolated DRMs, DIGs, CEMs, CEMMs or GEMs fractions are not pure preparations of rafts as they often contain other non-raft protein and/or lipid contaminations [37, 38, 44] (also see chapter 2 and 3).

1.1.2.3 Non-caveolar rafts and caveolar rafts or caveolae

Lipid rafts can be subdivided into two major sub-types: non-caveolar rafts and caveolar rafts, otherwise known as caveolae [45]. Both non-caveolar rafts and caveolae are cholesterol enriched membranes, with non-caveolar rafts presenting as planar complexes and caveolae presenting as invaginations that form little caves, through their association with the protein caveolin. Previously, caveolae have been defined in some papers as a different membrane microdomain than lipid rafts, but since caveolae fit into all the definition of rafts; it is now recognized as a sub-type of rafts [46]. Unlike lipid rafts, caveolae as microdomain

have only ever been found in the plasma membrane of cells and not on any other organelle membranes.

1.1.2.4 Lipid rafts and their functions

Lipid rafts have been implicated in many cellular functions and as raft proteomics and other biological techniques have evolved, more and more raft functions have been discovered. First of all, lipids and proteins are dynamically associated with each other in lipid rafts to form platforms important for membrane protein sorting and construction of signaling complexes [47]. Then, each individual rafts with their unique protein contents and functions can connect together to coordinate signaling transduction. The corollary is that disrupting rafts result in signaling inhibition.

Adaptor proteins like flotillins and caveolins are keys in membrane raft formations since many other functional proteins are recruited to them through their scaffolding domains. Reports show that transmembrane receptors like epidermal growth factor receptor (EGFR), G protein coupled receptor (GPCR) and insulin receptors are in raft domains [48-50], as well as some members in the Src family kinases like Src itself, Fyn and Yes (see chapter 2). Those kinases are able to phosphorylate receptors within rafts to regulate the downstream signaling events [51]. G proteins and Ras were found in rafts responsible for G protein signaling. Other proteins in rafts like V-ATPase are regulating the membrane potential (see chapter 2 and 3). Rafts are also involved in protein endocytosis and trafficking through either caveolae-mediated endocytosis that requires protein caveolins (see the next section) or raft-dependent endocytosis that depends on flotillins. Furthermore, rafts regulate cell migration through complexes with integrins and to this end, tyrosine phosphorylated cvaeolin-1 has been found

in focal adhesions [52]. Studies have suggested that T cell activation is organized inside rafts through the partitioning of T cell receptor (TCR), costimulators, signal transducers, and the actin cytoskeleton at the interface between the T cells and the antigen presenting cells (APC) [53]. Other people shown that B cell receptor (BCR) signaling also involves sorting by lipid rafts [54].

1.1.2.5 Caveolae

1.1.2.5.1 Caveolae and structural protein - caveolins

Caveolae are a special class of lipid rafts found in many cells and they are classically pictured as flask-shaped, stable invaginations of the plasma membrane. Because of their unique morphology, caveolae can be easily distinguished by electron microscopy, appearing when looking onto a plasma membrane from outside the cell as small caves with diameters in the range of 50 to 100 nm [11, 55]. When numerous, caveolae can have a substantial impact on the surface area of cells; ultrastructural analysis has shown that as much as 20% of adipocyte plasma membrane can be caveolae [56] (Figure 1.1).

The genesis of caveolae depends on the presence of caveolins, small, structural proteins that have also been observed at low levels in DRMs [57]. Caveolins interact directly with cholesterol [58] and DRMs have been observed to contain 3 to 4-fold more cholesterol when caveolins are present than in the caveolin-deficient cells [59]. Caveolae formation is inhibited when caveolin expression is knocked out [60, 61] and the human genome contains three caveolin proteins, caveolin-1, -2 and -3 (Cav1, 2 and 3) [62-64]. All three are integral but not transmembrane proteins targeted to the inner leaflet of the PM; Cav1 and 2 are expressed in most cells whereas Cav3 is muscle specific [65-68]. Caveolins themselves do

not have enzymatic activities, rather they homo- or hetero-oligomerize with other caveolins to form a coat that stabilizes caveolae and forces its concave structure; at the same time, they interact with other membrane proteins and recruit other cytosolic proteins to caveolae through their scaffolding domains (CSD) [69-72]. Besides caveolin, recent studies identified the Cavin protein family that are also associated with caveolae and act as a coat protein. As an example, in the absence of polymerase 1 and transcript release factor (PTRF)/Cavin1, caveolae flatten and caveolin-1 is released into the cell membrane [73]. Serum deprivation response (SDR)/Cavin2, SDR-related gene product that binds to C kinase (SRBC)/Cavin3 and muscle-restricted coiled-coil protein (MURC)/Cavin4 were later been identified which forms a multi-protein complex with Cavin1 [74-76].

Caveolae have been suggested to function in signaling events through the compartmentalization of signaling molecules interacting with caveolin proteins [77, 78]; the interactions are normally thought to have negative effects through the suppression of enzymatic activities [79, 80]. However, for cases like insulin receptor signaling, binding to caveolae has an activating function instead [81-84].

1.1.2.5.2 Caveolae-mediated endocytosis

Beside signal transduction, caveolae are also involved in vesicle transport through caveolae-mediated endocytosis; it differs from raft-dependent endocytosis through its requirement of caveolae [85]. Caveolae-mediated endocytosis is in large part defined as the cholesterol-sensitive, clathrin-independent internalization of ligands and receptors from the plasma membrane; it is regulated by various cellular components that include Cav1, cholesterol and dynamin, as well as regulators of the actin cytoskeleton [86]. Cav1 is

required for caveolae formation and evidence suggests that Cav1 can acts as a negative regulator of raft-dependent endocytosis [87]. Actin and actin-binding protein filamin restrict caveolae movement, so disruption of actin cytoskeleton induces rapid internalization of caveolar vesicles [88]. The internalization of ligands induces the actin cytoskeleton breakdown [89]. Chemical agents that disrupt membrane cholesterol also inhibit caveolae-mediated endocytosis; on the other hand, addition of cellular cholesterol increases the endocytosis through raft/caveolae [90-92]. Dynamin located at the neck of caveolae is required for the caveolae budding from the plasma membrane [93]. Phosphorylation of Cav1 at tyrosine 14 by Src kinase has been shown to be needed as the treatment of cells with tyrosine kinase inhibitors block caveolae endocytosis [94].

Simian virus 40 (SV 40) binds to GM1 and enter the cell through the caveolae-mediated endocytosis pathway. Live cell imaging has shown that when cells are stimulated by SV40, dynamin is transiently recruited to caveolae, actin polymerizes to form an actin tail and SV40 stays in a caveolin positive endosome called the caveosome [95, 96, 89]. Beside SV40, many other viruses and bacteria also interact and enter host through membrane caveolae, such as the human immunodeficiency virus (HIV) [97] and *Salmonella enterica* (see next section). Ligands like cholera toxin b-subunit (CT-b) and albumin internalize through raft-dependent endocytosis that requires caveolin [98, 99]. However, many ligands can enter cells via multiple endocytosis pathways depending on the situation [100] or switch between endocytosis pathways [101]. Distinct from clathrin-mediated endocytosis, it has been suggested that the use of caveolae for cellular intake allows pathogens to bypass the classical endosome–lysosome trafficking pathway and, as a consequence, avoid lysosomal degradation [102].

1.1.2.5.3 Caveolae and caveolins in health and disease

Since caveolae are places where signaling proteins interact and integrate directly or indirectly with caveolin scaffolding protein, ablations or mutations of caveolin proteins result in deformation or mislocalization of caveolae/caveolins and are usually associated with various diseases. With the availability now of caveolin null mice, caveolae and caveolin associated diseases can be studied more directly.

Early studies have observed that the NIH 3T3 cell line transformed by several different oncogenes express greatly reduced levels of Cav1 and caveolae [103]. A later study examined the expression level of Cav1 in human breast cancer cells, and found that Cav1 level is significantly reduced in human breast cancer cells compared with their normal mammary epithelial counterparts. Furthermore, Cav1 overexpression resulted in growth inhibition [104]. Loss of caveolae and down-regulation of Cav1 levels usually causes increased cell proliferation and accelerates tumourigenesis. Evidence from *Cav1*$^{-/-}$ null mice showed more susceptibility to carcinogen-induced tumorigenesis as they develop tumors at an increased rate [105]. Caveolae and Cav1 have been implicated in the development of human cancer, but Cav1 seems play different roles in various cancer cells; Cav1 acts like a tumor suppressor, on the other hand, it is required for tumor survival and growth [106]. Cav1 mutations detected in cancer cells cause the loss of caveolae and mislocalization of caveolin proteins [107, 108]. As one example, genetic analysis of human breast cancer samples revealed that up to 16% of these samples have a single Cav1 gene point mutation (P132L) [107]. This mutation (P132L) was later identified to be dominant-negative (DN) that cause the mislocalization of Cav1 to Golgi complex [108].

Muscle-specific Cav3 is closely linked to muscle degeneration diseases like muscular dystrophy [109]. Cav3 genetic mutations have also been identified that cause reduced cell surface Cav3 levels. In one study, researchers found that Golgi-associated mutants of Cav3 caused redistribution of plasma membrane protein – dysferin to internal compartment [110].

1.1.3 Other membrane microdomains

1.1.3.1 Tetraspanin-enriched microdomains (TEMs)

Tetraspanins are a class of integral membrane proteins containing, as their name suggests, four transmembrane domains and two extracellular loops [111]. They are expressed in all cells and tissues in almost all animal species [112]. In humans, the tetraspanin family comprises 33 proteins that are defined by their unique structural features. Tetraspanins can interact with each other and also with other proteins or factors on cell membranes, particularly in the plasma membrane, to form so called "tetraspanin web" or tetraspanin-enriched microdomains (TEMs) [113] (Figure 1.1).

Some tetraspanins are well characterized, such as CD9, CD81, CD82 and CD151; they do not have any known enzymatic activities in cells but rather they act as "organizers" to recruit other factors to TEMs. Tetraspanins have been reported to interact with integrins, growth factor receptors and many intracellular signaling molecules [114, 115]. Therefore, tetraspanin-associated microdomains are involved in a variety of physiological processes, such as immune cell activation, and cell migration, as well as cellular differentiation [113, 116]. Tetraspanin proteins are usually underrepresented in biochemical assays because they are small, hydrophobic and low abundant membrane proteins; however, due to their

functional significance (e.g., mutations in some tetraspanins are associated with human diseases like mental retardation [117]), TEMs are gaining more attention.

There is one report that tetraspanins are in lipid rafts because they can be associated with cholesterol through palmitoylated resides [10], but others believe that TEMs and rafts are two distinct membrane microdomains because tetraspanins appear to be resistant to cholesterol depletion [118]. Another possibility is that TEMs might reside next to lipid rafts, which would also explain why the two microdomains sometimes appear to share similar cell functions and facilitating signal transductions [119].

Like lipid rafts, TEMs or tetraspanin complexes can be separated from other membranes based on their biophysical properties. These complexes are insoluble in milder detergents (less hydrophobic) such as in 1% Brij-99 or CHAPS [118]; Firstly, cells are lysed in these detergents and then tetraspanins and their associated proteins are immuno-enriched using antibodies against tetraspanins [120, 121]. Stronger non-ionic detergents like Triton X-100 are not used to study TEMs because tetraspanins were not observed in DRMs after Triton X-100 extraction. Furthermore, studies have reported that Triton X-100 can affect homodimeric tetraspanin interactions, effectively solubilizing whole tetraspanin complexes (Table 1.1).

Table 1.1 Different biochemical and proteomic methods used for isolating or enriching membrane microdomains and comparison of their relative purity

Membrane microdomains	Methods				Purity
	Detergent	Detergent-free	Immunoisolation	Phase transfer	
Lipid rafts	Triton X-100, NP-40, CHAPS, Tween, Lubrol WX and Brij-96 [15, 122, 37, 123, 21, 124]	High salt and alkaline pH, membrane fragmentation using sonication [125, 126, 68]	[a]NA	NA	Cholesterol disruption drug [37] > Detergent > Detergent free
Caveolae	Triton X-100 [127, 77, 128]	High salt and alkaline pH, membrane fragmentation using sonication or Dounce [129, 125, 130]	Caveolin antibodies [131, 132]	NA	2D gel comparison [73] > Immunoisolation > Detergent > Detergent free
Tetraspanin-enriched microdomains	Brij-99, CHAPS [118]	NA	Tetraspanin antibodies [133-135]	NA	Immunoisolation > Detergent
GPI-anchored proteins	Brij-58, NP-40, CHAPS, Triton X-114 [136-138, 123, 139-141]	High salt and alkaline pH [137, 138, 123]	NA	Enzymatic cleavage by GPI-specific phospholipases [136-140]	Phase transfer > Detergent > Detergent free
Galectin lattices	NA	Lactose treatment [44] (also see chapter 3)	NA	NA	NA

a Not applied

1.1.3.2 GPI-anchored proteins (GPI-APs)

GPI-anchored proteins (GPI-APs) are otherwise soluble proteins localized on the outer leaflet of PM via the attachment of a glycosylphosphatidylinositol (GPI) moiety [142]. This is a classic example of a post-translational modification (PTM) determining the targeting, localization and function of proteins within cells. GPI-APs are present inside lipid rafts but they are only a sub-type of rafts. GPI-APs share some common sequence features as well, such as two hydrophobic regions on the N and C-terminus of the sequence, a hydrophilic spacer region and a ω-site located in the middle of the sequence, corresponding to the cleavage site where the phosphoglycan anchors are attached to the carboxy-termini. Moreover, the attachment takes place in the ER where the nascent protein is transferred to the pre-synthesized GPI anchor by a transamidase [143]. One interesting biophysical property of GPI-APs, conferred upon them by the GPI anchor itself, is their insolubility in non-ionic detergents such as Triton X-100 [32] (Figure 1.1).

GPI-APs' membrane localization places them exactly in the interface where cells communicate with their extracellular surfaces and thus GPI-APs mediate many cellular processes including cell–cell interactions, receptor recognition and cell signaling [144-146]. It is now quite clear that GPI-APs play important roles in human diseases and disorders; for example, one causative agent of neural degeneration, misfolded prion protein (PrP), is a GPI-AP [147]. On the other hand, many of the surface proteins of the malaria parasite, *Plasmodium falciparium*, are GPI-APs [148] and they are associated with host-pathogen recognition. GPI-APs have also been reported as candidate biomarkers of human hepatocellular carcinoma, as well as pancreatic and biliary carcinomas [149, 150]. Another

potential biomarker, folate receptor, is not only a marker for myeloid leukemia and chronic inflammatory diseases but also shows potential use in targeted drug delivery [151].

Transamidase recognizes certain constraints of the ω-site of native GPI-APs and thus bioinformatics approaches have been developed to exploit this, including the Big-Pi, DGPI and GPI-SOM predictors [152-154]. Another more sensitive, and certainly more specific, approach has integrated computational and experimental components [155]. However, while the available bioinformatics tools are very useful for predicting GPI-APs, which typically comprise 1–2% of eukaryotic genomes, very few have been confirmed biochemically since their initial description in the 1980s; the main difficulties is that GPI-APs are insoluble and typically present at very low levels in cells.

Since GPI-APs are insoluble membrane-anchored proteins, detergents were normally used to isolate or separate them from rest of the soluble proteins in cells like Brij-58, NP-40 or the Triton series; however, detergent free methods for studying GPI-APs have also emerged [123]. A comparative study of several detergents has also been done [141]. The GPI moiety itself is generally quite stable in the context of the cell but it can be released by enzymatic treatment using bacterial GPI specific enzyme phospholipases [156]. After the enzymatic cleavage, GPI-APs are released from membrane, making them soluble and thus they partition into the aqueous phase [136], allowing subsequent separation from rest of the membrane proteins. This strategy has been termed “modification specific proteomics” and has been used in several studies involving diverse higher eukaryotes, from plants to animals [137-140] (Table 1.1).

1.1.3.3 Galectin lattices

Galectin lattices are relative new membrane microdomains that have recently received much attention, although their roles in biophysical events are unknown, for the most part. Galectins are small β-galactoside-binding proteins that bind cell surface glycans especially N-glycans, they are made in the cytosol but secreted from cells [157]. There are 15 mammalian galectins; one of them, galectin-3 (Gal3), contains an oligomerization domain that enables oligomer formation, upon binding to glycoproteins resulting in the formation of heterogeneous cell surface lattices [158-160]. Galectin lattices are formed by multiple low affinity interactions, but the strength of the interactions can be dynamically modulated by protein glycosylation or galectin expression [161, 162]; once formed, the lattice can regulate a variety of cellular functions, including proliferation, migration and apoptosis [163, 164]. Since glycosylation is a common post-translational modification to secretory and membrane-anchored proteins, galectin lattices might be very numerous at the cell surface (Figure 1.1).

Lipid rafts and galectin lattices are believed to be closely connected: some galectin lattices might be formed within the boundaries of a raft through binding of raft glycoproteins. Recent work suggests that lipid raft stabilization is promoted by galectin-induced lattice formation [165, 166]. On the other hand, lattices have been shown to sequester proteins away from lipid raft domains, suggesting a role in regulating membrane dynamics by compartmentalization [44] (also see chapter 3). Lactose is commonly used to disrupt lattices by competing with cell surface glycans for galectin binding and it is used in galectin lattices study (Table 1.1).

1.2 *Salmonella enterica*

1.2.1 *Salmonella enterica* and human health

Salmonella is a rod-shaped, Gram-negative intracellular pathogen that is capable of infecting a variety of phagocytic and non-phagocytic cells. There are two recognized *Salmonella* species: *S. enterica* and *S. bongori*, which share high genetic similarity [167]. Unlike other bacterial pathogens, *Salmonella* is able to infect multiple hosts in human and animals, except *S. enterica* serovar Typhi and *S.* Paratyphi that are human specific. Most of the human pathogenic *Salmonella* serovars or strains belong to the *S. enterica* subspecies, including the most common *Salmonella* model system, *S.* Typhimurium, which can be cultivated and genetically manipulated and used in many of the *in vivo* and *in vitro* host-pathogen researches.

Each year, *Salmonella* causes nearly 1.3 billion cases of human disease, including in young children and ranging from diarrhea to a life-threatening systemic disease called typhoid fever that still causes hundreds of thousands of deaths in developing countries. *Salmonella* infections in livestock like chicken, pigs, cattle and their products also raises big food safety concerns since the potential for food-poisoning can result in big economic losses if even a single case is detected. In past years, antibiotics for *Salmonella* have been discovered. However, microbial resistance to those antibiotics has becomes a serious issue now; therefore, new antibiotic candidates are urgently needed which requires us to gain more knowledge towards *Salmonella* pathogenicity and host-pathogen interaction [168].

1.2.2 *Salmonella* pathogenesis

Upon oral *Salmonella* ingestion, the bacteria travel through the stomach and colonize the small intestine. From there, they start to enter enterocytes, M cells and dendritic cells and subsequently reach the submucosa, where they are internalized by resident macrophages and rapidly disseminate through the blood stream, finally accumulating in the mesenteric lymph nodes and, ultimately, the spleen [169]. *Salmonella* internalize into host cells via two different pathways, depending on the cell types. Phagocytes such as macrophages use phagocytic uptake to recognize and internalize bacterial pathogens. On the other hand, *Salmonella* can also invade phagocytic and non-phagocytic cells by their type III secretion systems (T3SSs). *Salmonella* delivery an array of specialized effector proteins into the host through two distinct T3SSs, encoded by pathogenicity island 1 (SPI-1 T3SS) and 2 (SPI-2 T3SS).

Salmonella first adheres to its host membrane surface and then it secretes bacterial effector proteins encoded by the bacterial pathogenicity island through their type III secretion system. The effector proteins induce dramatic rearrangement of the actin cytoskeleton resulting in host cell ruffling and rapid internalization of the bacteria [170, 171]. Once inside, *Salmonella* resides in a host membrane bound vacuole, much like phagosome but known as the *Salmonella* containing vesicle (SCV). As the SCV moves from the cell periphery to perinuclear positions, it accumulates early endosome and later endosome markers but their interactions with the SCV is transient and the markers are being rapidly removed [172]. Studies have shown that SCVs do acquire lysosomal glycoproteins but that the final fusion step with lysosomes is blocked, a step crucial for bacterial survival since it allows it to avoid the degradative environment of the phagolysosome [173]. In cultured epithelial cells and

macrophages, intracellular *Salmonella* replication starts after a 3 to 4 h lag phase after invasion. The replication is accompanied by the formation of a network of long tubular structures called *Salmonella*-induced filaments (SIFs) that radiate from the SCV [174]. The physiological function of SIFs is probably to help position the SCV close to the Golgi, thereby facilitating interception of endocytic and exocytic transport vesicles to obtain nutrients and/or membranes [175]; F-actin also polymerizes around SCVs at the same time, which is essential for the bacterial replication. The bacteria eventually kill their host cells and escape to infect other cells.

1.2.3 Type III secretion system and *Salmonella* effector proteins

Gram negative bacteria like *Salmonella* utilize T3SS to directly inject bacterial proteins called effectors into the host cells across bacterial and host membranes, where they interact with host proteins and manipulate host cell signaling, allowing the bacteria to invade and replicate. T3SS is a complex, needle-like structure composed of several sub-compartments made up of approximately 20 bacterial structural proteins. It also contains another set of proteins called 'translocators' that help to move the virulence factors - effector proteins into the host cytoplasm.

Most *Salmonella* virulence genes are located on two pathogenicity islands. SPI-1 encodes SPI-1 T3SS structural proteins, translocators as well as SPI-1 effectors. At least 15 effector proteins can be translocated by T3SS1 into the host cells [170]. Some of the early SPI-1 effectors like SopE, SopB, SipA and SipC induce actin rearrangement required for the internalization; other effectors involved in processes like host cell survival, inflammatory response and SCV or Sif biogenesis which happens at a later stage during the infection.

Evidence suggests that some effector proteins have multiple activities within the cell and that they work co-operated with each other. T3SS-2 is not as well-characterized as T3SS-1; they have been identified in recent years. The T3SS-2 apparatus is probably similar to T3SS-1 and translocates more than 20 SPI-2 effectors to the host. Roles of individual SPI-2 effectors still remain to be defined, but they are believed to be secreted and to function later in the infection. They play a critical role in promoting Sif formation, regulating SCV and Sif trafficking, as well as allowing replication of bacteria; T3SS-2 effectors also interfere with host cell ubiquitin pathways [176].

1.2.4 *Salmonella* infection and lipid rafts

Adherence to host cell surface is the first step in bacterial infection; studies have found that many bacteria, including *Salmonella*, target and interact with the host membrane through lipid rafts, specialized domains on the plasma membrane that are enriched in cholesterol (see review [177]). Rafts coordinate cellular reactions by clustered signaling proteins and factors; by targeting rafts, *Salmonella* are able to co-operate with the host signaling molecules that trigger the rearrangement of the cytoskeleton, membrane ruffing and result in internalization. On the other hand, *Salmonella* also requires intracellular cholesterol once it gets into the host. The incorporation of raft components into the SCV seems to have important consequences for the subsequent fate of the bacteria-containing phagosome, and may prevent the interactions with degradative compartments [102].

A study by Garner *et al.* has shown that cholesterol is essential for *Salmonella* uptake [178]. Depletion and chelation of plasma membrane cholesterol specifically inhibited bacterial internalization but not adherence, so the infection is essentially blocked at the

invasion stage. Furthermore, accumulated cholesterol at the *Salmonella* entry site was retained by SCV following pathogen internalization and the redistribution of membrane cholesterol is induced by SPI-1 T3SS. The entry also causes selective protein aggregation on the cell surface and some of these proteins internalize with the SCV but the protein levels decrease over time [179]. Another study looked at the immune recognition of *Salmonella*; their results suggested that the entire bacterial recognition system is based around the ligation of a GPI-anchored protein CD44 by bacterial components – endotpxin lipopolysaccharide (LPS) and the recruitment of multiple signaling molecules within the lipid rafts [180]. Strong evidence showing the relationship between *Salmonella* invasion and lipid rafts is the finding that one of the SPI-1 translocons - SipB is a cholesterol binding protein which is responsible for translocating effectors to the host cytosol. They also demonstrated that cholesterol depletion blocked effector translocation into cells [181]. Some recent researches have shown that *Salmonella* enters hosts not only through lipid rafts but through a specific subset of rafts known as caveolae. Lim *et al.* examined the entry of *Salmonella* using a human M-cell model; they found that increased caveolin-1 levels lead to enhanced *Salmonella* infection, whereas *Salmonella* transcytosis levels were significantly reduced by caveolin-1 siRNA knock down [182]. Later research from the same group examining age-dependent susceptibility to infection also found that *Salmonella* invasion increased in non-phagocytotic, senescent host cells in which caveolin-1 level was also increased. When raft structures were disrupted by methyl-β-cyclodextrin or siRNA-mediated knockdown of caveolin-1 in the senescent cells, *Salmonella* invasion was reduced markedly compared to that in nonsenescent cell; in contrast, over-expression of caveolin-1 led to increases *Salmonella* invasion in non-senescent cells [183].

Salmonella attack rafts as the entry site of invasion, once they get inside the host, they seem also require cholesterol. As SCV undergoes maturation, cholesterol accumulates in both macrophages and epithelial cells. At 20 h post infection the SCV cholesterol constitutes more than 30% of total cellular cholesterol [184]. In normal uninfected cells, only around 10% of cholesterol is intracellular [185]. The study also identified a GPI-anchored protein CD55 is recruited to the SCV; GPI-anchored proteins are markers of rafts [184]. The accumulation of cholesterol in the SCVs may suggest that *Salmonella* infection may affect the cholesterol biosynthesis or their transporting pathways. SPI-2 T3SS effectors PipB and PipB2 target to rafts of SCVs [186]. Other data showed that SPI-2 effector - SseJ function to esterify cholesterol and its esterification at the SCV are functionally important for intracellular bacterial survival [187]. Once *Salmonella* starts to replicate, cholesterol is also required, when inhibiting the first step in cholesterol biosynthesis pathway, bacteria proliferation has been reduced [188].

1.3 Qualitative and quantitative proteomics

1.3.1 Definition of proteomics and traditional techniques

Proteomics is the study of all proteins in a cell, an organelle, or an isolated complex system, including their expression, three-dimensional structure, localization(s), interaction(s), and modification(s) (as reviewed in Ref. [189]). An organism's proteome is in part determined directly by the genome encoding the primary amino acid sequences. Other factors affecting a proteome include alternative splicing to produce different transcripts from one gene and post-translational modifications (e.g., phosphorylation, ubiquitylation). Thus, the number of possible proteinaceous molecular species in a cell is far greater than the number of

genes. Moreover, the proteome of a cell is not static, as it changes in response to the external environments and internal cellular states.

The techniques used in proteomics include the traditional Edman degradation for determining the amino acid sequences; yeast two-hybird screens for studying protein-protein interactions; antibody-based methods such as parallelized immunoblotting, enzyme-linked immunosorbtive assays; and immunofluorescence microscopy [190]; as well as spectroscopic methods such as X-ray crystallography and nuclear magnetic resonance (NMR) for determining and probing the high resolution structure of all proteins in an organism. Both types of approaches focus on a single protein in each assay, or possibly two, three, or four, in the case of immunofluorescence.

1.3.2 Mass spectrometry (MS) - based proteomics

MS-based proteomics is a much higher content technology and currently the most popular technique in proteomics for directly measuring proteins; with a fully sequenced genome of the organism being studied and more discerning software tools, thousands of proteins can easily be identified and quantified from a few micrograms of protein sample with modern mass spectrometers [191].

Modem mass spectrometers consist of an ionization source, a region for selecting, fragmenting and measuring the ionized analytes, and a detector. Mass spectrometric measurements are carried out in the gas phase on ionized molecules. Electrospray ionization (ESI) and matrix-assisted laser desorption/ionization (MALDI) are the two techniques most commonly used to ionize large biomolecules for MS analysis. ESI can couple to liquid-based separation tools and is therefore used for analysis of complex samples. MALDI ionizes

samples from a dry, crystalline matrix and is used to analyze simpler sample mixtures. In mass spectrometry-based proteomics, peptides are more suited than proteins because of their lower molecular weights and higher ionizability; although the development of ionization techniques like surface-enhanced laser desorption/ionization (SELDI) made the ionization and detection of whole protein possible, in general, this is an inefficient and insensitive process.

Mass spectrometers do not measure mass per se, they measure the mass-to-charge (m/z) ratio of ions. Smaller peptides in the range of 7 to 30 amino acids in length are detected with much higher sensitivity and are better behaved in the gas phase. Trypsin is the favored enzyme for generating such peptides, not only because the sizes are optimal but also because of the basic arginine or lysine left on the carboxy-terminus of the peptide, which assists ionization and helps to direct fragmentation. Measuring only the mass of such peptides, however, is not sufficient to unambiguously identify them in most cases because there can be many peptides of a similar or identical mass in the entire complement of proteins encoded in a genome, e.g., anagramic peptide sequences. Instead, peptides can usually be unambiguously identified by interpreting the masses of ions that result from fragmenting the original peptide ion, a process known as tandem mass spectrometry or MS/MS. The mass spectrometer can first measure the mass of all peptides – precursor ion MS, and then select a number of peptides for fragmentation in the 'collision cell' by insert gas use for example collision-induced dissociation (CID), resulted in tandem fragment ion MS/MS spectra.

Previous limits on how quickly spectra could be acquired meant that only a single analyte could be analyzed at a time. Mass spectrometer technology has advanced considerably but even so, very complex protein samples are separated before MS analysis

using a variety of one, two, and three dimensions of separation to reduce the complexity of the sample prior to the peptides entering the mass spectrometer. 1D or 2D sodium dodecyl sulfate polyacrylamide gel electrophoresis (SDS-PAGE), isoelectric focusing, and various chromatographic methods are used most frequently in combination with reversed phase high-performance liquid chromatography (HPLC) or gas chromatography (GC) as the final separation method prior to the peptides being electrosprayed into the mass spectrometer [192]. A couple of protein enrichment techniques are often used before mass spectrometry proteomics analysis, especially, in the study of post-translational modified proteins. For example, lectin was used for binding of glycoproteins for many biomarker researches [193] and TiO_2 was applied to enrich phosphorylated proteins [194].

1.3.3 Instruments

There are many types of mass analyzers but those that are currently in use in proteomics labs are ion traps, time-of-flight (TOF) analyzers, quadrupoles and Fourier transform (FT) analyzers. These analyzers can be used alone or connected together in tandem to take advantages of each analyzer.

1.3.3.1 LTQ-Orbitrap

A linear trapping quadrupole (LTQ)-Orbitrap is the type of instrument used in most of the proteomics experiments present in this thesis. Introduced in 2005, it is an advanced machine with high mass resolution of up to 150,000, a high ion capacity, high mass accuracy of 2-5 ppm, a m/z range of at least 6000 and a dynamic range greater than 10^3, which makes it suited to analysis of complex protein samples [195].

Ionized molecules are first electrosprayed into the linear ion trap, a selected number of ions with given m/z ratios are then passed into the C-trap. The C-trap allows storage of a significant ion population and then its injection into the Orbitrap analyzer in a short pulse so that each m/z population forms a sub-microsecond pulse. The Orbitrap analyzer is an electrostatic trap wherein tangentially injected ions rotate around a central electrode. Since rotational frequency depends strongly on ion energies, angles and initial positions, the ion packets spread out quickly over the angular coordinate forming a thin rotating ring. The whole ring then oscillates along the central electrode harmonically with a period proportional to $(m/z)^{1/2}$ [196]. An LTQ-Orbitrap is capable of MS and MS^n analysis. MS survey scan collected in the Orbitrap measure the m/z ratios for all peptides, and then a couple of most abundant peptides at a given time were selected and fragmented in the ion trap for MS^n analysis.

1.3.3.2 Q-TOF

Quadrupole (Q) time-of-flight (TOF) mass spectrometer is also a hybrid instrument based upon a quadrupole and fastscan time-of-flight technology. Q-TOF instruments provide high sensitivity and accuracy with great reproducibility of peptides/proteins identification but its dynamic range is lower than that of an LTQ-Orbitrap.

In a Q-TOF, the sample is introduced through the interface and ions are focused using the hexapole ion bridge into the quadrupole MS. The flight path of ions after introduction changes 90°; this permits it to optically focus the kinetic energy of the ions to avoid shifts among different ions of the same m/z. The ions are then accelerated and travel to the reflectron. The reflectron makes the ions with same mass but different kinetic energy

arrive the detector at the same time result in high mass accuracy. A Q-TOF is capable of single MS or tandem MS/MS. Single MS only uses the TOF analyzer. In MS/MS, precursor ions are selected in the first quadrupole, undergo collision induced dissociation and the mass analysis of the fragment ions is performed in the TOF analyzer [197].

1.3.4 Qualitative proteomics and peptide/protein identification

Collision induced peptide fragmentation like CID results primarily in the cleavage of peptide amide bonds (NH-CO) through the lowest energy pathway. This leads to b and/or y-ions, depending on whether the charge is retained by the amino or carboxy-terminal fragments. *De novo* interpretation of such MS/MS spectra to derive the amino acid sequence of a peptide solely from the mass spectrometry peptide fragmentation data is challenging and often unsuccessful. On the other hand, if 'all' possible peptides from an organism are known from a genome sequence then it is a relatively simple matter to compare the fragment spectra with theoretical fragment spectra predicted from a database of all possible peptides in that organism to determine the identity of the observed peptide. It is much more difficult to identify proteins in organisms whose genomes are not sequenced because *de novo* sequencing of peptides is required. More extensive reviews on mass spectrometric analysis of peptides can be found elsewhere [198, 199].

A couple of database identification approaches have been developed and implemented into protein search engines such as the Peptide Sequence Tag which was first implemented in the PeptideSearch programme that use amino acids tag to match to a sequence from a database. SEQUEST used another algorithm that determines the overlap of theoretical and experimental spectrum. A probability-based matching approach is used in the

Mascot search engine that involving calculating the theoretically predicted fragments for all the peptides in the database. The predicted fragments are matched to the experimental fragments in a top-down fashion, starting with the most intense b- and y-ions. The spectrum overlap or fragment match are often given a score indicate the ranking of the identified peptide. When trying to identify hundreds or thousands of proteins there are very often false negative identifications. A false discovery rate can then be estimated by searching a decoy database consisting of reversed or scrambled sequences of the database used in the search. Post-translational modifications (PTMs) on peptides can be determined considering the potential mass different and resulting fragment ions that might result but this will increase the search space and lower the confidence of identification. Moreover, the sequence databases used for proteomics are far from optimal; some protein isoforms are not able to be distinguished. Furthermore, it is currently impossible to identify all proteins in a sample due to technical limitations of the mass spectrometer.

1.3.5 Quantitative proteomics and peptide/protein quantitation

Historically, proteomics has been largely qualitative, simply being used to identify which protein(s) are present in a sample, but quantitative proteomics approaches are gaining in popularity, allowing investigators to get at the specificity and functionality of the protein components in their samples. In a mass spectrum, the intensity of any given peptide (which is a proxy for a specific protein or proteins) is proportional to the concentration of that peptide in the sample. However, the ionizability of the peptide also has an enormous contribution to the signal measured for it, meaning that it is difficult to directly compare the intensities of two different peptides. Stable isotope dilution methods are the most accurate methods for

quantitative proteomics and the current choice for most groups with a serious interest in quantitative proteomics. However, two-dimensional gel electrophoresis (2DGE), with its unparalleled resolution, was favored historically.

Most quantitative proteomics approaches measure relative protein abundances between two or more samples [200], as opposed to determining absolute levels of proteins through the spiking of known amounts of isotope-labeled standards [201]. The wide range of technologies employed in quantitative proteomics has been reviewed extensively [202-204]. Three major groups are 1) label-free quantitation including spectral counting, ion intensity quantitation and 2DGE including 2D difference gel electrophoresis (2D DIGE) gel analysis. 2) metabolic labeling approaches like Stable Isotope Labeling of Amino acids in Cell culture (SILAC) and $^{14}N/^{15}N$ labeling 3) chemical labeling for example isotope-coded affinity tagging (ICAT) and isobaric tags for relative and absolute quantitation (iTRAQ). Details of SILAC and ion intensity quantitation are introduced in the next sections.

Semi-quantitative methods such as spectral counting have gained some popularity more recently [205]. The idea is that more abundant proteins have more tryptic peptides resulting in more MS/MS spectra; so the quantity is correlated with how many times peptides of a protein are sequenced in a given sample. This is a simple and fast method for quantifying proteins but there are problems with it, such as saturation and dynamic range; thus, spectral counting results often require much more validation than stable isotope dilution data. In 2DGE, the proteomes to be compared are each resolved by pI and molecular weight, with proteins being detected using one of a variety of protein stains. The staining intensity of each spot is proportional to the amount of that protein, allowing an easy method for quantifying the hundreds to thousands of protein spots visualized. Some of the pitfalls of 2DGE include

the resolution of protein isoforms, which makes quantitation challenging, and the difficulties in obtaining protein identifications from many spots. Samples in 2D DIGE are labeled with different fluorescent dyes prior to mix together and put in the same gel for analysis. Although label-free methods are easy to manipulate at the sample preparation stage and at relatively lost cost, the results are not as accurate as obtained from other relative quantitation methods. Metabolic labeling allows more accurate relative protein quantitation. Like SILAC (see section below), the $^{14}N/^{15}N$ method labels cells through metabolic incorporation on nitrogen; this requires that the cells be completely autotrophic for amino acids so it has mainly been used for bacteria and yeast. Chemical derivatizations to introduce isotope labels are similar in principle to SILAC in that the peptides from the two different conditions are encoded with different masses. The difference lies in how the isotopes are introduced; typically one or two types of functional groups on proteins or peptides are targeted with specific chemistry to introduce a new moiety containing an isotope label [206]. ICAT [206] is cysteine-specific tag which tag cysteine containing proteins or peptides only, whereas iTRAQ [207, 208] tags all peptides in samples. Chemical derivatization can be applied to any sample but it is based on the assumption that each sample is completely and specifically labeled, often an unsupported assumption for complex biological samples. Metabolic labeling can only be done on living cells whereas chemical labeling can be done on any proteome. SILAC or chemical approaches can be more expensive than 2DGE but the additional information obtained (e.g., protein IDs, more proteins quantified) is usually judged to be worth the cost. Although each method has its advantages and disadvantages, 2DGE is no longer very popular, whereas SILAC and some chemical derivatizations remain the most commonly used stable isotope dilution methods. Furthermore, the development of a complete labeled SILAC mouse [209]

and ^{15}N flies [210] means that metabolic labeling is now available for *in vivo* proteomics studies.

1.3.5.1 SILAC

In SILAC [203], the proteomes to be compared are mass tagged by growing the cells initially in media containing specific amino acids enriched in various isotopes, e.g., media containing either normal isotopic abundance arginine or arginine with all six carbon atoms replaced with ^{13}C. Essential amino acids are chosen to be labeled such as arginine (Arg), lysine (Lys) and leucine (Leu) and the two groups of cells are grown under identical conditions. After 5 to 6 cell passages, greater than 98% isotopic labeling can be achieved, then the two samples can be combined prior to protein isolation so that all downstream sample handling is carried out on the combined samples. The two heterobaric forms of the peptides are easily resolved by the mass spectrometer and the relative intensities of the light and heavy peptides give a measure of the relative amounts of the original protein between the two samples [211] (Figure 1.2). SILAC and other metabolic labeling methods normally can only be applied to cultured cells.

Figure 1.2 SILAC workflow

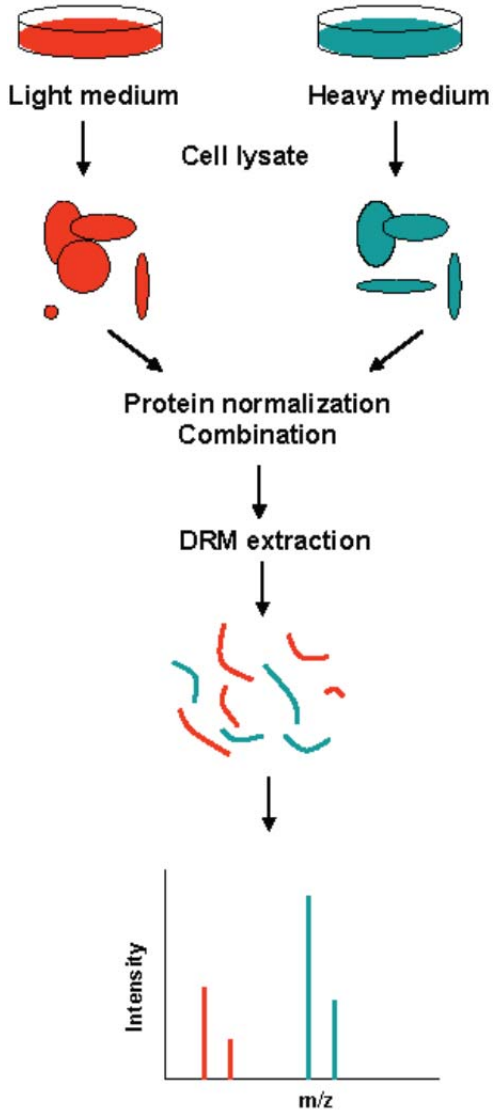

1.3.5.2 Label-free ion intensity quantitation

Ion intensity-based quantitation is one of the label-free methods. It is based on the comparison of the peak height (intensity) or peak area of the peptide precursor ions. The assumption is that the peak height or area of the peptide is proportional to the concentration of that peptide or the corresponded protein(s). Thus, two samples to be compared are

analyzed in series and then the peak heights of individual features common to the two analyses can be compared directly. This method depends strongly on the reproducibility of retention times on the chromatography system in front of the mass spectrometer. In some cases, precursor ion peaks to be compared are normalized and aligned with software assistance (see chapter 3) (Figure 1.3).

Figure 1.3 Label-free ion intensity quantitation work flow

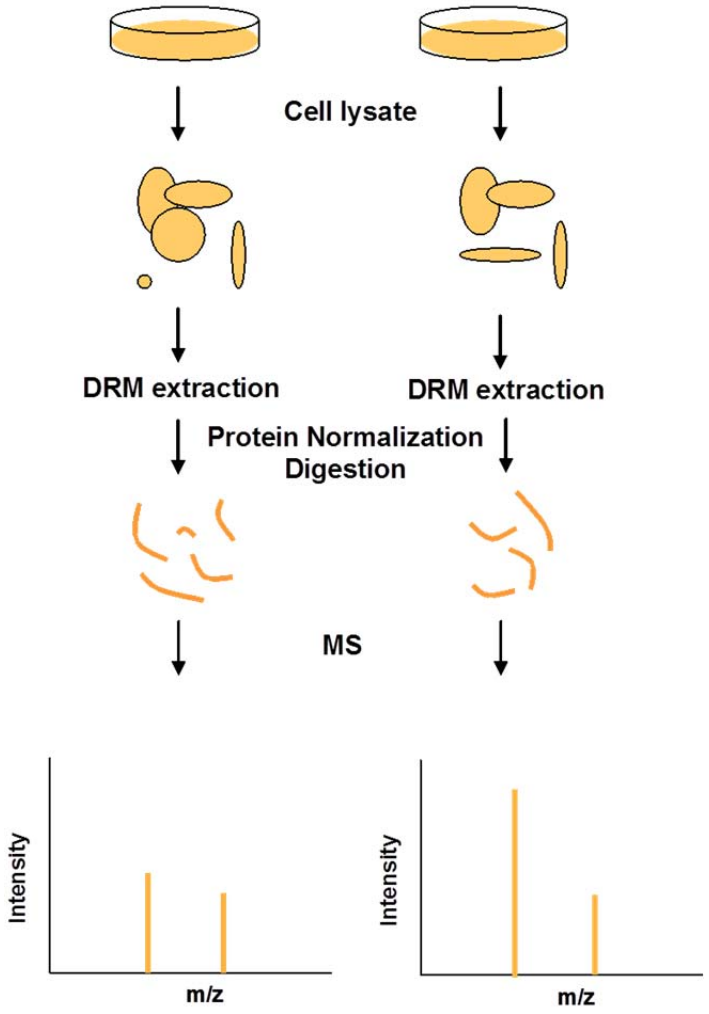

1.4 Quantitative proteomics applied to membrane microdomains

1.4.1 Biochemical approaches for membrane microdomain proteomics

1.4.1.1 Detergent-based methods to isolate rafts

Most lipid raft proteomics studies performed so far have taken advantage of the early observations that rafts, or cholesterol and sphingolipid-enriched membranes, are insoluble in cold, non-ionic detergents (e.g., Triton X-100) and that their low buoyant density allows their simple enrichment by density gradient centrifugation [21]. Typically, DRMs/rafts are separated from total cell lysate or membrane fractions solubilized with 1% Triton X-100 and further purified through a density gradient fractionation procedure comprised of three layers of sucrose at 45% (which contains the DRMs initially), 35% and 5%. After centrifugation at or near 200,000 relative centrifugal force (rcf), a purified DRM fraction can be isolated as a band from the 35 and 5% sucrose interference [9]. Although rafts are only a subset of DRMs [37], the two terms are often confused.

Triton X-100 is the most widely used non-ionic detergent for extracting DRMs. Several studies have examined the relative extraction properties of other detergents, including NP-40, CHAPS, Tween, Lubrol WX and several of the Brij series [15, 122-124]. All of these can be used to enrich raft marker proteins but the DRM proteome extracted with each are not consistent, with some proteins being extracted quite easily with one detergent and not with another. Other factors that contribute to the proteome variability include the abilities of detergents to promote domain formation and to break up some protein–protein interactions. A DRM proteomics study by *Blonder et al.* compared Brij-96 and Triton X-100 and concluded that Triton X-100 extracted more DRM material than Brij-96. Furthermore,

Triton X-100 increases the yield of DRM extraction but at the same time more non-DRMs were also observed, such as ribosomal proteins [122] (Table 1.1).

1.4.1.2 A detergent-free methods to isolate rafts

Another method for enriching rafts employs extraction of the cells in high salt, e.g., 500 mM Na_2CO_3, and high pH (≥11), followed by ultracentrifugation on a sucrose density gradient [68]. This approach also enriches some raft marker proteins but, surprisingly, fails to enrich GPI-anchored proteins. To compound this finding, the specificity of the high pH approach seems to be very poor, with as many as 75% of the proteins enriched in this way being non-raft proteins [37].

A related but likely even less stringent method for enriching rafts involves an initial total membrane enrichment step, followed by membrane fragmentation using sonication and then floatation of raft/DRM membranes on sucrose or Optiprep density gradients [125, 126]. This method seems to preserve more proteins, although a large fraction of those proteins have been otherwise demonstrated to be non-raft localized (Table 1.1).

1.4.1.3 Detergent-based and detergent-free methods to isolate caveolae

The first caveolae isolation experiment was based on the detergent-insolubility and the low-buoyant density of these membrane compartments [57]. The non-ionic detergent Triton X-100 was used to extract crude membranes from murine lung tissue, following which sucrose density ultracentrifugation was applied to enrich caveolae-rich membrane domains [77]. The purified membrane fractions, or DRMs, retain approximately 85% of caveolin and approximately 55% of a GPI-linked marker protein, while they exclude ≥98% of integral

plasma membrane protein markers and ≥99.6% of other organelle-specific membrane markers tested. However, the assumption here was that the purified DRMs were equivalent to caveolae, which seems highly unlikely given more recent results [37]. This technique has also been used to isolate caveolae from chicken smooth muscle cells where plasma membranes were subjected to several purification steps before detergent treatment [127].

To avoid artifacts with using detergents to extract membrane domains, detergent-free methods were developed to extract caveolae [126]. The initial step in all these processes is always mechanical disruption (e.g., a Dounce homogenizer or sonication) of cells, sometimes in high salt or alkaline pH conditions. Then the low-buoyant density of caveolae is enriched by floatation on a density gradient, similar to the detergent extraction method. The hope is that weakly-associating proteins are more readily retained by avoiding detergents and these methods have been used to study caveolae in human heart tissue [212], rat ventricular myocytes [129] and several cell lines [213, 130]. However, the downside of detergent-free methods is that the resulting low-density membrane fraction is probably even less enriched in caveolae, making their use as a caveolae model questionable (Table 1.1).

Regardless of the procedure, it is important to note that all the detergent-free and detergent-based enrichment procedures mentioned above cannot demonstrate, or at least have not demonstrated, the ability to separate lipid rafts from caveolae or vice versa. However, in a more recent study, *Yao et al.* [214] developed a modified sucrose gradient that can separate lipid rafts from caveolin-dependent caveolae, allowing the separation of the two in one experiment.

1.4.1.4 Silica coating and immunoisolation for the isolation of caveolae

In order to improve the purity of isolated caveolae, silica coating and immunoisolation were introduced more recently. Silica coating of plasma membranes was first applied by Caney and Jacobson in the early 80s to enhance the yield and purity of isolated PM of cells in culture [215]. The procedure consists of coating intact cells with dense, positively charged silica particles, which functions to increase the density of the PM for easier isolation and also to prevent vesiculation or lateral reorientation.

More recently, *Schnitzer et al.* applied this silica-coating approach to purify caveolae from luminal endothelial plasma membranes of rat lung. Cell surface membranes were isolated by differential centrifugation after coated with silica; then the PM pellet was homogenized in 1% Triton X-100 followed by sucrose density gradient to yield a DRM preparation containing caveolae [128]. A modified version of this procedure was also published later where caveolae were immunoisolated with the aid of a monoclonal anti-Cav1 antibody [131]. DRMs were isolated from sonicated plasma membranes with or without silica coating and then subjected to immunoprecipitation by anti-Cav1 coated magnetic beads. Similar immunoisolation procedures were also employed by another group to enrich caveolae from rat lung vasculature where the membrane fraction was ultracentrifuged in the presence of high salt prior to immunoenrichment [132] (Table 1.1).

1.4.2 Quantitative proteomics to better understand membrane microdomain

1.4.2.1 Quantitative proteomics approaches to more accurately determine the protein compliment of lipid rafts

Taking advantage of their detergent resistance is a simple and effective way to enrich lipid rafts and caveolae but DRM preparations are notoriously dirty, containing copurifying proteins from a wide variety of locations within the cell besides membrane microdomains. This fact has long been recognized by cell biologists studying lipid rafts and, as a result, the field has come to require that for a protein to be considered a bona fide component of rafts, its presence in DRMs must be shown to be sensitive to cholesterol disruption [216, 217] because the liquid crystal state of lipid rafts is completely dependent on the rigid lipid packing provided by cholesterol intercalation between phospholipid tails. Despite this standard in the lipid raft field, many proteomics groups have tried to equate the proteins identified in DRMs with lipid raft proteins and, as a result, the lipid raft community has largely ignored the proteomic studies of lipid rafts; much of the data simply contains far too high a rate of false positive assignments to be of any use. There are now several proteomics studies of DRMs that have also tested the sensitivity of each identified protein to cholesterol perturbation using methyl-β-cyclodextrin (MβCD). Initially, *Bini et al.* [15] used 2DGE to measure, among other things, the effects of MβCD on proteins in DRMs isolated from Jurkat T-cells. The authors observed that most proteins, including several unexpected proteins such as mitochondria-resident proteins, were sensitive to cholesterol disruption. As will be discussed, later studies have found that these proteins in fact are not sensitive to cholesterol disruption and closer examination of the original methodology suggests a possible reason for the discrepancy: *Bini et al.* normalized their preparations based on equal

amounts of protein but this was only after the DRM preparations had been made, which assumes that the treatment itself, i.e., MβCD, does not have a marked effect on the yield of DRM. The same year as the Bini study, however, *Foster at el.* reported a study where SILAC was used to quantify the impact of MβCD on 392 proteins identified in epithelium derived HeLa DRM preparation [37]. One additional finding of this study was that MβCD has an enormous effect on the DRM yield, explaining the discrepancy between this data and that of Bini. According to the known sensitivity of lipid raft proteins to this drug, three differentially sensitive groups are able to be classified into 'raft proteins', 'raft-associated proteins' and 'co-purifying proteins or contaminants', significantly, the non-raft group including mitochondrial and endoplasmic reticulum (ER) proteins that had been incorrectly assigned to rafts by DRM proteomics studies before. By using the quantitative proteomics approach, the inability to biochemically purify rafts was overcame and eliminated the contaminants that copurified with rafts in DRMs (Figure 1.4). The greater specificity afforded by this approach also demonstrated in an unbiased manner that lipid rafts are enriched in signaling proteins. This confirmed what most people already thought but until that point had not been demonstrated in an unbiased manner. There was a multitude of anecdotal reports of signaling proteins being enriched in rafts, of course, but no demonstration that this was a general phenomenon.

Figure 1.4 The use of SILAC and cholesterol depleting drug MβCD to determine the true components of lipid rafts

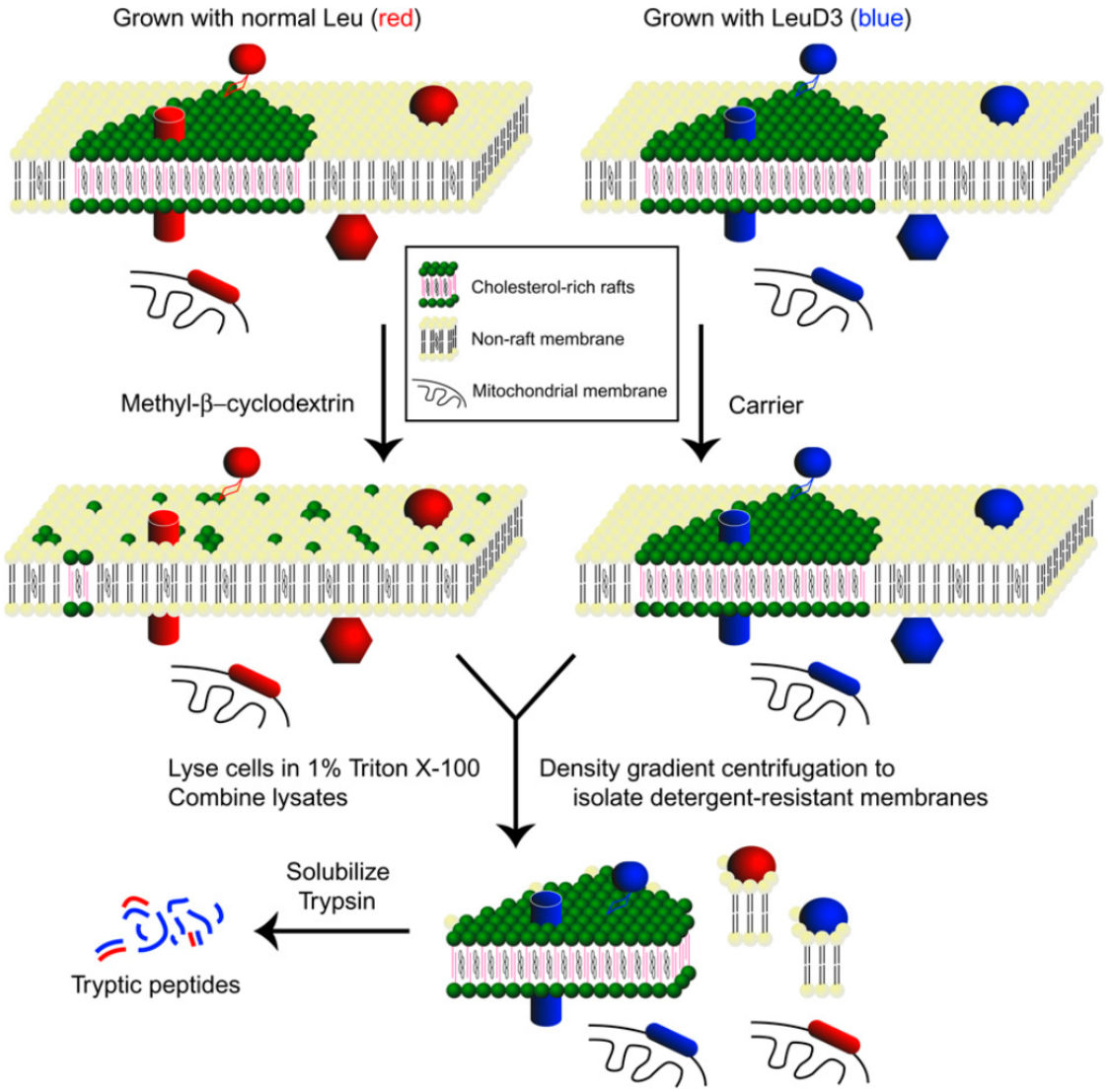

Figure adapted from *Foster et al.* Copyright (2003) National Academy of Sciences, USA. [37]. Two populations of HeLa cells were grown in normal isotopic abundance leucine (red) or $^{2}H_{3}$-leucine (blue) and then treated with carrier (blue) or MβCD (red) to disrupt rafts. The cells were then solubilized in ice cold Triton X-100 and equal amounts of proteins from the two samples were mixed together prior to isolation of DRMs by equilibrium density gradient centrifugation and LC-MS/MS. Peptides from proteins that are true components of lipid rafts should then present in the mass spectrometer with the heavy version (blue) much more abundant than the light (red), whereas copurifying non-raft proteins should present in roughly equal levels of light and heavy. In this scheme, mitochondrial proteins, endoplasmic reticulum components, and most cytosolic housekeeping proteins presented with roughly equal ratios, indicating that they are contaminants of the raft preparation.

Similar results in plant membranes have been confirmed by *Kierszniowska et al.* [218] using ^{15}N metabolic labeling and MβCD to define the sterol-dependent raft proteins in DRMs. In that study, they found many signaling proteins enriched in rafts, as well as cell wall-related proteins, suggesting that, in plants, rafts are anchored through the plant skeleton to the cell wall. In a study by *Yu et al.* [219], the change caused by ceramide-induced cholesterol displacement of immortalized Schwann cells was examined by SILAC. Here, the authors found ceramide-induced cholesterol depletion only partially decreased the association of caveolin-1 with rafts and had a minimal effect on changing the abundance of other lipid raft proteins such as flotillin-1 and G-proteins that are normally sensitive to MβCD treatment. However, the association of ATP synthase subunits with DRMs was increased by the treatment, confirming that it is not a raft resident protein. MβCD is the favored and most effective pharmacological agent for disrupting rafts, but does disruption with other compounds lead to the same conclusions? *Ledesma et al.* [220] compared the effect of sphingomylin depletion by fumonisin B1 to cholesterol depletion by MβCD on hippocampal neuron DRMs and quantified the differences using 2DGE. They concluded that the two drugs induced a similar decrease of raft protein content. The authors also identified proteins such as enolase, annexin, and Thy-1 membrane glycoprotein to be in cholesterol-depended rafts, contrary to other reports of the insensitivity of such proteins to cholesterol depletion [37].

1.4.2.2 Comparative proteomics of caveolae

As an object for biochemical study, caveolae are more tractable than lipid rafts because they can be easily seen by electron microscopy and their formation is dependent on

the structural protein caveolins. Neither detergent-based nor detergent-free methods yield pure caveolae and although immunoisolation of caveolae via caveolin can achieve a higher enrichment, it too leaves room for improvement. Along another vein, methods for resolving caveolae from cholesterol-rich rafts has only been described very recently [214]. Nonetheless, two groups have reported the application of quantitative proteomics to study caveolae composition: *Hill et al.* [73] used 2DGE to distinguish differences in the DRM proteome of mouse embryonic fibroblasts from both wild-type and Cav1 knockout mice. Because *cav1*$^{-/-}$ cells are devoid of identifiable caveolae by microscopy, proteins that are absent in *cav1*$^{-/-}$ DRMs compared with wild-type DRMs are reasonably expected to be components of caveolae. The 2DGE approach used by *Hill et al.* allowed the unbiased assignment of seven proteins to be unique to caveolae and one, Cavin1/Ptrf, was determined to be a coat protein of caveolae. In another study, *Oh et al.* [221] first identified aminopeptidase P to be associated with caveolin by silica coating and immunoisolation of caveolin-associated partners. Then, proteomic analysis of the isolated luminal endothelial cell plasma membranes that contain caveolae with the lung homogenates further revealed aminopeptidase P is particularly concentrated in caveolae. However, the use of more sensitive and higher-throughput quantitative proteomics approaches should enable a deeper coverage of the proteome of caveolae.

1.4.2.3 Using proteomics to understand membrane microdomain dynamics

The ultimate application of quantitative proteomics to the study of membrane microdomains is not simply to catalog their contents but rather to measure how their contents change during various dynamic processes and lipid rafts remain the quintessential

microdomain for such studies. In the case of lipid rafts, the focus is typically on identifying proteins that are recruited to rafts during signal transduction, especially in response to agonists that act to cluster rafts.

T-cell activation is closely connected with raft dynamics as the T-cell receptor (TCR) is a component of rafts and it recruits other proteins to these small platforms upon ligand engagement [53, 222-224]. *Bini et al.* [15] used 2DGE to follow the changes in the DRM proteome when TCR was activated by ligation with anti-CD3 monoclonal antibody cross-linking. They identified a small number of spots on their gels that increased during activation and these included known proteins involved in T-cell activation signaling pathway such as ZAP-70, Grb2, and phospholipase C. They also clustered raft-associated proteins based on their temporal raft association by examining the protein spot intensities at different time points after T-cell activation; the data strongly suggested that rafts are highly dynamic structures.

In a similar study by *Tu et al.* [225], normal Jurkat DRMs were compared with DRMs from anti-CD3/CD28 costimulated cells using 2DGE. The authors were particularly interested in the inducible association of activated IκB kinase complexes with rafts; they demonstrated that treatment of Jurkat cells with MβCD disrupted the assembly and activation of this raft complex and also interfered in anti-CD3/CD28-induced activation of a NFκB response element in the IL-2 promoter. A small number of proteins were found to be recruited to rafts after CD3/CD28 costimulation, e.g., heat shock proteins, vimentin, calmodulin, and a rhoguanine nucleotide dissociation inhibitor; however, these proteins are not well-known members of the TCR signaling pathways and the role they play once recruited to rafts remains unclear.

Von Haller et al. [226, 227] also used ICAT to quantify isolated DRMs from control, unstimulated cells and TCR/CD28 cross-linked cells separately and then the two samples were labeled with light and heavy ICAT reagents at the protein level before combining and digestion. The authors identified several recruited proteins but unfortunately left it up to others to follow these up and validate them. Another study, by *Gupta et al.* [16], also used ICAT to study the change of B-cell receptor (BCR) when ligated by anti-IgM. Here, ICAT labeling was performed at the peptide level where all Cys-containing peptides were labeled. Only four proteins identified showed altered localization, including two cytoskeletal proteins that suggested that the aggregation of rafts might be controlled by cytoskeletal remodeling and another structural protein, ezrin, was dissociated from rafts. Besides identifying proteins recruited to or displaced from rafts upon ligation, this study also looked at the change of post-translational modification of ezrin and they found threonine was dephosphorylated upon BCR ligation. Ezrin was released from the underlying actin cytoskeleton when BCR activated, indicating a transient uncoupling of lipid rafts from the actin cytoskeleton.

Quantitative proteomics has also been used to study other dynamic processes involving lipid rafts. *Yanagida et al.* [228] used spectral counting to investigate the changes in protein composition of DRMs during DMSO-induced differentiation of the human leukemia cell line HL-60 cells into neutrophilic lineage. They identified a group of proteins that were upregulated during differentiation, including known cell differentiation proteins such as CD11b/CD18 subunits of β_2-integrin MAC-1, CD35, and GPI-80, as well as other proteins such as flotillins and a group whose expression was down-regulated like G proteins, heat shock proteins. The authors then further quantified the absolute amount of nine DRM

proteins using spiked, isotope-labeled internal standards and concluded that the protein amounts nearly corresponded to the result obtained by spectra counting. *Blonder et al.* also reported the use of trypsin-mediated $^{18}O/ ^{16}O$ differential stable isotope labeling to compare the untreated DRMs and Iota-b toxin induced DRMs in Vero cells to explore the effects of iota b binding and iota a uptake through rafts [229]. Although markers of DRMs like flotillins and caveolins were identified and quantified with ratios close to one, meaning that their levels remain unchanged in response to the toxin, several other proteins were observed to change. The functional significance of these changes was not pursued.

Finally, the changes imposed on raft protein composition by platelet-derived growth factor (PDGF) stimulation was studied by *Maclellan et al.* [230] wherein they used both 2DGE analysis and ICAT labeling on primary smooth muscle cells to quantify the changes. Following a 15 min exposure to PDGF, 23 proteins were increased in protein abundance in rafts, whereas raft localization of only three proteins increased after 12 h of stimulation. The proteins recruited to rafts included GPI-anchored proteins, cytoskeletal proteins like actin, and endocytosis-related proteins such as clathrin, suggesting a role for rafts in regulation of PDGF-stimulated changes in the cytoskeleton.

1.5 Research aims and hypothesis

Lipid rafts and caveolae are the two most well-known and well-studied membrane microdomains present in the detergent-resistant membranes of cells but simple DRM isolations cannot be equated with lipid rafts or caveolae proteomes. One aim of this thesis was to extend this idea to several cell types and systems, using quantitative proteomics combined with drug treatments or genetic perturbations to explore the composition of these

intriguing domains. Previous raft proteomics studies have identified mitochondrial proteins in rafts, which are in disagreement with pervious findings from my supervisor [37]; leading to one of the hypotheses I have tested: That mitochondria do not contain lipid rafts, and lipid rafts do not contain mitochondrial proteins. Another aim of this work has been to look at the dynamic changes in the raft proteome during *Salmonella* infection by quantitative proteomics combined with time-course experiments to identify novel host targets of the bacteria. A high-content fluorescent-based screening assay for estimating the number of invaded bacteria was also been developed which will help with siRNA library screen later on.

2 Mitochondria do not contain lipid rafts and lipid rafts do not contain mitochondrial proteins

2.1 Introduction

Biological membranes form barriers, compartmentalizing cells into organelles or separating cells from their outside environment. They are composed of lipids and proteins at ratios ranging from 1:4 to 4:1 by mass, with the proteins conferring several capabilities, including ion transport, energy storage, and information transduction. The original fluid mosaic model [6] of membranes suggested a homogenous distribution of proteins and lipids across the two-dimensional surface, but more recent evidence suggests that membranes themselves are compartmentalized by uneven distributions of specific lipids and/or proteins into various microdomains [231]. Lipid rafts are one such class of microdomains that were originally defined biochemically as the low density detergent-resistant membrane (DRM) fraction of cells but that are now recognized as a subset of DRMs enriched in cholesterol and sphingolipids [19-23]. Cholesterol is thought to intercalate between the rigid hydrophobic tails of sphingolipids and saturated phospholipids, allowing a very tightly packed structure with unique biophysical characteristics compared with surrounding membranes. Lipid raft theory [17] proposes that certain proteins preferentially cluster into this unique environment, forming reaction centers essential for many cellular processes, such as cell signaling and trafficking [9, 17]. The diverse array of vital processes that rafts are implicated in make these membrane microdomains an interesting subject for proteomic characterization.

At least two dozen proteomic investigations of DRMs have been reported since 2001 (reviewed elsewhere [232]), and without exception, all have found certain mitochondrial proteins to be present in the preparations, particularly mitochondrial ATP synthase subunits

and the voltage-dependent anion selective channels (VDACs). Mitochondria are quite dense, however, so they should not migrate upwards in the standard DRM preparation. Thus, there are two possible explanations for the observation of mitochondrial proteins in DRMs: 1) mitochondria themselves contain bona fide lipid rafts or another detergent-resistant membrane microdomain, or 2) the localization of proteins such as the ATP synthase subunits or VDACs is not restricted to the mitochondria. We have addressed an aspect of the former possibility previously using stable isotope labeling by amino acids in cell culture (SILAC) to encode the sensitivity to cholesterol disruption into a proteomic analysis of DRMs [37]. We were able to demonstrate that the "mitochondrial" proteins in DRMs are not sensitive to cholesterol disruption by methyl-β-cyclodextrin (MβCD), the standard test applied to putative lipid raft components [216, 217]. While these findings suggested that ATP synthase subunits and VDACs are not in rafts, several other more recent studies have claimed otherwise [233, 123, 130]. Here, we use quantitative proteomics and multiple subcellular fractionation procedures to approach the issue of mitochondrial proteins being in lipid rafts from several angles in three different cell types to conclude that there are no rafts in mitochondria and that there are no mitochondrial proteins in cell surface rafts.

2.2 Experimental procedures

2.2.1 Material sources

The following materials were obtained from the indicated commercial sources: normal DMEM, Roswell Park Memorial Institute (RPMI)-1640 medium, L-glutamine, penicillin/streptomycin, SuperSignalWest PicoChemiluminescent detection system and BCA assay kit, HEPES, sodium pyruvate, and cell culture trypsin (ThermoFisher, Nepean, Ontario,

Canada); FBS, both qualified and dialyzed forms (Invitrogen, Burlington, Ontario, Canada); L-lysine and L-arginine-deficient DMEM and RPMI-1640 (Caisson Labs, North Ogden, UT); L-lysine, L-arginine, methyl-β-cyclodextrin, Triton X-100, sodium deoxycholate (SDC), DTT, iodoacetamide, and Percoll (Sigma-Aldrich, St. Louis, MO); $^{2}H_4$-lysine, $^{13}C_6$-arginine, $^{13}C_6{}^{15}N_2$-lysine, and $^{13}C_6{}^{15}N_4$-arginine (Cambridge Isotope Laboratories, Cambridge, MA); sequencing grade modified porcine trypsin solution (Promega, Madison, WI) and protease inhibitor cocktail tablets with EDTA (Roche Diagnostics, Mannheim, Germany). Antibodies used and their commercial sources were as follows: a-flotillin-2 (BD Transduction, San Jose, CA), a-ATP synthase subunit b (Molecular Probes, Burlington, CA), and horseradish-peroxidase-conjugated anti-mouse secondary (Bio-Rad, Hercules, CA). The three cell lines used here, HeLa, swiss-3T3, and Jurkat, were all obtained from the American Type Culture Collection (Manassas, VA).

2.2.2 Cell culture and SILAC

HeLa and 3T3 cells were maintained in DMEM supplemented with 10% FBS (v/v), 1% L-glutamine (v/v), and 1% penicillin/streptomycin (v/v) at 5% CO2 and 37°C. Jurkat cells were maintained suspended in cell culture flask in RPMI-1640 supplemented with 10% FBS (v/v), 1% L-glutamine (v/v), 1% penicillin/streptomycin(v/v), 10 mM HEPES, and 1 mM sodium pyruvate at 5%CO2 and 37°C. Double and triple SILAC labeling was conducted as described [234], allowing a 200-fold increase in the cell population during labeling. We will henceforth refer to the different labels as 0/0 for the normal isotopic abundance Lys and Arg, 4/6 for $^{2}H_4$-Lys and $^{13}C_6$-Arg, and 8/10 for $^{13}C_6{}^{15}N_2$-Lys and $^{13}C_6{}^{15}N_4$-Arg. To obtain enough material for effective proteomic analysis, six 15 cm plates of confluent adherent cells

(HeLa and 3T3) or 1.6×10^8 suspension cells (Jurkat) were used for each of the 0/0 and 4/6 conditions for isolation of rafts from whole cells. In the triple label experiment used for determining the presence of mitochondrial rafts, we used fifteen 15 cm plates or 4.0×10^8 cells for the 0/0 and 4/6 conditions and three 15 cm plates or 0.8×10^8 cells for the 8/10 condition. All cells were serum starved (18 h for HeLa, 9 h for 3T3, and 20 h for Jurkat) to deplete free cholesterol before MβCD treatment, mitochondria isolation, or DRM isolation.

To determine the optimal MβCD concentration for each cell type, serum-starved HeLa, 3T3, and Jurkat cells in six-well plates were treated with the compound for 1 h at several concentrations between 5 and 20 mM. Cell viability was assessed after the treatment by visual inspection, and the maximum ([MβCD]max) dose that did not cause detectable cell death was used in all further experiments (HeLa, 10 mM; 3T3, 5 mM; Jurkat, 5 mM). As the effects of MβCD on some raft proteins can often be subtle, our goal in this optimization was to maximize the concentration used for each cell type.

2.2.3 Whole cell membrane (WCM) preparation

Three 15 cm plates of 0/0 labeled HeLa or 3T3 cells were washed three times with ice-cold PBS and then scraped into homogenization buffer (250 mM sucrose, 10 mM Tris-HCl, and 0.1 mM EGTA, pH 7.4) with protease inhibitor cocktail added fresh separately. Cells were lysed by forcing them through a 25 G syringe. Unbroken cells and large pieces of debris were pelleted down for 10 min, 4°C at 600 relative centrifugal force (r.c.f.), and the supernatant was saved by spinning down for 30 min, 4°C at 166,000 r.c.f.

2.2.4 Mitochondria isolation

Mitochondria were isolated as described with some modifications [235]. Briefly, serum starved cells were washed three times with PBS and then scraped or resuspended into homogenization buffer (250 mM sucrose, 10 mM Tris-HCl, and 0.1 mM EGTA, pH 7.4) with protease inhibitor cocktail added fresh. Cells were lysed by forcing them through a 25 G syringe; cell breakage was tracked using phase contrast microscopy and was continued until at least 95% of the cells were broken. Lysates were then centrifuged for 10 min at 600 r.c.f. to pellet unbroken cells and nuclei. The supernatant from this step was collected and centrifuged for a further 10 min at 5,000 r.c.f. to pellet crude mitochondria. The pellet was resuspended in homogenization buffer and recentrifuged under the same conditions. Following this, the pellet was resuspended and mitochondria were resolved in 20% Percoll (in 10 mM Tris-HCl and 0.1 mM EGTA, pH 7.4) as a white band near the top of the tube after centrifugation for 60 min at 65,000 r.c.f. The band was extracted by puncturing the site of the centrifuge tube with a 22 G syringe and drawing solution out. The extracted band was then diluted 3-fold in PBS, and mitochondria were pelleted by centrifugation for 30 min at 65,000 r.c.f. The final mitochondria pellet was washed once with ice-cold PBS. All isolation steps were carried out at 4°C.

2.2.5 Detergent-resistant membrane (DRM) preparation

Detergent-resistant membranes (DRMs) were extracted from isolated mitochondria (0/0 condition treated with [MβCD]max for 30 min at 4°C where indicated) or serum starved cells (0/0 condition treated with [MβCD]max for 1 h at 37°C where indicated) or 4/6 labeled cells as described [37] with minor modifications. Briefly, cells were solubilized in lysis

buffer [1% Triton X-100, 25 mM MES, pH 6.5, and protease inhibitor cocktail] by endover-end rotation for 1 h. Relative protein concentrations of cell lysates were determined using the Coomassie Plus kit (Pierce, Nepean, Ontario, Canada), and equal masses of protein from each SILAC condition were mixed together. The combined lysates were mixed with an equal volume of 90% sucrose (in 25 mM MES, 150 mM NaCl, pH 6.5, MES-buffered saline [MBS]) and transferred into the bottom of an ultracentrifuge tube. On to this was layered 5 ml of 35% sucrose in MBS and then enough 5% sucrose in MBS to fill the tube. These gradients were then centrifuged for 18 h at 166,000 r.c.f. The white, light-scattering band appearing between 35% and 5% sucrose after centrifugation corresponded DRMs, and this was extracted using a 22 G syringe. The sucrose was diluted out approximately 3-fold with MBS and membranes were further pelleted by centrifugation at 166,000 r.c.f. for 2 h. Finally, the DRM pellet was washed once with ice-cold MBS prior to further processing for proteomic analysis. All isolation steps were carried out at 4°C.

2.2.6 Protein correlation profiling with SILAC and DRM preparation for linear sucrose gradient

A total of 8.0×10^8 Jurkat cells were used for the 0/0 linear gradient condition, and 5.0×10^8 Jurkat cells were used for the 4/6 nonlinear control condition. A crude DRM lysate was prepared from 0/0 and 4/6 Jurkat cells as above. A linear sucrose gradient was prepared by mixing 6 ml each of 30% and 10% sucrose in MBS into a centrifuge tube with a linear gradient mixer. A 1 ml 5% sucrose cushion was layered on top of the linear gradient, followed by the 0/0 extracted DRMs. The nonlinear control condition was prepared by mixing 4/6 cell lysate with an equal volume of 90% sucrose in MBS and then layering 5 ml

35% and 5 ml 5% sucrose on top as above. After centrifuging the gradients for 18 h at 166,000 r.c.f., 12 1 ml fractions were extracted from the bottom curvature of the linear gradient tube, and one 3 ml fraction was collected at the 35–5% interface of the nonlinear condition. Fractions were diluted and pelleted as above and then resuspended in 1% SDC. The seven final linear samples were single fractions or combinations as follows: A (fraction 1 to fraction 2), B (3, 4), C (5), D (6), E (7), F (8, 9), and G (10–12), with fraction 1 being the bottom (most dense) fraction and 12 being the top fraction. The protein concentrations were measured by BCA assay. Equal amounts of protein from the 0/0 linear samples and 4/6 nonlinear samples were mixed for the protein correlation profiling (PCP) with SILAC [236].

2.2.7 Western blotting

Equal volumes of the seven linear fractions and of the nonlinear fraction (on average 15 mg protein) were combined with protein sample buffer, separated by 12% SDS-PAGE, transferred to polyvinylidene difluoride membrane, and blocked with 5% milk powder. Primary antibodies were used as follows: a-flotillin-2, diluted 1 in 200 for 1 h; and a-ATP synthase subunit b, diluted 1/250 for 18 h. Horseradish-peroxidase-conjugated anti-mouse secondary was used at 1/4,000 and signal detected with the SuperSignalWest PicoChemiluminescent detection system.

2.2.8 Liquid chromatography-tandem mass spectrometry, database searching, and data analysis

Most analyses described here involved direct analysis of an in solution digestion of the samples in question. In solution digestions in SDC were carried out exactly as described

[234] with protein pellets being solubilized directly in SDC and then subjected to trypsin digestion. For each sample, ~5 mg of digested peptides were analyzed by liquid chromatography-tandem mass spectrometry (LC-MS/MS) on a LTQ-Orbitrap (ThermoFisher, Bremen, Germany) exactly as described [234]. For the DRM versus whole cell membrane (WCM) comparison experiment, DRM pellets were resuspended in Triton lysis buffer. Protein concentrations were measured by Bradford assay for both DRM and WCM samples; equal amounts of protein were mixed and then pelleted down. In this experiment only, digested peptides were then further fractionated by strong cation exchange chromatography into five fractions using 0, 20, 50, 100, and 500 mM NH4CH3COO as described [237] and analyzed as above on an LTQ-Orbitrap.

MS/MS were extracted using the Extract_MSN.exe tool (v3.0; ThermoFisher) at its default settings, and the spectra were searched against the International Protein Index human (v3.37; 69,164 sequences) or mouse (v3.35; 51,490 sequences) databases using Mascot (v2.2; Matrix Science) using the following criteria: tryptic specificity with up to one missed cleavage; ±5 parts-per-million and ±0.6 kDa accuracy for MS and MS/MS measurements, respectively; electrospray ionization-ion trap fragmentation characteristics; cysteine carbamidomethylation as a fixed modification; N-terminal protein acetylation, methionine oxidation, $^{2}H_4$-Lys, $^{13}C_6$-Arg, $^{13}C_6{}^{15}N_2$-Lys, and $^{13}C_6{}^{15}N_4$-Arg as variable modifications as necessary. Proteins were considered identified if we observed at least two unique peptides with mass errors <3 parts-per-million, at least seven amino acids in length, and with Mascot IonsScore >25. These criteria yielded an estimated false discovery rate of ~1% using a reversed database search. Quantitative ratios were extracted from the raw data using MSQuant (http://msquant.sourceforge.net), which calculates an intensity-weighted average of

within-spectra ratios from all spectra across the chromatographic peak of each peptide ion. For automatic quantitation, only those proteins with a coefficient of variation (CV) <50% were accepted with no further verification. For proteins with high CVs or with only one quantified peptide, the chromatographic peak assignment was manually verified or rejected. Analytical variability of SILAC data in the types of experiments performed here is typically <20% in our hands, and biological variability was addressed in these experiments by performing at least three independent replicates of each experiment.

For the linear gradient experiments, spectra were extracted using MaxQuant [238] and searched against the International Protein Index Human database using the same parameters as above except for a ±0.5 kDa requirement for MS/MS accuracy. MaxQuant was then employed again to extract quantitative data, either SILAC ratios or PCPs. The resulting ratios for 0/0 linear fractions A to G relative to the 4/6 nonlinear control (light/heavy) were corrected for the volume of sample used and normalized to the greatest intensity fraction to view individual protein profiles. Principal component analysis (PCA) was performed on this seven-dimensional data set in MatLab as follows: the data set was converted into its corresponding covariance matrix, and the eigenvalues and eigenvectors were obtained, the eigenvectors corresponding to the greatest and second greatest eigenvalues (vectors PC1 and PC2) were used to define a plane, and protein data points were projected onto the plane to generate a two-dimensionalplot. Data were then subjected to complete linkage hierarchical clustering using Cluster software [239], and the results were viewed using MapleTree (http://mapletree.sourceforge.net).

2.3 Results

2.3.1 The cholesterol-dependent DRM proteome is similar across cell types

The DRM proteomes of at least a dozen different cells and tissues are now available [233, 15, 229, 240, 241, 37, 16, 242, 220, 18, 243, 230, 123, 130, 244-248, 225, 249, 226, 227]. However, it is extremely difficult, if not impossible, to purify any organelle to homogeneity [250], and the single-step centrifugation used to enrich rafts is no exception, so without rigorous controls a DRM proteome cannot be equated with a raft proteome. In an effort to distinguish resident lipid raft proteins from other proteins copurifying in DRMs, we previously developed a quantitative approach to mass encode the cholesterol dependence of DRM proteins from HeLa human cervical carcinoma cells prior to LC-MS/MS analysis [37]. In this way, a more accurate raft proteome can be measured because the two defining characteristics of raft proteins are measured in a single experiment: sensitivity to cholesterol disruption and enrichment in a low density membrane fraction. To estimate the similarity among raft proteomes from different cell types, we applied this method to two additional cell types commonly used in lipid raft and other cell biology investigations, 3T3 mouse fibroblasts and human Jurkat T lymphocytes.

Cell lines differ in their sensitivity to the cholesterol disrupting agent MβCD, so we initially determined the maximum sublethal dose of the drug for each cell line, [MβCD]max: 10 mM for HeLa and 5 mM for 3T3 and Jurkat. For each cell type, we then labeled two populations of cells with normal isotopic abundance (0/0) or stable isotope enriched (4/6) forms of lysine and arginine (see Experimental procedures) prior to treating one of the two populations with MβCD. For these experiments, we chose to treat the unlabeled cells so that any proteins sensitive to the treatment would present mostly in the labeled form rather than

the reverse because then any exogenous protein (e.g., keratins, trypsin, and serum components) would have the same SILAC spectral signature as a true raft component. The low density DRM fraction from each of the three cell types appeared quite different at the macroscopic level, with widely varying amounts of material isolated from each (data not shown). Despite this, 200 to 300 DRM proteins could typically be identified from <5 mg of total protein loaded into the mass spectrometer from each of the cell types, with SILAC ratios measurable for the large majority of these. By sorting the control:MβCD ratios in decreasing order, we found that the overall distribution of cholesterol sensitivity (Figure 2.1) in all three cell types was similar to our previous observations for HeLa DRMs alone [37]. Namely, there was a portion of the proteins displaying extreme sensitivity to cholesterol disruption, a group with intermediate sensitivity, and a group that did not appear to be sensitive to MβCD at all. Where they were identified, known raft proteins all fell into the group with high ratios, including heterotrimeric guanine nucleotide binding proteins (G-proteins), YES tyrosine kinase, Src tyrosine kinase, SNAP-23, and aminopeptidase N. According to the known sensitivity of lipid raft proteins to this drug [217], we previously classified the three differentially sensitive groups into raft proteins, raft-associated proteins, and copurifying proteins or contaminants [37].

Figure 2.1 Ratios of control:MβCD treated in decreasing order

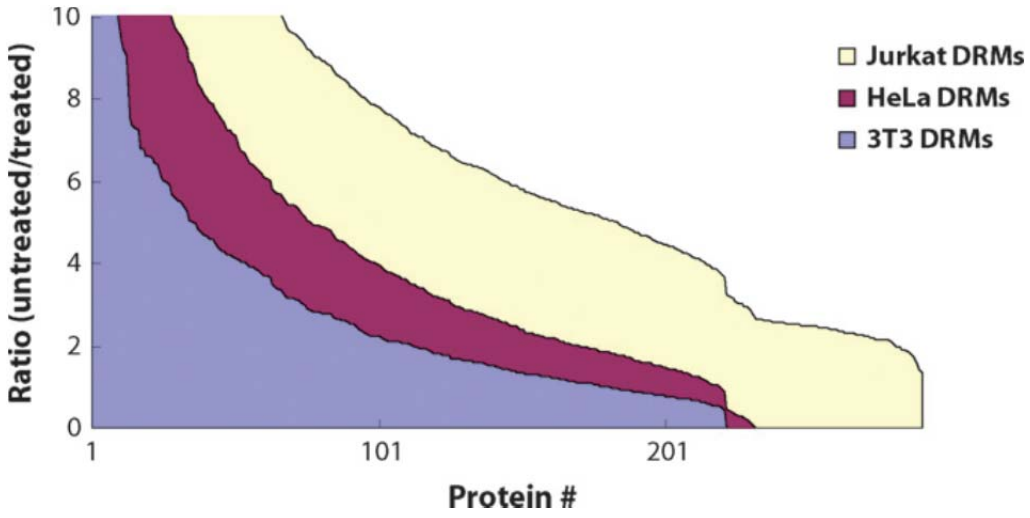

Ratios for detergent-resistant proteins identified and quantified by MSQuant were plotted from largest to smallest for all three cell types: HeLa, 3T3 and Jurkat.

Our application of the same method across multiple cell types now allows us to address the issue of how similar raft proteins are among different cell types. There are numerous reports of DRM proteomes from different cell types, but without the unbiased classification of DRM proteins enabled by our SILAC approach, comparison among those studies is difficult. In general, signaling enzymes, such as protein kinases, protein phosphatases, and G-proteins, were enriched among the proteins with high ratios relative to DRMs as a whole. Structural proteins of microfilaments, such as actin, myosin, and vimentin, were identified with intermediate ratios, suggesting a possible dependence of raft structure on the cytoskeleton consistent with recent studies of hemagglutinin dynamics at subdiffraction resolution [251] (Table 2.1). Likewise, the proteins with lower SILAC ratios were consistent across all cell types and generally included nuclear proteins and highly abundant cytosolic components, as would be expected. With few exceptions (e.g., mitochondrial trifunctional enzyme subunits, mitochondrial heat shock proteins, and prohibitin), all proteins classically

considered to be localized to mitochondria (we will henceforth refer to this group of proteins as "mitochondrial proteins" even though the localization being discussed may not be in a mitochondrion per se) also had relatively low ratios, suggesting that these are also simply copurifying contaminants and not true raft proteins. However, since previous groups [233, 242, 123, 130] have reported some of these to be true components of rafts, we were tempted to explore further the presence of these proteins in DRMs. These published studies leave open two possibilities: 1) that mitochondria themselves contain detergent-resistant microdomains or other low density structures that co-purify with rafts or 2) that conventional cell surface rafts are enriched in mitochondrial proteins. Thus, we have designed SILAC-based approaches to test these two scenarios with our null hypothesis, H_0, being that the mitochondrial proteins found in DRMs are simply just contaminants and not real components of rafts.

Table 2.1 Examples of DRM proteins identified and quantified with their ratios in three cell types tested

Protein names	Ratios (H/L)		
	HeLa	3T3	Jurkat
Guanine nucleotide-binding proteins G	>2.5	>5.5	>11.4
Proto-oncogene tyrosine protein-kinase Yes	5.5±1.6	4.7±1.3	12.5±9.4
Proto-oncogene tyrosine-protein kinase Src	ND	1.6±0.6	6.5±0.5
Aminopeptidase N	6.5±2.9	4.8±0.7	ND
SNAP-23	3.9±0.4	5.9±3.0	13.3±4.4
Fructose-bisphosphate aldolase A	9.4±1.9	3.7±2.1	6.4±3.2
Vacuolar ATP synthase subunits	<1.3	<0.8	ND
Vimentin	ND	2.8±0.7	4.6±1.8
ATP synthase subunits, mitochndrial precursor	<1.0	<1.8	<3
Voltage dependent anion selective channel proteins	<0.7	<0.7	<2.2
Heat shock proteins, mitochondrial precursor	<2.2	<1.7	<2.8
Caveolin 1 α, β	<1.2	<1.0	ND

ND, not detected

2.3.2 Do mitochondria contain lipid rafts?

Of the two possibilities, this one seems less likely since one of the hallmarks of rafts is their high cholesterol content, and mitochondria contain very little cholesterol. Despite this, the possibility has been suggested before [15], so we tested this formal possibility using a triplex version of SILAC that would allow us to evaluate whether mitochondrial proteins in DRMs are enriched when DRMs are isolated directly from purified mitochondria (Figure 2.2). Mitochondria are enriched from two of the three cell populations and treated with (0/0) or without (4/6) MβCD. DRMs are then isolated from the two mitochondrial preparations and from the third untreated, unfractionated cell population (8/10). In this scheme, only proteins that are sensitive to cholesterol disruption (high 4/6:0/0 ratio) and truly coming from mitochondria (high 4/6:8/10 ratio) would be considered components of mitochondrial rafts. Such proteins would be expected to fall in the upper right quadrants of the plots in Figure 2.3, but, as predicted, those areas of the graphs were essentially empty for all three cell types. In HeLa, 3T3, and Jurkat cells, only a few proteins had ratios indicating potential mitochondrial rafts. However, in each case, these numbers represented <2% of the total proteins identified and quantified, and none of them is actually a known component of the mitochondria.

Figure 2.2 The use of SILAC to determine the origin of proteins in DRMs

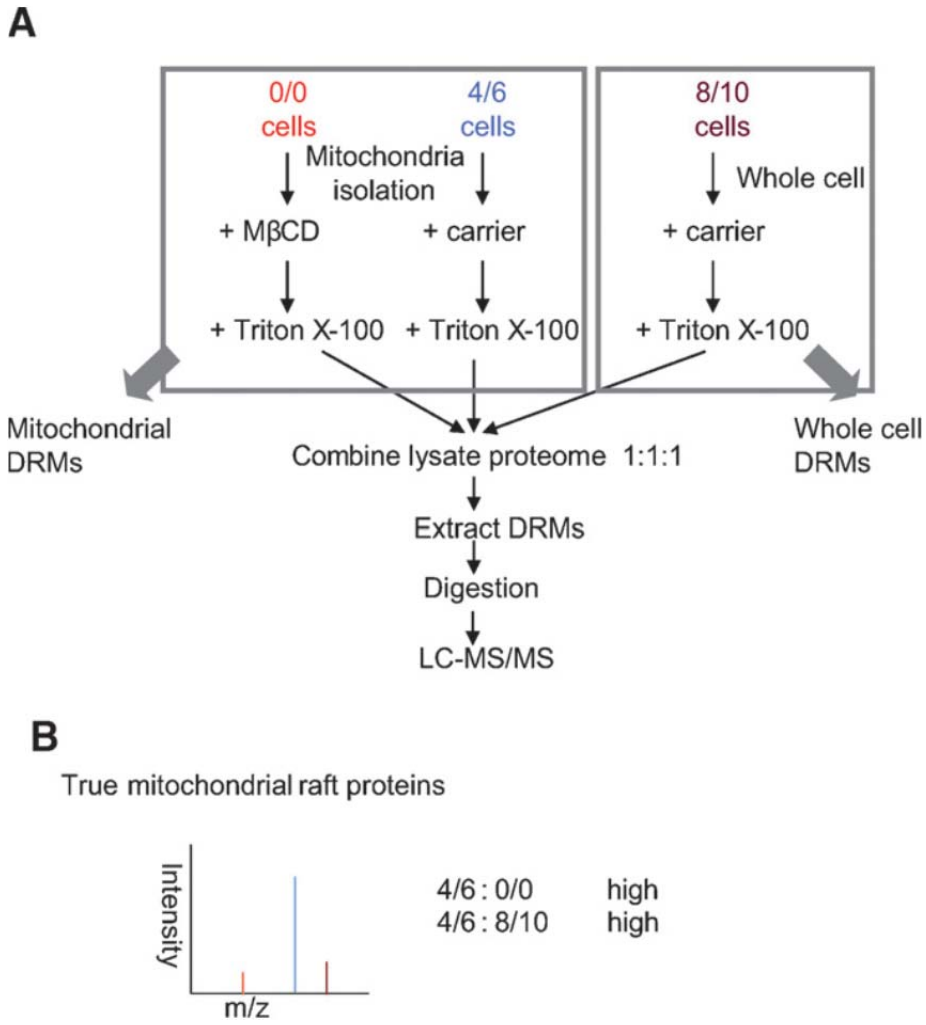

A: Cells were grown in three SILAC media separately containing normal isotopic abundance Lys and Arg (0/0), $^{2}H_4$-Lys and $^{13}C_6$-Arg (4/6), or $^{13}C_6{}^{15}N_2$-Lys and $^{13}C_6{}^{15}N_4$-Arg (8/10). Mitochondria from both 0/0 and 4/6 cell populations were isolated (see Experimental procedures), and then 0/0 mitochondria were treated with the cholesterol-disrupting drug MβCD. Afterwards, 0/0 and 4/6 mitochondria preparations were solubilized in Triton X-100. At the same time, whole 8/10 cells were also solubilized with Triton X-100. Equal amounts of protein from all three extracts were mixed prior to isolation of DRMs by floatation on a sucrose density gradient, and then the proteins were subsequently analyzed by LC-MS/MS. B: True mitochondrial raft proteins should have high 4/6:0/0 ratios indicating their sensitivity to cholesterol disruption, while high 4/6:8/10 ratio would indicate that proteins are coming from mitochondria.

Figure 2.3 Results of triple label SILAC experiments for all three cell types: HeLa, 3T3, and Jurkat

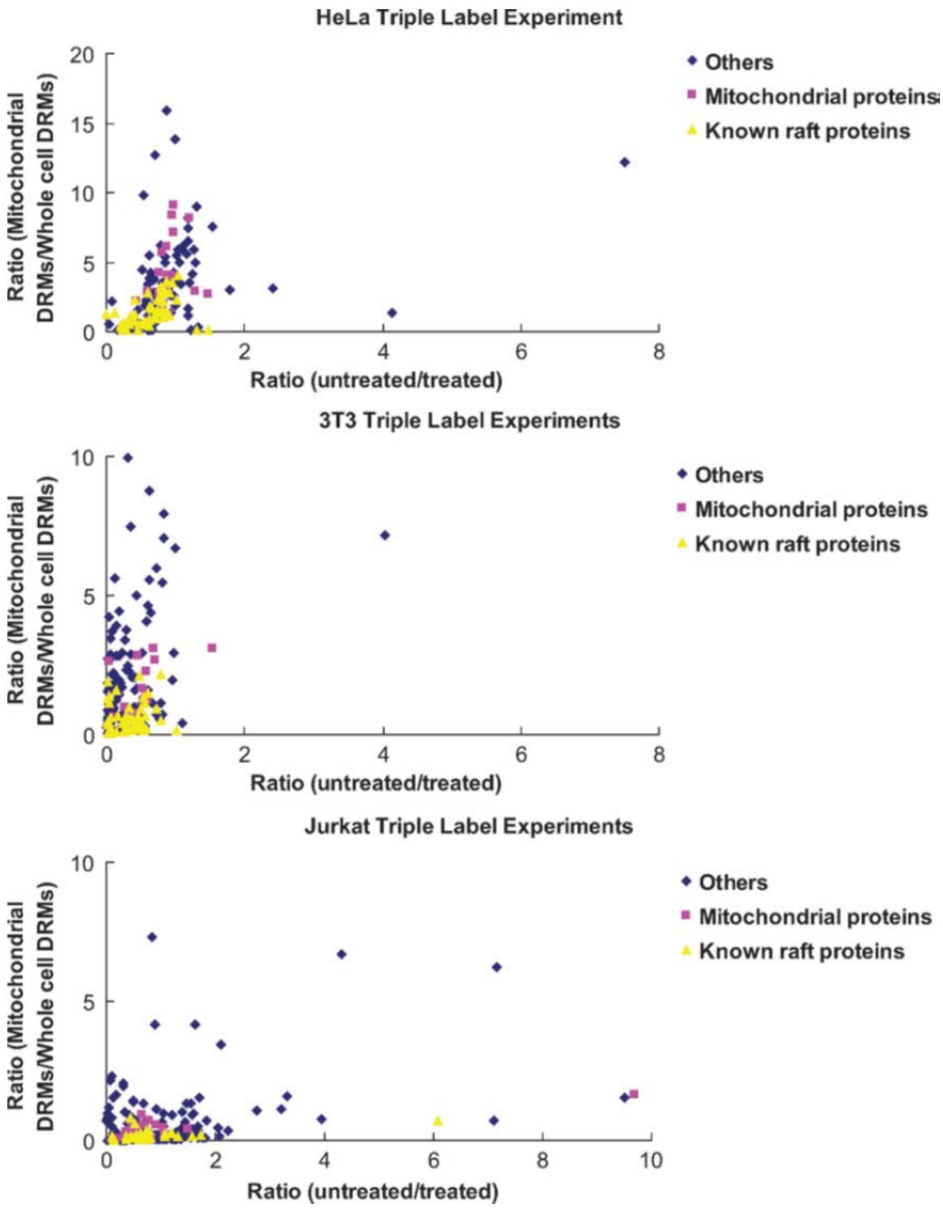

One dot corresponds to one identified and quantified protein that has both untreated/treated (4/6:0/0, abscissa) and mitochondrial DRMs/whole cell DRMs (4/6:8/10, ordinate) ratios. The graphs represent 165 proteins for HeLa, 196 for 3T3, and 294 for Jurkat.

2.3.3 Do plasma membrane rafts contain mitochondrial proteins?

To test the possibility that some classical mitochondrial proteins inhabit a second subcellular location, namely, plasma membrane lipid rafts, we tested the degree to which proteins are enriched in DRMs relative to WCMs in HeLa and 3T3 cells. WCMs were isolated from 0/0 cells, and DRMs were isolated from 4/6-labeled cells. As described in Experimental procedures, the 4/6-labeled cells were treated with 1% Triton X-100 for 1 h prior to floatation on a sucrose density gradient. Finally, this DRM preparation was mixed with the oppositely labeled WCM, the mixed membranes were pelleted, solubilized in deoxycholate, and the proteins were heat denatured and digested to peptides. To probe more deeply into the DRM versus WCM proteome, we used strong cation exchange chromatography to fractionate digested peptides before LC-MS/MS. In this scheme, proteins enriched by the DRM procedure should display a high DRM:WCM ratio, including any and all lipid raft proteins.

Several hundred quantifiable proteins were identified in this analysis (see Experimental procedures for details of protein identification criteria), with DRM:WCM ratios ranging from essentially zero to three, four, or even ten. We were reassured to find that many typical plasma membrane, nonraft proteins were not enriched in the DRM preparation, including large transmembrane proteins and the sodium/potassium-transporting ATPase (Figure 2.4). Interestingly, without exception all mitochondrial membrane proteins identified were also not enriched in DRMs. These included the mitochondrial components previously claimed to be in lipid rafts, including voltage-dependent anion selective channel proteins and ATP synthase subunits. Furthermore, in this system all the MβCD-sensitive proteins we have observed previously (Figure 2.1) [37] were enriched in DRMs.

Figure 2.4 The enrichment of DRM over WCM

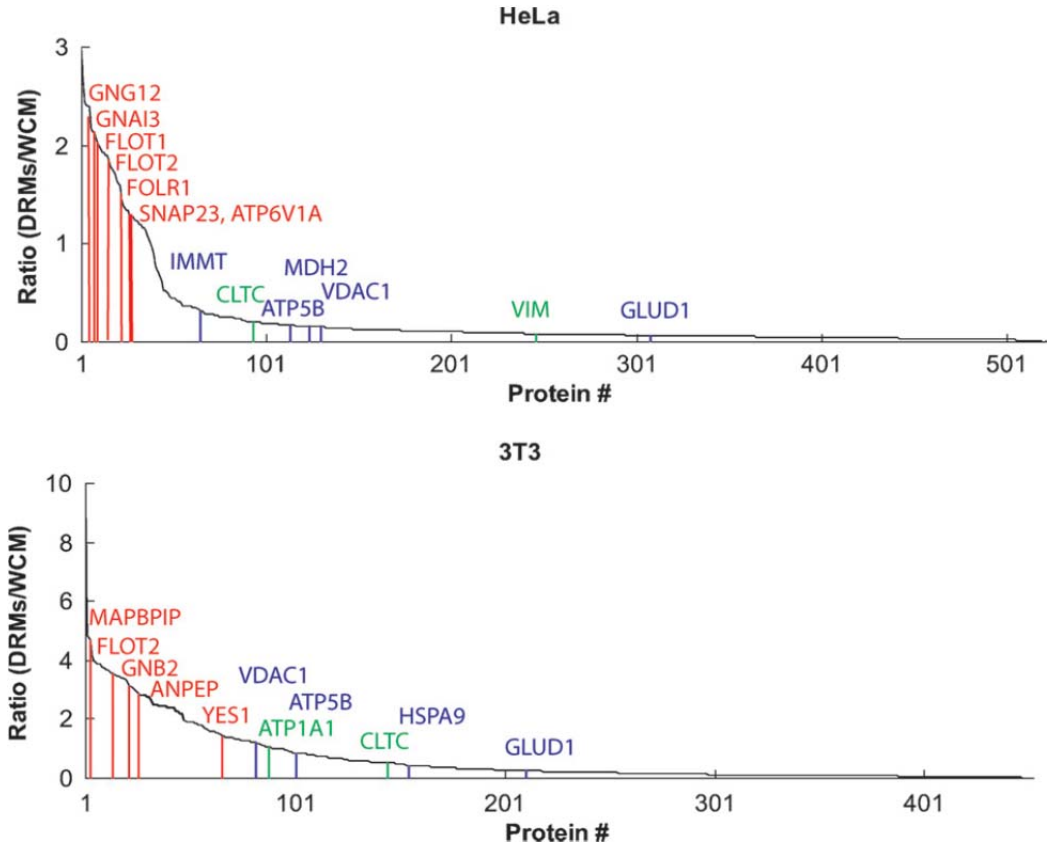

Abundance ratios for proteins in DRMs versus WCMs were plotted in decreasing order. Proteins with higher ratios are enriched in DRM relative to WCM. All previously known or identified raft proteins fell into the group with high ratios, whereas mitochondrial proteins, especially mitochondrial membrane proteins, are not enriched in DRMs. Some examples of raft, mitochondrial, and plasma membrane marker proteins are indicated here as red, blue, and green lines respectively. GNG12, guanine nucleotide binding protein G(I)/G(S)/G(O) subunit γ-12 precursor; GNAI3, guanine nucleotide binding protein G; FLOT1, Flotillin-1; FLOT2, Flotillin 2; FOLR1, folate receptor a precursor; SNAP23, isoform SNAP-23α of synaptosomal-associated protein 23P; ATP6V1A, vacuolar ATP synthase catalytic subunit A; IMMT, isoform 1 of mitochondrial inner membrane protein; CLTC, isoform 1 of clathrin heavy chain 1; ATP5B, ATP synthase subunit β, mitochondrial precursor; MDH2, malate dehydrogenase, mitochondrial precursor; VIM, vimentin; GLUD1, glutamate dehydrogenase 1, mitochondrial precursor; MAPBPIP, mitogen-activated protein binding protein-interacting protein; GNB2, guanine nucleotide binding protein G(I)/G(S)/G(T) subunit β-2; ANPEP, aminopeptidase N; YES1, proto-oncogene tyrosine-protein kinase Yes; ATP1A1, isoform long of sodium/potassium-transporting ATPase subunit α-1 precursor; HSPA9, stress-70 protein, mitochondrial.

2.3.4 Do mitochondrial proteins really co-migrate with rafts?

The classical discontinuous gradient system for isolating DRMs has a very low resolution: essentially anything with a density that falls between that of 5% and 35% sucrose would appear to co-migrate. Thus, while mitochondrial proteins and rafts appear to co-migrate in this system, they may resolve if subjected to a higher-resolution separation on a linear density gradient. To this end, we applied detergent solubilized Jurkat cells onto a continuous, linear sucrose gradient from 10–30% sucrose (see Experimental procedures). One white, light-scattering band was observed after ultracentrifugation, similar to that obtained with the nonlinear gradients but more diffuse and centered at ~15% sucrose. Western blotting of fractions taken from this gradient revealed that the raft marker flotillin-2 and the mitochondrial ATP synthase β subunit showed different distribution patterns (Figure 2.5A). The profile of flotillin-2 was centered at 14–17% sucrose, corresponding to the light scattering band mentioned above, but ATP synthase β was distributed toward the higher density fractions. While only based on two proteins, these data suggest that rafts and mitochondrial proteins may not co-migrate.

To test the co-migration of rafts and mitochondrial proteins more generally, we used PCP-SILAC [236, 252] to measure the distribution of proteins across a linear density gradient (Figure 2.5B). As expected, profiles of known raft proteins (flotillin-1, flotillin-2, p56-LCK kinase, and G-protein subunit β-1 as examples) peaked in the same fraction as flotillin-2 measured by Western blotting (Figure 2.5A). By contrast, the ATP synthase subunits β and α, as well as VDAC-1 and VDAC-2, peaked at higher densities of sucrose. The nonraft plasma membrane marker transferrin receptor 1 exhibited a peaked profile

shifted toward the detergent-soluble fractions, and detergent-soluble β-actin was greatest in intensity in the low density detergent-soluble fraction.

To visualize these trends on a larger scale, rather than just looking at selected profiles, complete linkage hierarchical clustering was performed on the PCP-SILAC data using the CLUSTER program [239]. The resulting tree bifurcated at its base into two groups (Figure 2.5C). One group contained the common mitochondrial proteins found in DRMs, the ATP synthase subunits and VDACs, as well as many proteasome subunits, ribosomal subunits, and ribonucleoproteins. The second group contained the common raft and raft associated proteins (including the flotillins, G-protein subunits, p56-LCK kinase, and V-ATPases). It also contained the nonraft plasma membrane and nuclear membrane proteins and all the cytosolic proteins, including cytoskeletal proteins. The raft proteins themselves clustered to one small branch separated from a larger branch containing the cytosolic proteins.

The clustering data were confirmed by another orthogonal method, PCA. PCA is a technique that can be used to reduce multidimensional data to its principal components (PCs), which are linear combinations of all the variables [253]. The PCs summarize the greatest correlated variation of the data set. PC1 and PC2, representing the greatest and second greatest correlated variation, respectively, are graphed for the PCP-SILAC data in Figure 2.5D, and the same trends seen in the clustering are observed. The ATP synthase subunits and VDACs cluster tightly and separately (bottom left) from the classical raft and raft-associated proteins (bottom center). The proteasome, ribosomal subunits, and ribonucleoproteins make a diffuse grouping (top left), and the cytosolic and cytoskeletal proteins mainly cluster (far right). The nuclear membrane and nonraft plasma membrane proteins appear in the transition between the raft and cytosolic proteins. These groupings

confirm what was seen in the hierarchical clustering: that accepted raft proteins exhibit a different profile from the mitochondrial contaminants, ATP synthase subunits, and VDACs.

Figure 2.5 The separation of rafts and mitochondrial proteins in a linear sucrose gradient

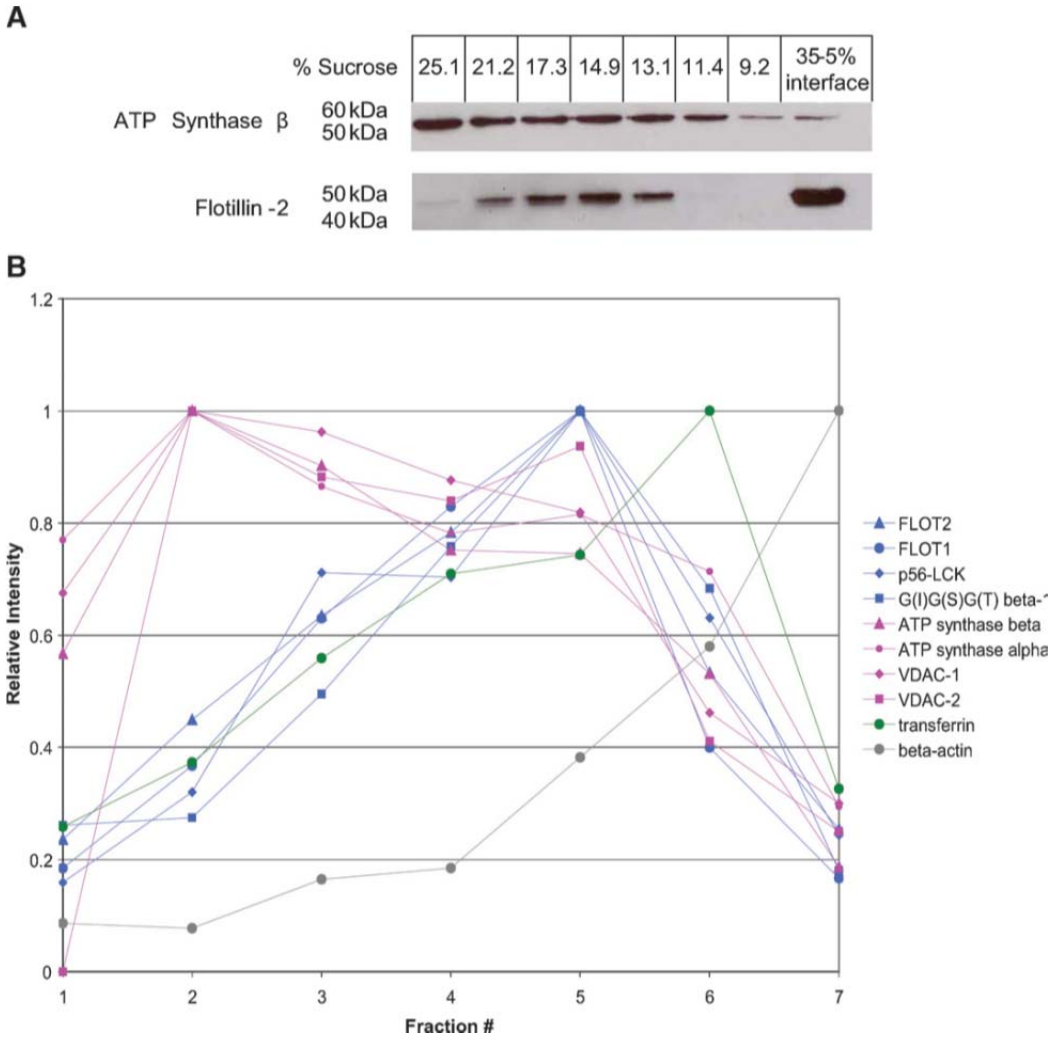

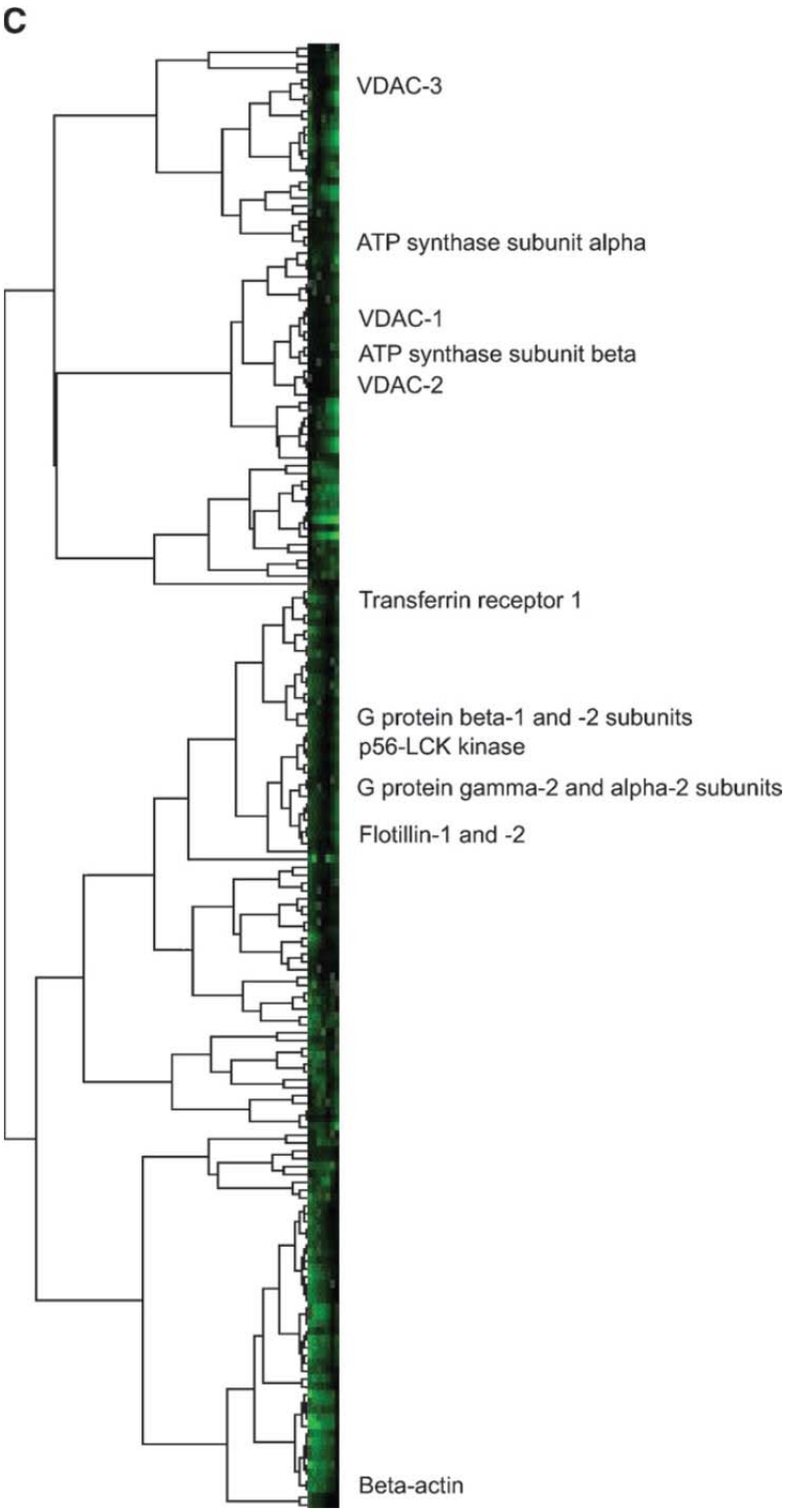
C
VDAC-3
ATP synthase subunit alpha
VDAC-1
ATP synthase subunit beta
VDAC-2
Transferrin receptor 1
G protein beta-1 and -2 subunits
p56-LCK kinase
G protein gamma-2 and alpha-2 subunits
Flotillin-1 and -2
Beta-actin

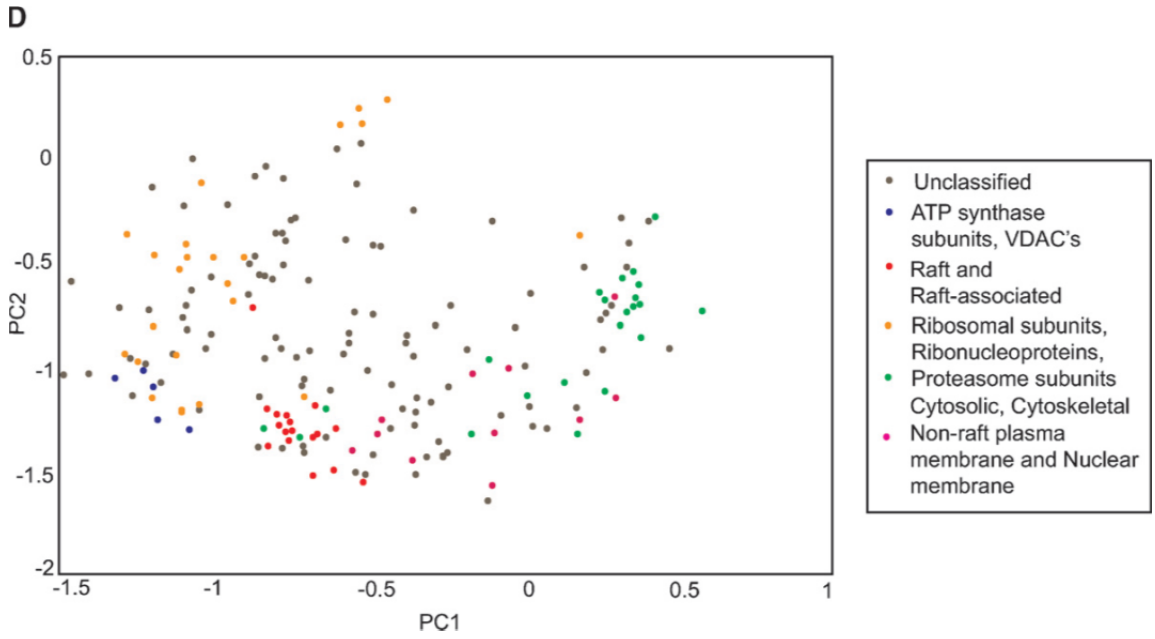

A: Western blot of the lipid raft marker flotillin-2 and the mitochondrial ATP synthase β subunit in fractions taken from a linear sucrose gradient and a nonlinear gradient showing different distribution patterns. B: Some examples of protein profiles or protein distributions across the linear density gradient by PCP-SILAC. C: Hierarchical clustering on the PCP-SILAC data showing the separation of rafts and mitochondrial proteins into two distinct groups. D: PCA analysis on the PCP-SILAC data.

2.4 Discussion

Based on the number of publications in PubMed, lipid rafts and/or caveolae have been an extremely popular subcellular domain for proteomic investigations [232], equivalent perhaps to mitochondria [254] and certainly more so than phagosomes [255]. Prior to the advent of proteomics, rafts were considered to be exclusive to the plasma membrane and membranes immediately up- and downstream of the plasmalemma (i.e., late Golgi/*trans*-Golgi network and endosomes/phagosomes). Likewise, the protein constituents of rafts were thought to be typical plasma membrane proteins, such as glycosylphosphatidylinositol-anchored proteins and Src-family tyrosine kinases [9], so the discovery of mitochondrial proteins in DRM preparations came as a surprise. One of the great advantages of proteomics is its unbiased nature; it took proteomics to discover mitochondrial proteins in DRMs simply

because no one thought to look for them previously. However, biochemical subcellular fractionations typically never yield absolutely homogenous preparations [250], so here we have sought to demonstrate whether mitochondrial proteins are bona fide components of plasma membrane lipid rafts or if they are present in DRMs for another reason. Thus, our null hypothesis was that mitochondrial proteins copurify in DRMs but are not localized in lipid rafts.

Our data certainly support the presence of mitochondrial proteins in DRMs, with several dozen of the most abundant [256] mitochondrial proteins being identified with many peptides each. Without exception, however, none of the proteins were sensitive to cholesterol disruption across three different cell types used as model systems for human epithelia (HeLa), mouse fibroblasts (swiss-3T3), and human T lymphocytes (Jurkat). The failure of any of these mitochondrial proteins to satisfy the cholesterol sensitivity test, the gold standard for a lipid raft protein [217], suggests that they simply copurify with lipid rafts in the DRM preparation. If mitochondrial proteins are specific components of rafts, then one prediction would be that they should be relatively enriched in DRMs versus whole cells or the entire membrane complement of whole cells. To test this hypothesis, we measured the degree of enrichment of proteins in DRMs versus a WCM preparation, and, indeed, mitochondrial proteins were not enriched in DRMs, again suggesting that they are simply contaminants. Furthermore, using a triplex SILAC scheme to simultaneously measure sensitivity to drug treatment and relative enrichment in a subcellular biochemical fraction, we also demonstrated that the mitochondrial proteins in question are indeed enriched in mitochondrial preparations, as one would expect, but that they are not sensitive to cholesterol disruption. And finally, by using high-resolution linear density gradients to better resolve the components of DRMs,

classical lipid raft proteins and mitochondrial components showed different distribution profiles across the gradient, lending more support to the thesis that mitochondrial proteins are copurifying contaminants of the normal DRM preparation.

We are cognizant of four potential caveats that complicate the interpretation of our data. First, in trying to demonstrate the widespread lack of cholesterol sensitivity of mitochondrial proteins in DRM preparations, we were unable to reanalyze the more than two dozen different cells or tissues whose DRM proteomes have been reported (for review, see [232]). Thus, it is conceivable, although we feel it unlikely, that mitochondrial proteins could demonstrate sensitivity to MβCD in other cell types. Second, in the triplex SILAC experiments described in Figure 2.2, we were unable to obtain a completely homogenous preparation of mitochondria, although it was no worse than for other published proteomic analyses of mitochondria [257, 256]. However, for our purposes, homogeneity is not essential because we are only interested in relative enrichment in mitochondrial DRMs, and having a small but detectable contamination from other membranes actually allows a more quantitative assessment of enrichment versus an "all or nothing" response. Third, while Triton X-100 insolubility is the most widely used method for enriching rafts, other detergents, as well as detergent-free methods, yield proteomes with subtly different protein complements [1]. We have previously shown that the high pH/carbonate method [126] has even more cholesterol-insensitive proteins in it than Triton X-100-prepared DRMs [37] and that mitochondrial proteins are similarly insensitive to cholesterol depletion. We have not, however, shown the insensitivity to cholesterol disruption of mitochondrial proteins in DRMs prepared using detergents other than Triton X-100. Lastly, the conditions required to disrupt rafts, serum starvation followed by severe cholesterol starvation, amount to an extremely

harsh environment for the cells, and this could substantially disturb intracellular organelles. Again, we believe the impact of such a perturbation on our conclusions to be minimal because we have confirmed the effects by treating isolated mitochondria with MβCD. Severe cholesterol depletion likely does have some effects on the biosynthetic and endosomal systems, but since there is very little movement of membranes from these compartments to the mitochondria, such effects in the whole-cell experiments would also not appreciably detract from our conclusions.

In summary, we find that we are unable to reject our stated null hypothesis that mitochondrial proteins identified in previous raft studies are actually contaminants of the DRM preparation. We find no evidence that rafts are in mitochondria or that mitochondrial proteins are in rafts.

3 Differential impact of caveolae and caveolin-1 scaffolds on the membrane raft proteome

3.1 Introduction

Plasmalemmal proteins and lipids can segregate into different subdomains, forming tightly packed, lipid-ordered phases enriched in specific subsets of proteins. Collectively known as lipid rafts, these structures can be biochemically enriched in a low-density detergent-resistant membrane (DRM) fraction [1]. This compartmentalization helps to coordinate various activities of raft-associated proteins [9, 17], making the domains a subject of great interest for cell biologists [258] and proteomics scientists alike [250]. Formation of caveolae, a subtype of rafts characterized by morphologically distinctive invaginations of the plasma membrane depends on the presence of the protein caveolin-1 (Cav1) [80]. Recent comparative proteomic analyses of DRMs from wild-type and *Cav1*$^{-/-}$ fibroblasts identified PTRF (Polymerase I and transcript release factor) or cavin-1 as a crucial regulator of caveolae formation [73]. Other cavin family proteins were subsequently identified with varying roles regulating caveolae formation, dynamics and size [259, 74-76]. The requirement for proteins other than Cav1 in caveolae formation argues that Cav1 functions outside of caveolae [260, 80, 38].

Despite these successes, it remains difficult to study the composition of caveolae because of a lack of effective tools; DRM preparations contain not just caveolae but other types of raft domains and many other contaminants, particularly from mitochondria [37, 261]. Likewise, detergent-free methods of enriching caveolae are at least as fraught with complications [1]. However, combining biochemical methods with genetic manipulation of relevant proteins can be an effective approach to probe the composition of these structures.

The Golgi enzyme β-1,6-N-acetylglucosaminyltransferase V (Mgat5) modifies N-glycans, generating high affinity ligands for galectins that then lead to the genesis of another membrane domain, the galectin lattice [262]. *Mgat5*-deficiency reduces mammary tumor growth and metastasis formation but Cav1 expression was inversely proportional to tumor size in *Mgat5*$^{-/-}$ mice, suggesting that Cav1 expression impacts on tumor growth only in the absence of Mgat5 and the galectin lattice [263, 264]. These observations led to the development and characterization of three cell lines: 1) *Mgat5*$^{+/+}$ mammary carcinoma cells derived from wild-type tumors that express Cav1 and caveolae; 2) *Mgat5*$^{-/-}$ cells from small tumors that express Cav1 but no detectable caveolae; 3) *Mgat5*$^{-/-ESC}$ cells from large tumors that express minimal Cav1 protein and that have escaped (ESC) the growth limitations imposed by the lack of Mgat5 [264]. Further characterization revealed that noncaveolar Cav1 in *Mgat5*$^{-/-}$ cells form high molecular weight oligomers and inhibit epidermal growth factor receptor (EGFR) signaling and endocytosis, as well as dynamics of the GM1-ganglioside binding raft marker cholera toxin b-subunit (CT-b) [264, 265]. Intriguingly, whereas Cav1 inhibits EGFR signaling, EGFR is not associated with caveolae in the absence of ligand [87], suggesting that Cav1 scaffolds may represent a Cav1 regulatory domain [265].

Collectively, these observations suggest a model where caveolae, Cav1 scaffolds, and Cav1-free raft domains represent functionally distinct subtypes of lipid rafts whose expression may explain many of the discordant reports of Cav1 regulation of cellular signaling. However, apart from a few marker proteins, e.g. Cav1 and PTRF, the protein composition of caveolae and Cav1 scaffolds remains uncertain. Here we use super-resolution microscopy to show that Cav1 scaffolds represent homogenous, sub-diffraction limit domains whose size and distribution differ from that of caveolae. We also analyzed the DRM

proteome of cells containing Cav1/caveolae (*Mgat5*$^{+/+}$), Cav1 scaffolds only (*Mgat5*$^{-/-}$), or no Cav1 or caveolae (*Mgat5*$^{-/-ESC}$) and compared the data with that of DRMs from wild-type and *Cav1*$^{-/-}$ MEFs (mouse embryonic fibroblasts). Our results show that expression of Cav1 scaffolds but not caveolae significantly depletes proteins, including signaling G proteins, from the raft proteome suggesting that caveolae and Cav1 scaffold expression differentially impacts on the protein composition and signaling potential of lipid raft domains.

3.2 Experimental procedures

3.2.1 Materials and cell lines sources

The following materials were obtained from the indicated commercial sources: Dulbecco's Modified Eagle's Medium (DMEM), L-glutamine, penicillin and streptomycin, BCA assay kit and cell culture trypsin (ThermoFisher, Nepean, Ontario, Canada); Fetal bovine serum, both qualified and dialyzed forms, Alexa-488 coupled secondary antibody, ProGold and Lipofectamine 2000 (Invitrogen, Burlington, Ontario, Canada); L-Lys- and L-Arg-deficient DMEM (Caisson Labs, North Ogden, UT); L-Lys, L-Arg, methyl-β-cyclodextrin (MβCD), isoproterenol, Triton X-100 (Tx-100), sodium deoxycholate (SDC), dithiothreitol, iodoacetamide, lactose, sucrose and Alexa-546 coupled-CT-b (Sigma-Aldrich, St.Louis, MO); $^{2}H_4$-lysine, $^{13}C_6$-arginine, $^{13}C_6{}^{15}N_2$-lysine, and $^{13}C_6{}^{15}N_4$-arginine (Cambridge Isotope Laboratories, Cambridge, MA); Sequencing grade modified porcine trypsin (Promega, Madison, WI); Protease inhibitor mixture tablets with EDTA (Roche Diagnostics, Mannheim, Germany); Coomassie Plus kit (Pierce, Nepean, Ontario, Canada); Protein A Sepharose beads (Amersham Biosciences, Sweden); Mouse protein nonspecific IgG

(Biomeda, Foster city, CA). Antibodies used and their sources were as follows α-PTRF (BD Transduction, San Jose, CA); α-actin, α-caveolin-1 (Santa Cruz Technology, Santa Cruz, CA). The *Mgat5*$^{+/+}$, *Mgat5*$^{-/-}$, *Mgat5*$^{-/-ESC}$ cell lines were cultured as previously described [264].

3.2.2 Cell culture and SILAC

Both duplex and triplex stable Isotope Labeling by Amino acids in Cell culture (SILAC) labeling was conducted as described previously [37]. Before labeling, all Mgat5 cells were maintained in DMEM supplemented with 10% fetal bovine serum (v/v), 1% L-Gln (v/v), and 1% penicillin/streptomycin (v/v) at 5%CO2 and 37°C then transferred to SILAC medium with dialyzed fetal bovine serum plus Lys and Arg isotopologs; cell populations were amplified 200-fold in the labeling media to achieve complete labeling. Here we refer to the different labels as "0/0" for the normal isotopic abundance Lys and Arg, "4/6" for $^{2}H_{4}$-Lys and $^{13}C_{6}$-Arg, and "8/10" for $^{13}C_{6}{}^{15}N_{2}$-Lys and $^{13}C_{6}{}^{15}N_{4}$-Arg. For each analysis, six 15-cm plates of Mgat5 cells were used per condition for detergent-resistant membrane extractions, quantitative co-immunoprecipitations and MβCD treatment experiments. For the MβCD treatment experiment, all 0/0 and 4/6 labeled *Mgat5*$^{+/+}$ cells were serum starved for 5 h to deplete free cholesterol before MβCD treatment and DRM extraction. 0/0 cells were treated with 5 mM MβCD for 1 h at 37 °C with 4/6 untouched. WT and *Cav1*$^{-/-}$ MEFs were maintained in normal DMEM medium as 'label-free' samples [73]. Two 15 cm plates of MEF cells were used per each cell type for detergent-resistant membrane extraction prepared in parallel. For the lactose/sucrose treatment experiment, five 15 cm plates of labeled Mgat5 cells were used for each of the 0/0, 4/6 and 8/10 conditions for the treatment and subsequent

detergent-resistant membrane extraction. In this experiment, 35% confluent 0/0 and 4/6 *Mgat5*$^{+/+}$ cells were treated by adding 20 mM lactose or sucrose, respectively, directly to the growth medium for 2 days with 8/10 cells as the control.

3.2.3 Detergent-resistant membrane (DRM) preparation

DRMs were extracted from normal or treated SILAC cells as described previously [37] and as section 2.2.5. Each plate would typically yield between 10 to 20 ug of DRM protein. All steps above were carried out at 4 °C.

3.2.4 Quantitative co-immunoprecipitation

Caveolae were precipitated from both detergent and detergent-free extracts of *Mgat5*$^{+/+}$ cells. In the detergent method, 0/0 and 4/6 *Mgat5*$^{+/+}$ cells were lysed in Tx-100 for 1 h; 4, 8, or 20 ug of caveolin-1 antibody or protein nonspecific IgG were added to 4/6 and 0/0 lysate respectively. After adding Protein A Sepharose beads, both the lysates were rotated for 2 h at 4 °C, after which the beads were pelleted at 600 r.c.f. for 10 min and, washed three times with ice-cold phosphate-buffered saline buffer. Finally, the beads were solubilized in 100 ul 1% SDC in 50 mM Tris (pH 8.0), heated for 10 min 99 °C with mixing at 1400 rpm; the protein concentration of both the supernatants were measured by BCA assay and combined at a 1:1 protein ratio. In the detergent-free method, cells were scraped in homogenization buffer (250 mM sucrose, 10 mM Tris-HCl, and 0.1 mM EGTA, pH 7.4) with Protease Inhibitor Mixture added fresh, and then lysed by passage through a 25-G needle syringe until >95% of the cells were broken by examining under microscope. All

nuclear and cell debris were pelleted at 16,000 r.c.f. for 10 min, and then Tx-100 was added to the supernatant to extract DRMs and allowed to incubate for 1 h. The remainder of the detergent-free procedure was the same as the detergent method except 10 ug of caveolin-1 ab and IgG were used.

3.2.5 Western blotting

Ten micrograms of whole cell lysate from *Mgat5*$^{+/+}$, *Mgat5*$^{-/-}$, and *Mgat5*$^{-/-ESC}$ were combined with SDS sample buffer, separated by 12% SDS-PAGE, transferred to polyvinylidene difluoride membrane and blocked with 5% milk powder. Primary antibodies were used as follows: α-caveolin-1 diluted 1 in 200 for 1 h; a-PTRF, 1/100 for 1 h and α-actin, 1/100 for 1 h. Horseradish peroxidase conjugated anti-mouse secondary was used at 1/4000 and signal detected with SuperSignalWest PicoChemiluminescent detection system.

3.2.6 Transfection and Immunofluorescence

Mgat5$^{+/+}$, *Mgat5*$^{-/-}$, and *Mgat5*$^{-/-ESC}$ cells were plated and 24 h later transfected with Gαs-GFP [259] using Lipofectamine 2000. Twenty-four hours after transfection, cells were incubated with or without Alexa-546 coupled-CT-b (1/400) for 20 min at 4 °C and fixed with methanol/acetone (50%/50%v/v) at -20 °C. For the isoproterenol experiments, one hour before treatment, complete media was replaced with serum-free DMEM. Gαs-GFP transfected cells were then incubated with or without Alexa- 546 coupled-CT-b as described above. Next, the cells were washed with warm phosphate-buffered saline and incubated with

10uM isoproterenol for 15 min at 37 °C. The cells were then fixed for 20 min with 4% paraformaldehyde (PFA) at room temperature, and permeabilized with 0.2% Tx-100. In both cases, preparations were extensively washed with phosphate-buffered saline containing 100 uM Ca^{2+} and 100 mM Mg^{2+}, blocked with 1% bovine serum albumin and then the cover slides were incubated sequentially with the primary and secondary antibodies. Cover slides were mounted in Gelvatol for confocal analysis and images acquired using an Olympus Fluoview 1000 confocal microscope. Pearson's coefficients were calculated from individual cells (11–19 cells) using ImagePro Plus and ImageJ software.

For the stimulated emission depletion microscopy (STED) microscopy, Mgat5 cells were fixed in 3% paraformaldehyde, permeabilized with 0.2% Triton X-100 and blocked with 1% bovine serum albumin before incubation with anti-Cav1. Cells were then incubated with Alexa488 α-rabbit secondary antibody and then mounted in ProGold for confocal STED analysis. Images were acquired using a Leica SP5 STED CW microscope (courtesy of Vladimir Zhukarev, Leica). Signal dynamic range was adjusted for each STED and confocal image acquisition (gain ~800 V for confocal images and ~1000 V for STED images) and images processed using a median filter radius of 3 and application of a 30–255 intensity threshold to 8-bit images. Area of Cav1-positive structures was measured with ImageJ software, and the averages of individual cells pooled to obtain the mean of all cells from independent experiments. Statistical analysis was performed on GraphPad Prism software: to determine p values unpaired T tests were performed between two different conditions using 95% confidence intervals.

3.2.7 LC-MS/MS, database searching and data analysis

All analyses here involved in solution digestions in 1% SDC (50 mM Tris, pH 8) with protein pellets or bead-bound protein in the pull-down experiments being solubilized directly in SDC and then subjected to trypsin digestion. Protein solutions were reduced (1 ug dithiotreitol/50 ug protein), alkylated (5 ug iodoacetamide/50 ug protein) and digested (1 ug trypsin/50 ug protein) as described [234]. For each sample, 5 ug (measured by BCA method) of digested peptides were analyzed by liquid chromatography-tandem mass spectrometry (LC-MS/MS) on a LTQ-OrbitrapXL (ThermoFisher, Bremen, Germany). The LTQ-OrbitrapXL was on-line coupled to Agilent 1100 Series nanoflow HPLC instruments using a nanospray ionization source (Proxeon Biosystems) holding columns packed into 15-cm-long, 75-um-inner diameter fused silica emitters (8-um-diameter opening, pulled on a P-2000 laser puller from Sutter Instruments) using 3-um-diameter ReproSilPur C18 beads. Buffer A consisted of 0.5% acetic acid, and buffer B consisted of 0.5% acetic acid and 80% acetonitrile. Gradients were run from 6% B to 30% B over 60 min, then 30% B to 80% B in the next 10 min, held at 80% B for 5 min, and then dropped to 6% B for another 15 min to recondition the column. The LTQ-OrbitrapXL was set to acquire a full-range scan at 60,000 resolution from 350 to 1500 Th in the Orbitrap and to simultaneously fragment the top five peptide ions in each cycle in the LTQ. In all experiments, digested peptides were also further fractionated by strong cation exchange chromatography into five fractions using 0, 20, 50, 100, and 500 mM of NH4CH3COO or 10 fractions using 0, 10, 20, 50, 75, 100, 150, 200, 350, and 500 mM of NH4CH3COO as described [234] and analyzed as above on an LTQ-OrbitrapXL.

Protein identification and quantification were done using Proteome Discover (v.1.2, ThermoFisher, Bremen, Germany) and Mascot (version2.3, Matrix Science) to search against the International Protein Index (IPI) Mouse (version 3.69, 110,771 sequences—common serum contaminants and human keratins added and all reversed sequences were concatenated) database with the following criteria: electrospray ionization-ion trap fragmentation characteristics, tryptic specificity with up to one missed cleavages; ±10 parts-per-million and ±0.6 Da accuracy for MS and MS/MS measurements respectively; cysteine carbamidomethylation as a fixed modification; N-terminal protein acetylation, methionine oxidation, deamidation (NQ), duplex ($^{2}H_4$-Lys, $^{13}C_6$-Arg) or triplex ($^{13}C_6{}^{15}N_2$-Lys and $^{13}C_6{}^{15}N_4$-Arg) SILAC modifications as appropriate; peptide false discovery rate was set at 1%. Quantitation was done using a mass precision of 2 ppm (three times the mass precision is used to create extracted ion chromatograms). After extracting each ion chromatogram, Proteome Discoverer runs several filters to check for, among other things, interfering peaks and the expected isotope pattern, and peptides that do not meet all the criteria are not used in calculating the final ratio for each protein. The ratios presented in the various tables are the raw measured ratios, with the exception of the *Mgat5*$^{-/-}$ versus *Mgat5*$^{-/-ESC}$ comparison, where the ratios were standardized around a mean of 1.0. We consider proteins identified if at least two peptides were observed. Analytical variability of SILAC data in the types of experiments performed here is typically <30% on average and biological variability was addressed in these experiments by performing at least three independent replicates of each experiment.

Label-free quantitation was performed using Mass Profiler Professional and MassHunter (Agilent) software based on area-under-the curve method (Figure A.1). In this procedure, at least four biological replicates of DRMs (4 ug each) from WT and *Cav1*$^{-/-}$

MEFs were analyzed by LC-MS (i.e. only MS1 spectra acquired) using 160 nl (75 mm×150 um) high capacity C18 reverse phase HPLC-chip with 55 min gradient from 0 to 45% acetonitrile on a 1200 Series nano HPLC and Chip-Cube Q-TOF 6510 (Agilent Technologies) with Vcap set at 1850 V and the fragmentor voltage set at 175 V. MassHunter Qualitative Analysis software was used to extract the 1000 most abundant molecular features between 100 and 3200 Th, defined by precursor ion m/z, retention time (RT) and intensity. Statistical analysis of the extracted molecular features was performed using Mass Profiler Professional (Agilent) to generate MS/MS target lists with features significantly up-regulated in either WT or *Cav1*$^{-/-}$ DRM. The following settings were used in generating the inclusion list: minimum absolute abundance = 1000 counts, minimum # of ions = 2, 2+ or greater charge state required; compound alignment: RT window 0.1% + 0.15 min, mass window 5.0 ppm + 2.0 mDa; flag filter at least four out of eight samples have acceptable value; frequency filter retain entities that appear in at least 100% of samples in at least one condition; p value cut off 0.001, fold-change cut-off of 100; features that only present in one of the two cell types were selected. Inclusion list exportation settings: RT window ±0% + 0.1 min, number of precursor ions per compound limited to 1, minimum ion abundance 1000 counts, export monoisotopic m/z, prefer highest abundance charge state(s). The inclusion lists were imported into MassHunter and the target sample (MEF WT or *Cav1*$^{-/-}$ DRM) were subjected to targeted MS/MS in which the instrument selects the included m/z at a specific retention time window for MS/MS. This method obviously relies on highly reproducible chromatography so we examined the reproducibility of our Chip-LC-MS system using repeated injections of PC3 DRM samples. Total ion chromatograms (TICs), base peak chromatograms (BPCs), peptide and protein identifications are all highly reproducible, with the large majority of proteins and

peptides identified in all replicates (Figure A.2). Mass spectra extraction, database searching and quantitative ratios were performed using Spectrum Mill software (Agilent, A03.03) against NCBInr Mouse database (83233 Sequences). Cysteine carbamidomethylation was used as a fixed/mix modification. Other parameters include up to two missed cleavages for trypsin; ±20 ppm and ±50 ppm accuracy for MS and MS/MS measurements respectively. Positive identification required a protein score > 11, peptides with score > 10 and % SPI (Scored Peak Intensity) > 60.

3.3 Results

3.3.1 Cav1 scaffold domains by STED microscopy

As previously reported [87, 265], Cav1 expression in *Mgat5*$^{-/-}$ cells is greatly reduced relative to *Mgat5*$^{+/+}$ cells and in *Mgat5*$^{-/-ESC}$ cells it is eliminated essentially completely. Expression of PTRF/cavin-1 is significantly reduced in both *Mgat5*$^{-/-}$ cell lines (Figure 3.1A); this is consistent with its requirement for caveolae formation [73] but also for stable Cav1 expression [266]. Thus, *Mgat5*$^{+/+}$ cells potentially have caveolae, Cav1 scaffolds and noncaveolar lipid rafts, *Mgat5*$^{-/-}$ cells have Cav1 scaffolds and noncaveolar lipid rafts and *Mgat5*$^{-/-ESC}$ only contain noncaveolar lipid rafts (Figure 3.1B). This is consistent with the hypothesis that the functional noncaveolar, Cav1-positive domains in *Mgat5*$^{-/-}$ cells are different from caveolae in *Mgat5*$^{+/+}$ cells.

Figure 3.1 The Mgat5 cell lines

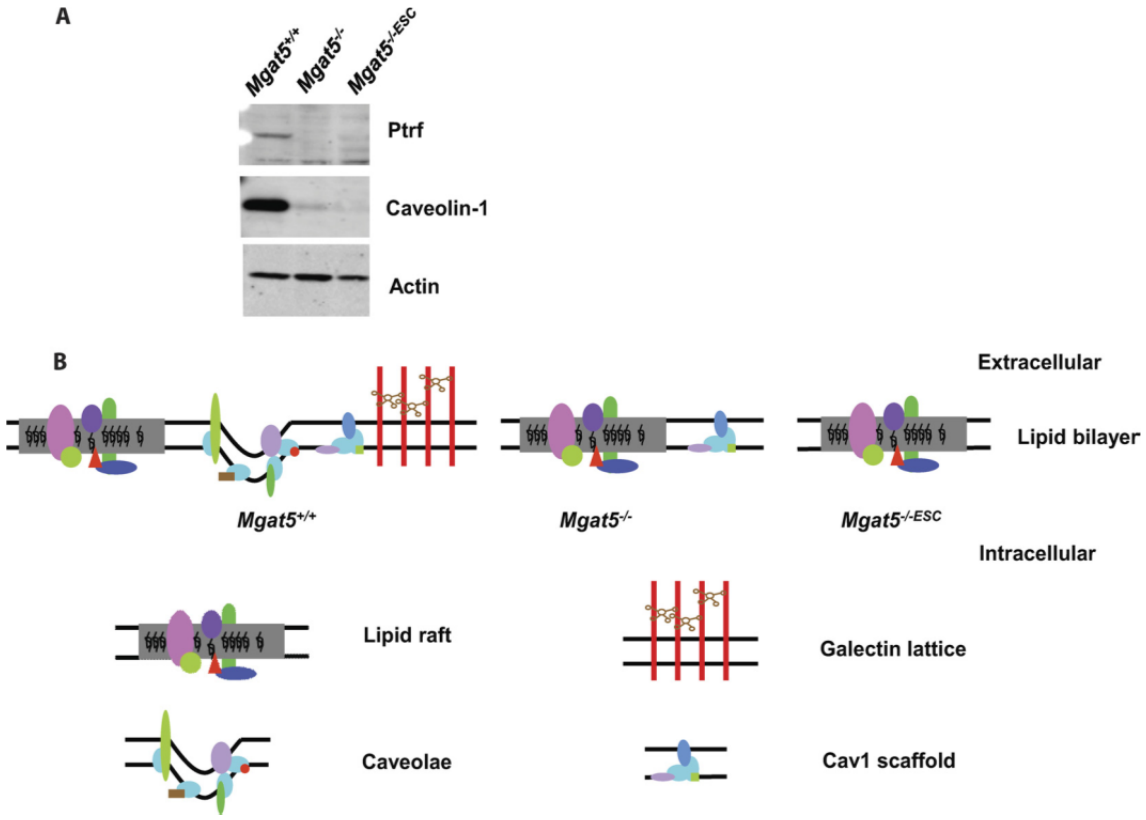

A, Western blot showing the Cav1 and PTRF levels in Mgat5 cells, actin as a loading control. B, Model of *Mgat5*$^{+/+}$, *Mgat5*$^{-/-}$, and *Mgat5*$^{-/-ESC}$ showing noncaveolar lipid raft, caveolae, galectin lattice, and Cav1 scaffold on the plasma membrane.

Indeed, confocal images show that Cav1 is distributed in larger clusters in caveolae-expressing *Mgat5*$^{+/+}$ cells compared with *Mgat5*$^{-/-}$ cells (Figure 3.2A). Super-resolution imaging of Cav1 in *Mgat5*$^{+/+}$ and *Mgat5*$^{-/-}$ cell lines using STED allows us to resolve many more and much smaller-diameter spots than with conventional confocal microscopy (Figure 3.2B and C). This state-of-the-art imaging method did not offer a significant advantage when analyzing *Mgat5*$^{+/+}$ cells as the spot size hovered around the resolution of diffraction-limited microscopy. However, in *Mgat5*$^{-/-}$ cells, STED was able to accurately measure what confocal

could not: average spot size in these cells was 128 ± 10 nm. Of particular interest, Cav1 in *Mgat5*$^{+/+}$ cells presented a highly variable spot size, even in STED images, perhaps because of the presence of both individual caveolae clusters and Cav1 scaffolds. Cav1 spot size in *Mgat5*$^{-/-}$ cells was highly homogeneous. This suggests that Cav1 scaffolds are uniform suboptical resolution domains smaller than and distinct from caveolae.

Figure 3.2 STED and confocal analysis of Cav1 labeled structures in *Mgat5*$^{+/+}$ and *Mgat5*$^{-/-}$ cells

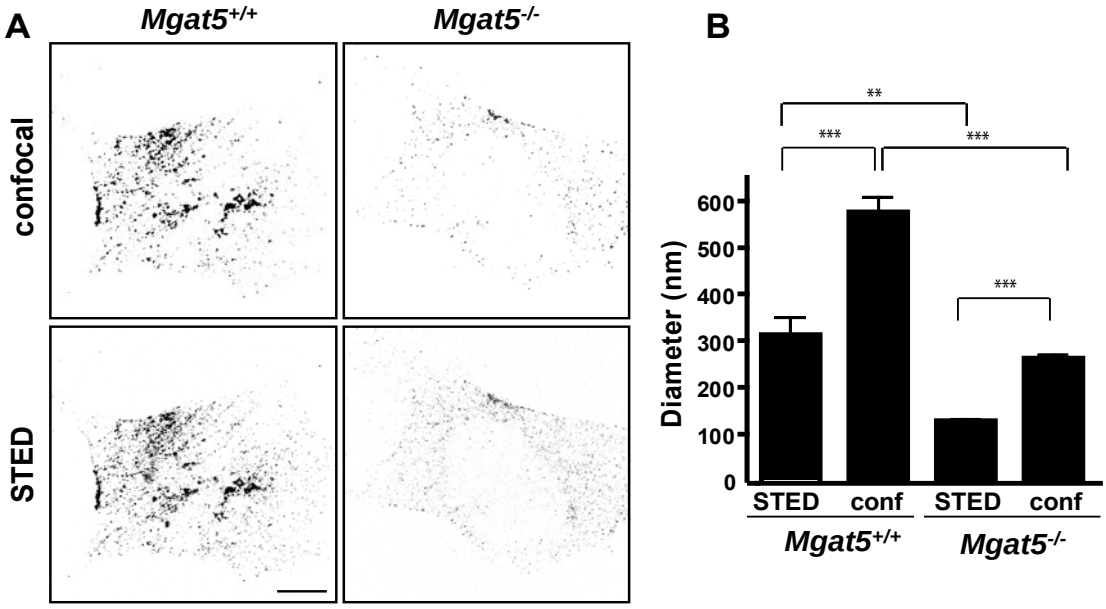

C

	Mgat5$^{+/+}$		Mgat5$^{-/-}$	
	STED	confocal	STED	confocal
# cells	12	12	11	11
Spots/cell	1284	503	712	179
SD	1106	593	291	303
Mean Area (nm²)	88330	269200	12890	54550
SD	67260	102600	1880	9342
Mean Predicted Diameter	313.1	575.9	127.8	262.7
SD	125.7	110.5	9.615	22.28

A, *Mgat5*$^{+/+}$ and *Mgat5*$^{-/-}$ cells were stained for Cav1 and analyzed by confocal and STED microscopy as indicated. Signal dynamic range was adjusted for each STED and confocal image acquisition (gain ~ 800 V for confocal images and ~1000 V for STED images) and images processed using a median filter radius 3 and application of a 30–255 intensity threshold to 8-bit images. Bar: 10 um. B, The mean diameter (±S.E.) of Cav1-positive structures from STED and confocal images for *Mgat5*$^{+/+}$ and *Mgat5*$^{-/-}$ cells was quantified for 11–12 cells from three independent experiments. ** $p < 0.05$, *** $p < 0.005$. C, Quantified data for the diameter of Cav1-positive structures from STED and confocal images is presented in table form.

3.3.2 The DRM proteome of caveolae and Cav1 scaffold expressing cells

As these cell models appear to have distinct caveolar structures, we then turned to mass spectrometry based proteomics to characterize the differential protein composition of DRMs from these cells [267, 37, 268]. *Mgat5*$^{+/+}$ cells were mass encoded with SILAC and then combined with equal masses of protein from light-labeled *Mgat5*$^{-/-}$ or *Mgat5*$^{-/-ESC}$ cells; DRMs were subsequently purified and analyzed by mass spectrometry. A high heavy:light ratio for a protein detected in this scheme would suggest that it is enriched in the *Mgat5*$^{+/+}$ cell DRMs and therefore potentially associated with caveolae (Figure 3.3). To assign a protein as specific to the DRMs of one cell type or another, we opted to use a cut-off set at two population standard deviations away from the mean ($\bar{x} + 2\sigma$) for three or four biological replicates. In a binary comparison of *Mgat5*$^{+/+}$ versus *Mgat5*$^{-/-}$, this yielded 66 proteins specific to *Mgat5*$^{+/+}$ DRMs and 33 proteins specific to *Mgat5*$^{-/-}$ DRMs, out of more than 400 proteins identified. There was also roughly twice the number of proteins identified in *Mgat5*$^{+/+}$ DRMs versus *Mgat5*$^{-/-ESC}$ (100 versus 51 out of 700 total protein identifications) (Figure 3.4). The *Mgat5*$^{+/+}$-specific subset includes Cav1, the raft marker protein flotillin as well as PTRF/cavin-1 and SDPR/cavin-2. Comfortingly, the SILAC ratios validated our immunoblotting (Figure 3.1A), with Cav1 showing very large *Mgat5*$^{+/+}$/*Mgat5*$^{-/-ESC}$ and *Mgat5*$^{+/+}$/*Mgat5*$^{-/-}$ ratios. PTRF/cavin-1 showed a 7:1 *Mgat5*$^{+/+}$/*Mgat5*$^{-/-}$ ratio and very large (>10) *Mgat5*$^{+/+}$/*Mgat5*$^{-/-ESC}$ ratio. These proteomic data confirm the graded expression of Cav1 from *Mgat5*$^{+/+}$/*Mgat5*$^{-/-}$/*Mgat5*$^{-/-ESC}$ cells as well as the elevated expression of PTRF/cavin-1 in *Mgat5*$^{+/+}$ cells relative to both *Mgat5*$^{-/-}$ and *Mgat5*$^{-/-ESC}$ cells.

Figure 3.3 The use of SILAC to determine proteins that are differentially expressed in the detergent-resistant membrane of Mgat5 cells

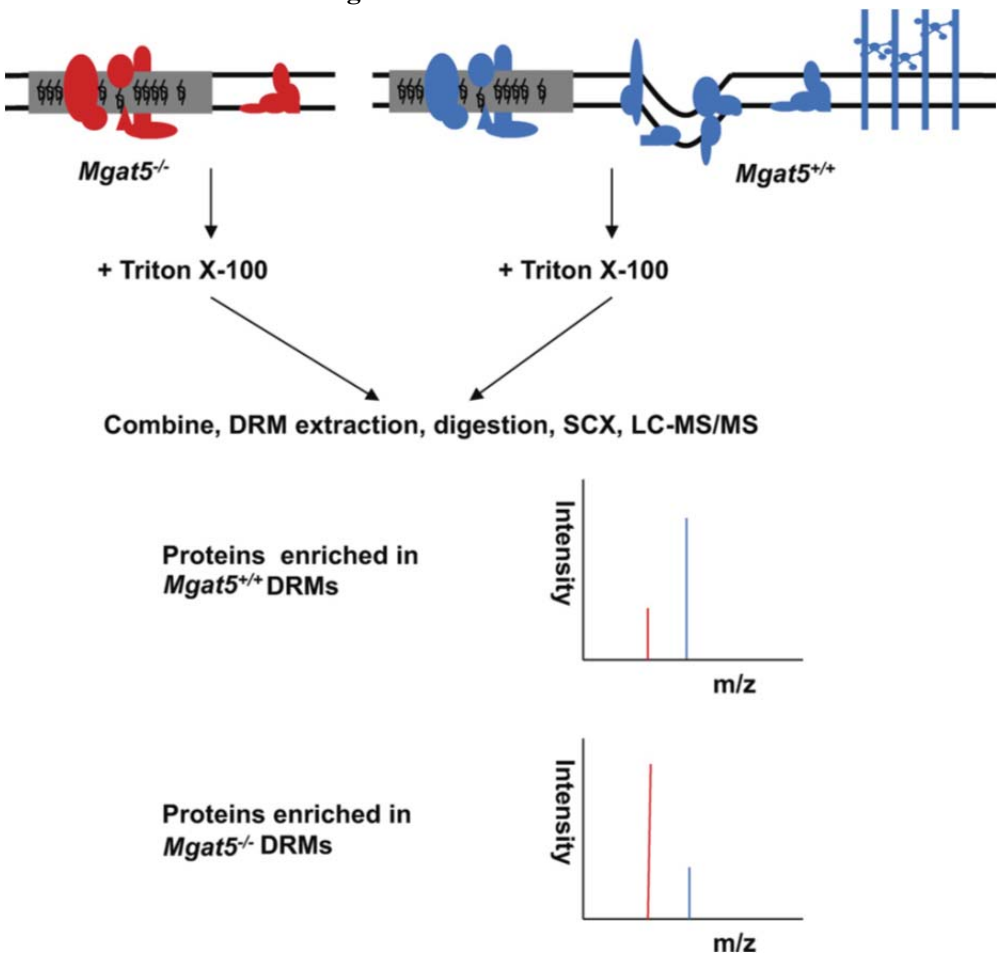

4/6 labeled *Mgat5*$^{+/+}$ cells were compared with 0/0 labeled *Mgat5*$^{-/-}$ or *Mgat5*$^{-/-ESC}$ and 4/6 labeled *Mgat5*$^{-/-}$ with 0/0 labeled *Mgat5*$^{-/-ESC}$. Cell lysates were combined at equal mass prior to DRM extraction. Here, the figure showing an example of *Mgat5*$^{+/+}$ versus *Mgat5*$^{-/-}$. Proteins enriched in *Mgat5*$^{+/+}$ are having relative high ratios and are the caveolae proteins; lower ratio ones are proteins enriched in the *Mgat5*$^{-/-}$ DRMs.

Figure 3.4 Proteins enriched in DRMs or membrane rafts of each of the Mgat5 cells tested and compared

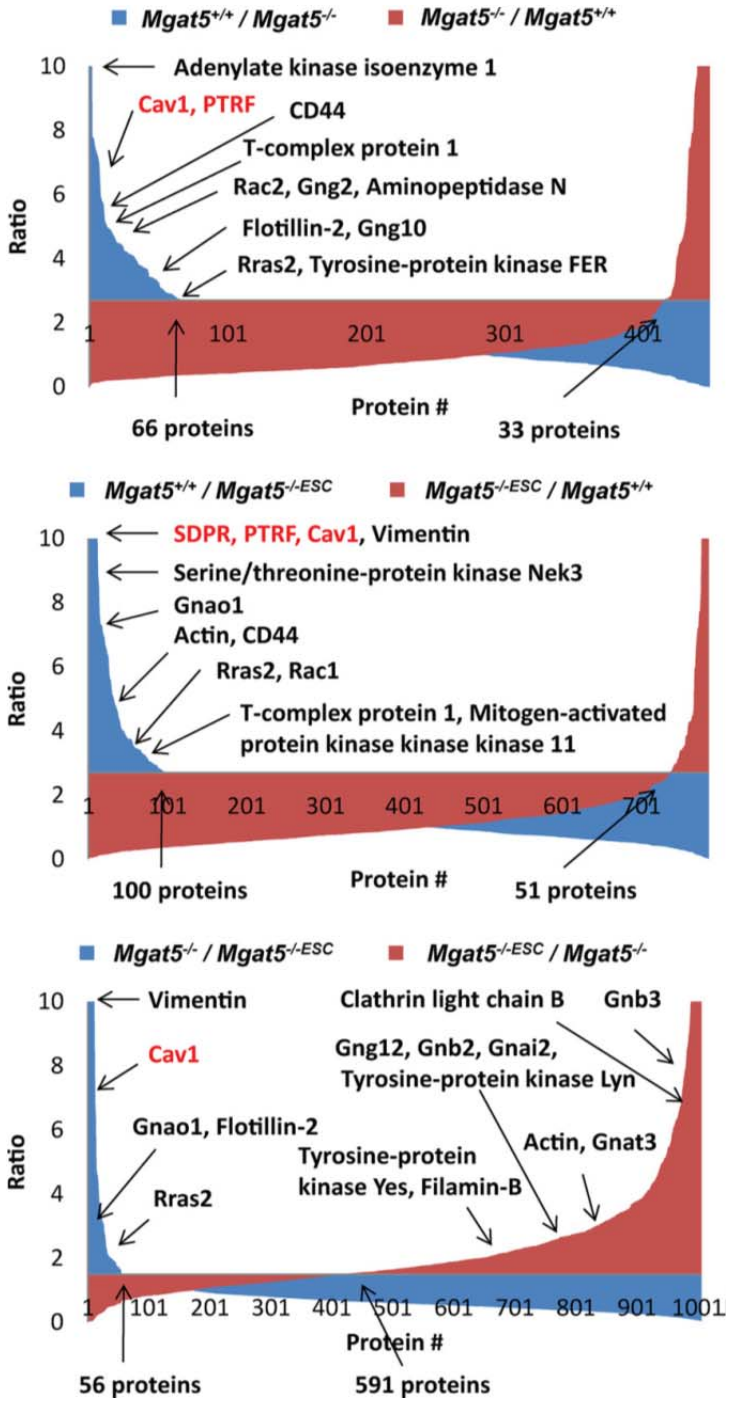

Proteins identified and quantified in each of the comparisons were sorted in decreasing ratio. for *Mgat5*$^{+/+}$ versus *Mgat5*$^{-/-}$ and *Mgat5*$^{+/+}$ versus *Mgat5*$^{-/-ESC}$ was 2.7 and for Mgat5$^{-/-}$ versus *Mgat5*$^{-/-ESC}$ was 1.5.

Ingenuity Pathways Analysis showed that the proteins enriched in *Mgat5*$^{+/+}$ relative to either *Mgat5*$^{-/-}$ or *Mgat5*$^{-/-ESC}$ cells were highly relevant to cellular movement and morphology, cellular assembly and organization and cell signaling (Figure A.3). Supporting this analysis, common proteins enriched in *Mgat5*$^{+/+}$ relative to either *Mgat5*$^{-/-}$ or *Mgat5*$^{-/-ESC}$ cells include Actin, Cav1, Flotillin, Rac, R-Ras, CD44, Aminopeptidase N and several heterotrimeric G-protein subunits (Table 3.1). The very high enrichment of heterotrimeric G-proteins suggests that their localization in DRMs depends on caveolae formation and that loss of caveolae results in reduction of this class of proteins from membrane rafts. In order to orthogonally validate the specificity of proteins identified in the SILAC/Mgat5 data, we used a label-free mass spectrometry approach to compare DRMs from WT and caveolin-1 knock out (*Cav1*$^{-/-}$) mouse embryonic fibroblasts (MEFs); reassuringly, there was at least 30% overlap between the caveolae-specific proteins identified between the two methods, which differed in both the cell type and analytical approach.

Table 3.1 Heterotrimeric G protein enrichment in proteomic analyses

Mgat5$^{+/+}$ vs. *Mgat5*$^{-/-}$		*Mgat5*$^{+/+}$ vs. *Mgat5*$^{-/-ESC}$		*Mgat5*$^{-/-ESC}$ vs. *Mgat5*$^{-/-}$		Quantitative CoIP		Non treated vs. MβCD treated *Mgat5*$^{+/+}$		MEF WT/ Cav$^{-/-}$
Names	**Ratios**	**Names**	**Ratios**	**Names**	**Ratios**	**Names**	**Ratios**	**Names**	**Ratios**	**Names**
Gng2[1]	4.48	Gnao1	7.33	Gnb3	7.28	Gng12	7.12	Gnat3	10.09	Gng10
Gnb4	3.85	Gnaq	2.76	Gng10	6.08	Gnb2l1	1.78	Gnb3	6.51	Gnai2
Gnaq	3.69	Gng2	2.51	Gng2	4.96	Gnai2	0.75	Gnb4	6.02	Gnb1
Gna13	3.42	Gna13	2.15	Gnb4	2.9	Gnb2	0.72	Gna11	4.35	
Gng10	3.36	Gna11	2.14	Gnb1	2.89	Gnb1	0.66	Gnai2	4.03	
Gnao1	2.99	Gnb3	1.96	Gnat3	2.7			Gnb2	4.02	
Gnai2	2.95	Gnb4	1.88	Gnai1	2.65			Gnaq	3.96	
Gnb2	2.91	Gnb2	1.84	Gna11	2.58			Gnai3	3.96	
Gng12	2.82	Gng12	1.68	Gnai3	2.5			Gng10	3.43	
Gnb1	2.47	Gnb1	1.62	Gna13	2.41			Gnb1	3.27	
Gnai3	1.91	Gnai2	1.51	Gnas-1	2.39			Gnas-1	3.16	
Gng5	1.68	Gng5	1.25	Gng12	2.38			Gna13	2.98	
Gna11	1.48	Gnai3	1.2	Gnai2	2.37			Gnas-3	2.91	
		Gnas-1	0.8	Gnb2	2.37			Gng12	2.73	
		Gng10	0.62	Gnb2l1	2.16			Gng5	2.71	
		Gnat3	0.62	Gnaq	1.97			Gnao1	2.45	
		Gnai1	0.61	Gng5	1.63			Gnb2l1	1.73	
				Gng7	0.74			Gng2	1.72	
				Gnao1	0.32					

[1] Shading in cells indicates which proteins satisfied the $\bar{x} + 2\sigma$ requirement for enrichment.

To validate the distribution of heterotrimeric G-proteins in and out of rafts and caveolae, we determined the extent of colocalization of Gαs-GFP with the GM1-ganglioside binding raft marker CT-b and with Cav1. Gαs-GFP shows increased colocalization with CT-b in *Mgat5*$^{+/+}$ cells relative to *Mgat5*$^{-/-}$ or *Mgat5*$^{-/-ESC}$ cells. It also shows increased colocalization with Cav1 on *Mgat5*$^{+/+}$ cells relative to *Mgat5*$^{-/-}$ (Figure 3.5). We further assessed surface Gαs-GFP expression in the cell lines and its response to β-adrenergic receptor activation with isoproterenol (Figure 3.6). Consistent with its elevated raft expression in *Mgat5*$^{+/+}$ and *Mgat5*$^{-/-ESC}$ cells, Gαs-GFP showed increased surface distribution in these cells relative to *Mgat5*$^{-/-}$ cells. Upon treatment with isoproterenol, surface expression in *Mgat5*$^{+/+}$ cells was lost and, importantly, partially colocalized with CT-b in internal vesicles, as previously reported [269]. This validates the increased expression of heterotrimeric G-proteins seen in the DRM proteomic analysis and suggests that caveolae expression promotes recruitment of heterotrimeric G-proteins to both caveolar and noncaveolar raft domains.

Figure 3.5 Increased colocalization of Gαs-GFP with Cholera Toxin b and Cav1 in *Mgat5*$^{+/+}$ cells

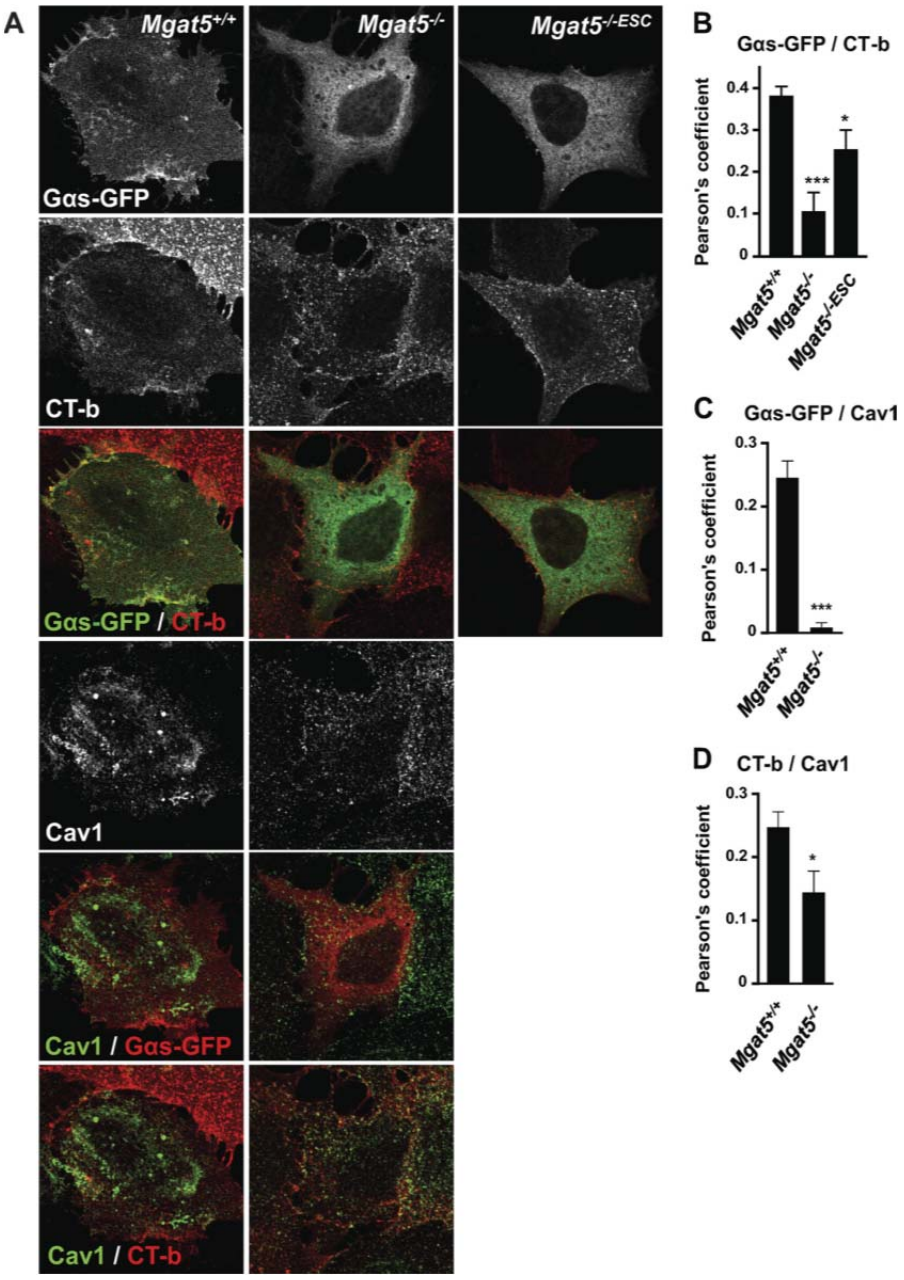

A, *Mgat5*$^{+/+}$, *Mgat5*$^{-/-}$ and *Mgat5*$^{-/-ESC}$ cells were transfected with Gαs-GFP and incubated with Alexa-546 coupled-CT-b before staining for Cav1. Pearson's coefficient revealed the level of colocalization between Gαs-GFP and CT-b (B), Gαs- GFP and Cav1 (C) and Cav1 and CT-b (D). Pearson's colocalization coefficients for Gαs-GFP and CT-b colocalization are shown for *Mgat5*$^{+/+}$, *Mgat5*$^{-/-}$, and *Mgat5*$^{-/-ESC}$ cells and colocalization with Cav1 for *Mgat5*$^{+/+}$, and *Mgat5*$^{-/-}$ cells. Graphs represent 10–18 cells from one representative experiment over four independent experiments. * $p < 0.05$, *** $p < 0.005$. Bar: 10 um.

Figure 3.6 Gαs-GFP is internalized upon activation with isoproterenol in *Mgat5*$^{+/+}$ and *Mgat5*$^{-/-ESC}$ cells

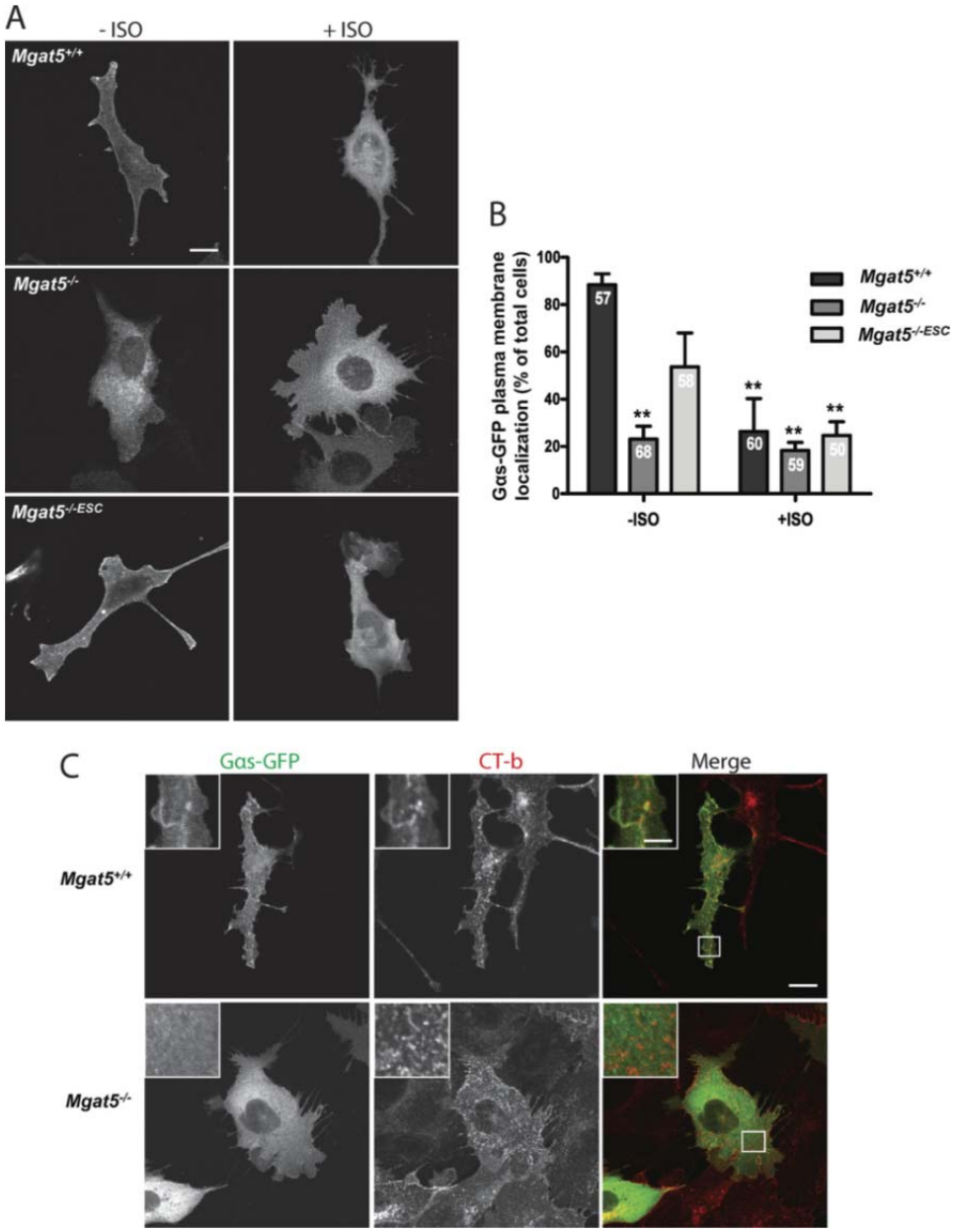

A, *Mgat5*$^{+/+}$, *Mgat5*$^{-/-}$, and *Mgat5*$^{-/-ESC}$ cells were transfected with Gαs-GFP and incubated with 10 uM isoproterenol (ISO) for 15 min at 37 °C. Representative images of Gαs-GFP in the three cell lines are shown. B, Gαs-GFP expressing cells were scored based on Gαs-GFP plasma membrane expression in the presence and absence of isoproterenol treatment. The total number of cells counted from three independent experiments is shown for each condition (within columns). ** $p < 0.01$ compared with *Mgat5*$^{+/+}$ without isoproterenol. Bar: 10 uM. C, *Mgat5*$^{+/+}$ and *Mgat5*$^{-/-}$ cells were transfected with Gαs-GFP and incubated with Alexa-546 coupled-CT-b at 4 °C for 20 min. Next, DMEM containing 10 uM isoproterenol was added to the cells for 15 min at 37 °C before fixation with PFA. Confocal images of Gαs-GFP (green) and Ct-b (red) are shown. Bar: 10 uM, zoom bar: 3 uM.

A dramatic bias was observed in the *Mgat5*$^{-/-}$ versus *Mgat5*$^{-/-ESC}$, with almost 600 proteins expressed dominantly in the *Mgat5*$^{-/-ESC}$ cell rafts and only 56 in *Mgat5*$^{-/-}$ (Figure 3.4). This suggests that whereas caveolar Cav1 expression recruits proteins to rafts, noncaveolar Cav1, or Cav1 scaffolds, restricts the DRM proteome. Indeed, Gαs-GFP association with CT-b-labeled rafts was increased in *Mgat5*$^{-/-ESC}$ cells relative to *Mgat5*$^{-/-}$ cells (Figure 3.5). Supported by the proteomics data, 17 out of the 19 heterotrimeric G-proteins identified in *Mgat5*$^{-/-}$ versus *Mgat5*$^{-/-ESC}$ meet the $\bar{x} + 2\sigma$ criteria and are therefore enriched in the *Mgat5*$^{-/-ESC}$ DRMs (Figure 3.4 and Table 3.1). Moreover, many of the proteins (e.g. Actin, Filamin-B, Tyrosine kinase Yes) enriched in the caveolae-containing *Mgat5*$^{+/+}$ DRMs were also identified with high ratios here, meaning they are restored in the *Mgat5*$^{-/-ESC}$ DRM when there is no Cav1 expression in the cell. Ingenuity Pathways Analysis showed that *Mgat5*$^{-/-ESC}$ DRMs are enriched in proteins involved in signaling, growth, assembly and cell movement as well as proteins related to cancer and cell death (Figure A.3). That we were only able to detect 33 proteins enriched in the *Mgat5*$^{-/-}$ DRM proteome versus *Mgat5*$^{+/+}$ and 57 versus *Mgat5*$^{-/-ESC}$ cells suggests that Cav1 scaffolds interact with a narrower set of proteins than whole caveolae. The dramatic enrichment of DRM proteins in *Mgat5*$^{-/-ESC}$ cells, in which loss of Cav1 scaffolds restores EGF signaling and CT-b movement and endocytosis [87, 265], suggests that Cav1 may indirectly regulate raft composition.

3.3.3 Galectin lattice regulation of raft composition

Mgat5$^{-/-}$ or *Mgat5*$^{-/-ESC}$ were lack of lattice compared to *Mgat5*$^{+/+}$ beside caveolae. To specifically determine whether the galectin lattice affects raft protein composition, we

performed quantitative proteomic analysis of DRM from untreated *Mgat5*$^{+/+}$ cells and cells treated with lactose or sucrose (Figure A.4). The raft association of the vast majority of the more than 700 proteins detected was not significantly affected by disruption of the galectin lattice with lactose (Figure 3.7A) and overall protein abundance ratios were highly similar for both lactose vs. sucrose and lactose vs. untreated samples (Figure 3.7B). 181 proteins accumulated in rafts upon disruption of the galectin lattice for lactose versus control and 66 for lactose versus sucrose, while only 4 proteins were displaced from rafts by lactose treatment for either condition (Figure 3.7C). Proteins whose raft association increased upon disruption of the galectin lattice included Src (isoform 2), protein kinase Yes and the β-Adrenergic receptor 2a (Figure 3.7A), suggesting that the raft localization of signaling proteins is affected by the galectin lattice. Indeed, disruption of the galectin lattice in *Mgat5*$^{+/+}$ results in accumulation of many proteins in DRMs, so galectin lattice opposes entry of many proteins into DRMs.

Figure 3.7 Galectin lattice limits protein accumulation in rafts

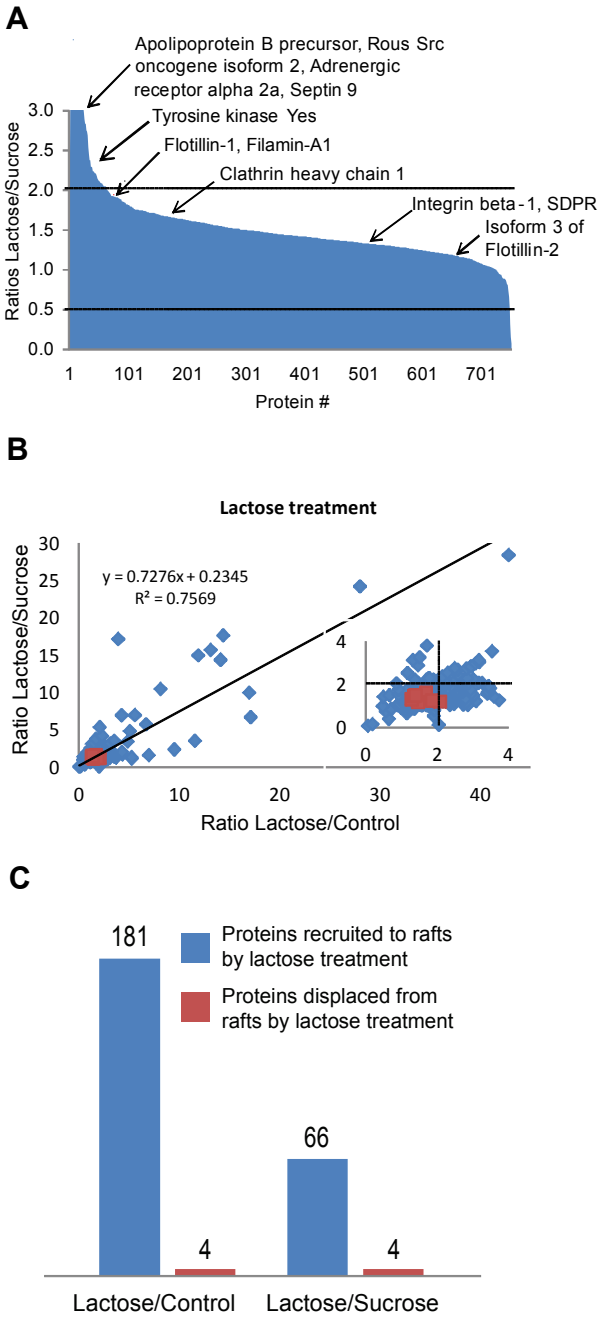

A. Graphical representation of all proteins identified in the proteomics study with decreasing ratios of lactose/sucrose. Some examples of proteins are indicated. B. Protein ratios of lactose/sucrose plotted over lactose/control show the high correlation between the two. Red dots are cadherin and catenin. C. Number of proteins recruited to and displaced from rafts upon lactose treatment show that lattice formation predominantly prevents protein accumulation in rafts.

3.3.4 Cav1 and cholesterol-dependence of the caveolar DRM proteome

To complement the subcellular fractionation approach above, we also immunoisolated Cav1-containing structures from DRMs of *Mgat5*$^{+/+}$ cells and quantitatively compared the composition of this preparation versus a nonspecific IgG control using SILAC (Figure 3.8A and B). Of more than 400 proteins identified and quantified from four independent experiments, 94 proteins exceeded $\bar{x} + 2\sigma$; these include Cav1 and Cav2 with the highest ratios and most peptides identified, PTRF/cavin-1, heterotrimeric G-proteins, filamin, and actin (Figure 3.8C). Among the 94 Cav1-associated proteins, eight of them were also identified to be caveolae associated in the *Mgat5*$^{+/+}$ versus *Mgat5*$^{-/-}$ and *Mgat5*$^{+/+}$ versus *Mgat5*$^{-/-ESC}$ comparisons (148 caveolae proteins identified in total, either present in *Mgat5*$^{+/+}$ versus *Mgat5*$^{-/-}$ and/or *Mgat5*$^{+/+}$ versus *Mgat5*$^{-/-ESC}$) (Figure 3.9A), meaning some of the DRM-associated proteins in caveolae-expressing cells associate with Cav1. The presence of heterotrimeric G-protein subunits and other signaling proteins supports the role of caveolae formation in the recruitment of these proteins to lipid rafts by Cav1 but also suggests that raft association of G proteins may occur independently of Cav1 and caveolae (Table 3.1).

Figure 3.8 Co-immunoprecipitation of caveolin-1 associated proteins in *Mgat5*$^{+/+}$ DRMs

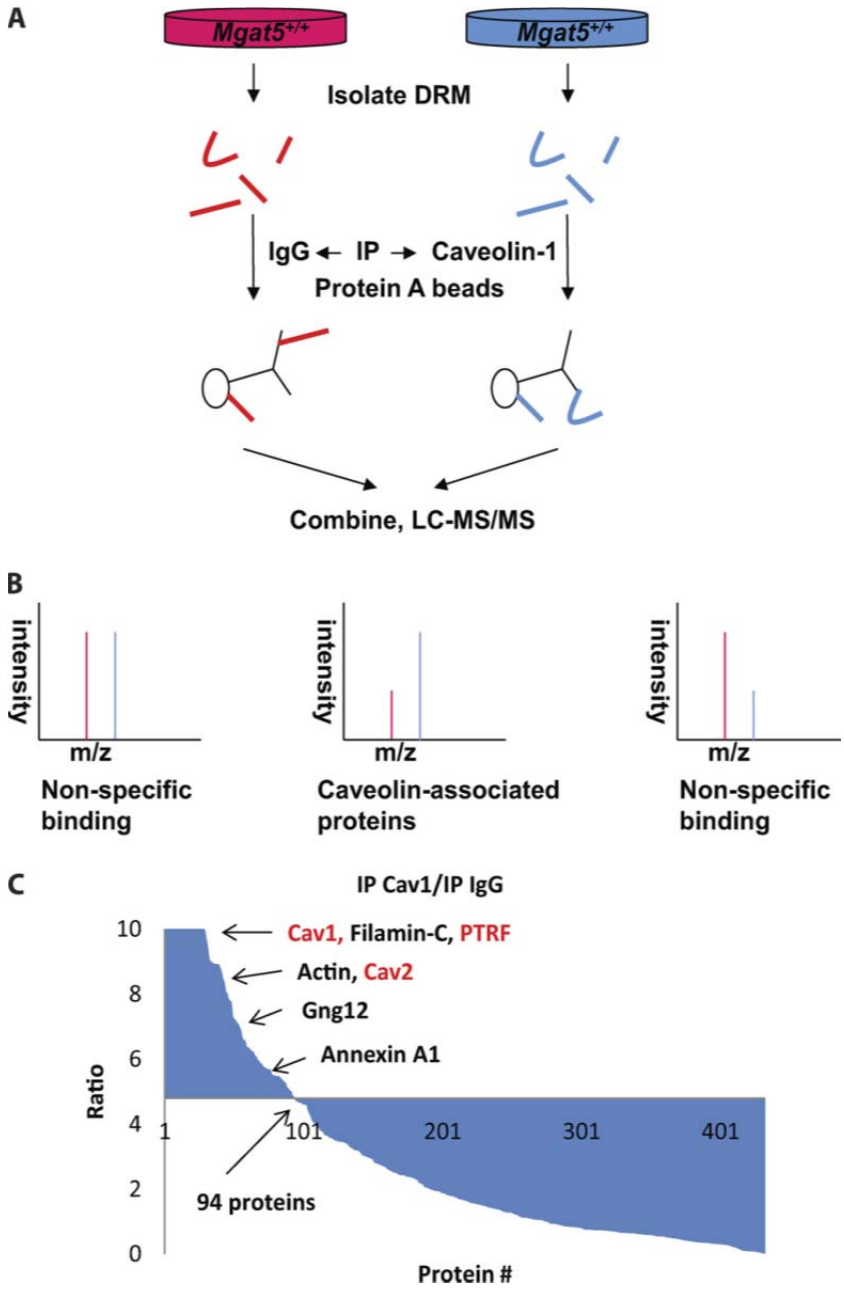

A, *Mgat5*$^{+/+}$ cells were labeled 0/0 and 4/6 and then DRMs were extracted from the two separately. 0/0 DRMs were IP with nonspecific IgG and 4/6 with caveolin-1 antibody. Finally, the two pull-downs were combined as one sample. B, Spectra of caveolin-1 associated proteins are ones with high ratios and nonspecific binding partners are having low ratios or relative equal ratios. C, Result of the quantitative co-IP experiment showing ratios in decreasing order over protein numbers. = 4.8.

Figure 3.9 Overlap of protein identifications

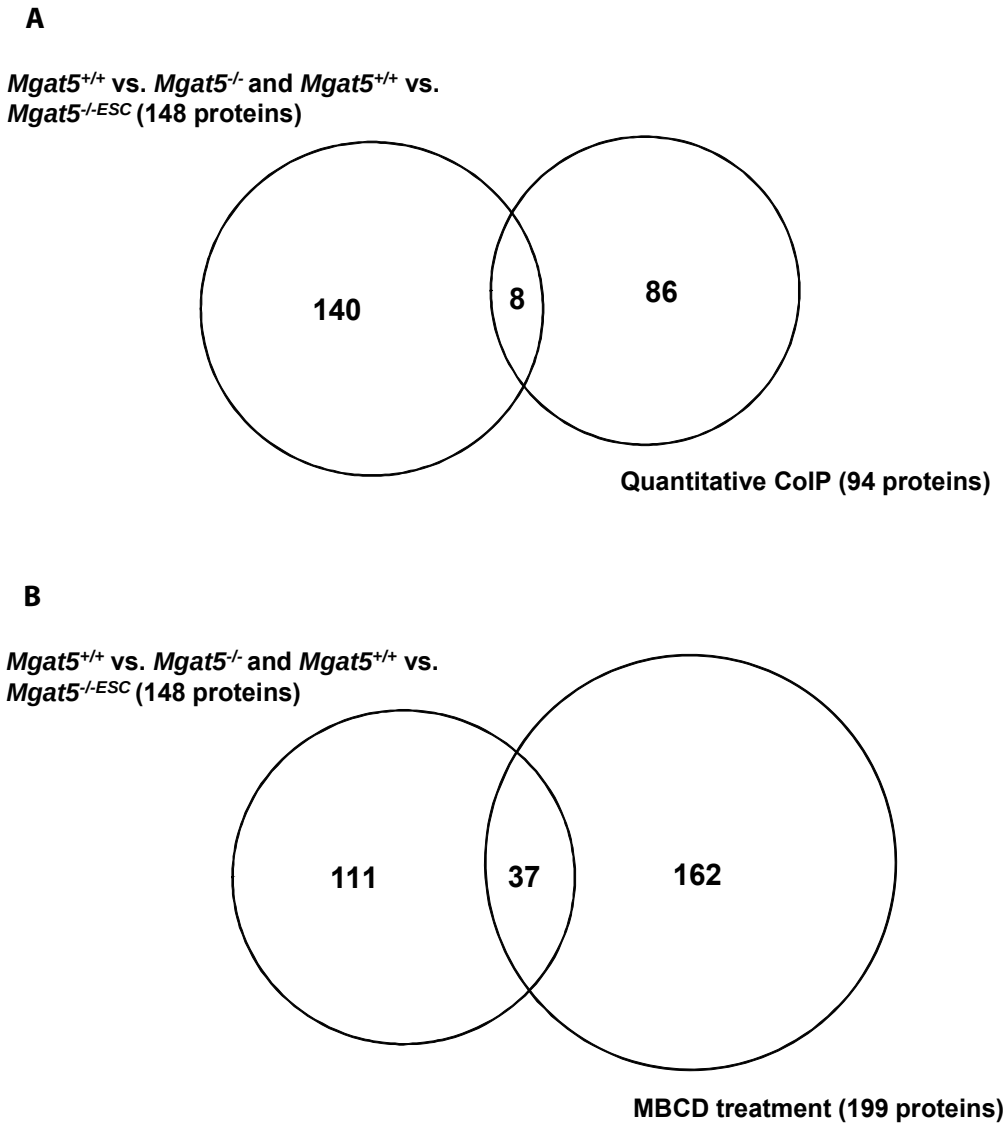

A, Proteins identified to be enriched in *Mgat5*$^{+/+}$ rafts relative to *Mgat5*$^{-/-}$ or *Mgat5*$^{-/-ESC}$ were compared with proteins identified to be associated with protein caveolin-1 in the quantitative co-IP experiment. B, Proteins identified to be enriched in *Mgat5*$^{+/+}$ rafts relative to *Mgat5*$^{-/-}$ or *Mgat5*$^{-/-ESC}$ were compared with proteins showed to be sensitive to MβCD treatment.

In order to test how many of the caveolae proteins identified are actually components of lipid rafts or raft-dependent proteins, we next measured the cholesterol-dependence of the caveolae proteins identified here [37]. Three biological replicates of DRM analyses from MβCD-treated versus untreated *Mgat5*$^{+/+}$ cells identified more than 1000 proteins with nontreated and treated ratios ranging from over 10 to less than 1. Of the 199 proteins depleted by MβCD, 37 of them were previously identified as caveolae proteins from the DRM comparison experiments (Figure 3.9B) and 47 are in caveolae and/or Cav1-associated, when taking into account the Cav1 immunoisolating experiments. Consistent with the raft enrichment of heterotrimeric G-proteins in *Mgat5*$^{+/+}$ cells, all 18 heterotrimeric G-protein subunits identified have high ratios, indicative of their cholesterol-dependent raft localization (Table 3.1). Similarly, other signaling proteins (e.g. tyrosine kinase Fyn and Yes, R-Ras) and vimentin and filamin were strongly affected by MβCD, consistent with a previous study [38] (Figure 3.10).

Figure 3.10 MβCD treatment for identifying cholesterol sensitive lipid raft proteins in *Mgat5*$^{+/+}$

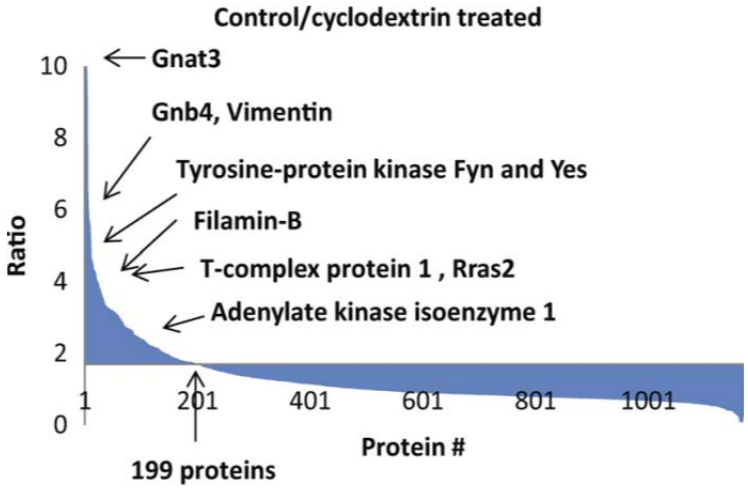

Results showing the ranking of proteins' sensitivity toward MβCD treatment over protein numbers. = 1.7.

3.4 Discussion

Rafts have fascinated cell biologists for over twenty years and proteomicists for almost half that time. Although it is clear that multiple distinct classes of rafts exist, as opposed to a continuum of sizes and compositions, it is equally clear that existing biochemical methods are insufficient to tease apart these subtleties. Cav1 is a critical regulator of raft domains and here we have taken advantage of the distinct states of caveolin and caveolae in a series of cell lines derived from wild-type and *Mgat5*$^{-/-}$ mammary tumors to identify how caveolar and noncaveolar Cav1 impact on the protein composition of detergent-resistant membranes in cells. To our knowledge, all previous biochemical preparations of rafts and/or caveolae have contained nonraft contaminants that complicate any interpretation of the data without resorting to biased selection of "real" raft proteins [232]. Two recent studies have used *Cav1*$^{-/-}$ cells [267, 73] to identify some of the proteins in caveolae but other

than Cav1 itself and members of the cavin family of proteins, none of the other reported proteins seem likely to be functional components of caveolae. Beyond simply extending the catalogue of caveolar proteins, our identification here of many signaling proteins in DRMs reinforces the role of rafts as cellular signaling platforms and reveals that caveolae and rafts seem to be particularly enriched for heterotrimeric G protein subunits.

In a similar fashion to the data presented here (Figure 3.5 and 3.6), Cav1 knockdown in C6 glioma cells reduces Gαs association with lipid rafts and reduces Gαs-GFP internalization in response to β-adrenergic receptor activation with isoproterenol [269]. Our results further suggest that Cav1 expression independently of caveolae, i.e. Cav1 scaffolds, is particularly associated with reduced lipid raft association of G proteins. Cav1 regulation of GPCR and G protein signaling therefore appears to be associated not just with Cav1 expression but also by the relative expression of caveolae and Cav1 scaffolds. Reduced expression of Cav1 and of PTRF, as shown here in *Mgat5*$^{-/-}$ cells, will result in Cav1 scaffold expression. However, impairment of endothelial VEGF signaling by transgenic expression of Cav1 independently of increased caveolae [270] suggests that caveolae and Cav1 scaffolds can co-exist and function independently in the same cell to regulate signaling. Indeed, the extent to which caveolin-cavin expression and stoichiometry impacts on relative expression of caveolae, Cav1 scaffolds and noncaveolar lipid rafts and their regulation of signaling pathways, including but not limited to G proteins, remains to be determined.

Intriguingly, our data also suggest that caveolin expression is not the only determinant of protein composition of caveolar domains, which is in agreement with other reports that cavin proteins also play a major role in caveolae formation [74, 75, 73, 76]. In *Mgat5*$^{-/-}$ cells where Cav1 is found at the cell surface but where caveolae do not form, more

than twice as many proteins come out of DRMs as go in, indicating that the caveolae structure itself has a dramatic impact on caveolae and membrane raft composition. This is consistent with STED measurements suggesting that the Cav1 scaffolds at the membrane of these cells exist as much smaller domains than whole caveolae in wild-type cells. Minimal Cav1 oligomers have been reported to consist of ~15 Cav1 monomers whereas caveolae have been proposed to contain ~144 Cav1 molecules [65, 271]. Although we cannot predict the precise size of Cav1 scaffolds, the highly homogeneous and reduced size of Cav1 staining in *Mgat5*$^{-/-}$ cells lacking caveolae suggests that Cav1 scaffolds might correspond to minimal Cav1 oligomers that subsequently combine to form caveolae. The fact that Cav1 scaffolds restrict the raft proteome to a greater extent than caveolae suggests that recruitment to caveolae impacts on Cav1 interaction with proteins and its regulation of raft domains.

Our data allow us to resolve one class of rafts, i.e. caveolae, away from the others found in DRMs and demonstrate the existence of distinct Cav1-associated subtypes. Because the set of proteins enriched in Cav1 IPs and the set impacted by *Mgat5*$^{-/-}$ or *Mgat5*$^{-/-ESC}$ cells (Figure 3.4 versus Figure 3.8) do not completely overlap, it suggests that the proteins that copurify with Cav1 but that are not affected by caveolae disruption may represent a subclass of Cav1 domains distinct from classical caveolae. At the same time, however, the immunoisolation of Cav1-containing structures has some caveats. Although we tried to enrich membranes before detergent extraction and subsequent Cav1 immunoisolation, some typically nuclear and cytosolic proteins clearly remain: whether this reflects the real composition of Cav1-containing structures or simply copurifying contaminants will require more study. As a general comment, we have found that it can be very difficult to obtain sufficient enrichment of the desired targets when immunoisolating membranes from

detergent solubilized cells. Immunoisolation is used frequently and effectively to enrich vesicles and other membrane-bound organelles so we suspect that the presence of detergents and the associated micelles result in more nonspecific interactions.

Using a panel of cell types with varying caveolae statuses, as well as subdiffraction limit microscopy and conventional confocal microscopy, we show that caveolae and Cav1 scaffolds differ in size and impact differently on the protein composition of lipid raft domains. Together with noncaveolar raft domains, these therefore represent functionally distinct subtypes of lipid rafts. Differential raft protein composition in Cav1 scaffold expressing *Mgat5*$^{-/-}$ cells argues that both Cav1 and its cavin-dependent ability to form caveolae impact on raft composition and function defining novel biological roles for caveolae.

4 Temporal changes in host cell surface and internal rafts upon *Salmonella* infection by SILAC

4.1 Introduction

Salmonella is a life threatening facultative intracellular bacterium that invades many cell types and causes millions of human and animal deaths every year. Upon infection, *Salmonella* attaches to the surface of cells, secreting effector proteins into the host through a type III secretion system (T3SS) encoded on *Salmonella* pathogenicity island 1 (SPI-1) and these effectors facilitate the bacteria's internalization into the host cell [170]. The bacteria then stays in a membrane bound compartment termed *Salmonella* containing vacuole (SCV). Once in SCVs, another T3SS encoded on the *Salmonella* pathogenicity island 2 (SPI-2) secretes a different set of effector proteins that guide maturation of SCV, allowing the bacteria to replicate and eventually escape the host cell [175]. Many host cell signaling events are triggered by dozens of effector proteins secreted into the host at different times during the infection process.

Salmonella targets host cells not randomly but through lipid rafts [177]. The specific receptor *Salmonella* uses is not known but *Salmonella* could be attaching to rafts in order to use them as a signaling platform for inducing the rearrangement of the cytoskeleton, which leads to membrane ruffling and eventually results in the bacteria becoming internalized. Disrupting rafts by depleting membrane cholesterol blocked the *Salmonella* uptake but not the attachment to the host [178]. The translocon protein SipB encoded by SPI-1 is a cholesterol binding protein that is responsible for translocating effectors to the host cytosol [181]. *Salmonella* does not only depend on cell surface cholesterol, intracellular cholesterol

is also required once *Salmonella* enters the host. The amount of intracellular cholesterol increases as the SCV forms and matures [184]. The accumulated cholesterol at the bacteria entry site is retained by the SCVs and raft localization on the SCVs might be important for its subsequent fate; e.g., it could prevent their eventual fusion with degradative lysosomes [102]. Two recent studies have demonstrated the involvement of caveolin-1 during *Salmonella* internalization [183, 182], so it would appear that *Salmonella* target this particular subdomain of rafts. Interestingly, both membrane cholesterol and caveolin levels are proportional to the rate of *Salmonella* uptake.

Quantitative proteomics techniques have identified how the raft proteome changes upon T cell activation [53], how the Golgi proteome changes after *Salmonella* infection [272] and the host interacting partners of SPI-2 effectors [273]. That *Salmonella* use lipid rafts/caveolae for entering cells is mainly supported by measurements of membrane cholesterol, no study has directly examined the changes that rafts/caveolae undergo upon infection. In this study, we applied SILAC to examine the proteome changes in rafts/caveolae at several points during early invasion through to SCV maturation and bacteria replication. During this time the raft proteome is highly dynamic, with dozens of proteins coming into or leaving rafts at least once. One protein in particular that is recruited to rafts is caveolin-1, seemingly confirming the role of this protein in *Salmonella*'s entrance into its host through caveolae-mediated endocytosis [183, 182]. Other novel raft proteins that may be responsible for *Salmonella* invasion and intracellular survival were also identified, opening up many avenues for future functional studies.

4.2 Experimental procedures

4.2.1 Material sources and *Salmonella* strains

The following materials were obtained from the indicated commercial sources: Dulbecco's Modified Eagle's Medium (DMEM), L-glutamine, penicillin/streptomycin, gentamicin, normal goat serum (NGS), BCA assay kit and cell culture trypsin (ThermoFisher, Nepean, Ontario, Canada); Fetal bovine serum (FBS, both qualified and dialyzed forms), Alexa anti-rabbit 488 and Alexa anti-mouse 568 coupled secondary antibodies, DAPI Nucleic Acid Stain, ProLong Gold antifade reagent and Lipofectamine 2000 (Invitrogen, Burlington, Ontario, Canada); L-Lys- and L-Arg-deficient DMEM (Caisson Labs, North Ogden, UT); L-Lys, L-Arg, methyl-β-cyclodextrin (MβCD), Triton X-100 (Tx-100), sodium deoxycholate (SDC), dithiothreitol, iodoacetamide, filipin III, calcium phosphate ($CaCl_2$) (Sigma-Aldrich, St.Louis, MO); $^{2}H_4$-lysine, $^{13}C_6$-arginine, $^{13}C_6{}^{15}N_2$-lysine, and $^{13}C_6{}^{15}N_4$-arginine (Cambridge Isotope Laboratories, Cambridge, MA); Sequencing grade modified porcine trypsin (Promega, Madison, WI); Protease inhibitor mixture tablets with EDTA (Roche Diagnostics, Mannheim, Germany); Coomassie Plus kit (Pierce, Nepean, Ontario, Canada). Nuclear-ID Red DNA Stain (Enzo Life Sciences, Plymouth Meeting, PA); Paraformaldehyde (PFA) (Canemco Marivac Supplies, Canton de Gore, Quebec, Canada); siRNA used are: ON-TARGETplus SMARTpool - Human CAV1 and ON-TARGETplus non-targeting pool (Dharmacon, Lafayette, CO); Antibodies used and their sources were as follows: rabbit α-caveolin-1 (Santa Cruz Technology, Santa Cruz, CA), Mab to *Salmonella* (Meridian Life science, Memphis, TN). The cell line used here is HeLa, obtained from the American Type Culture Collection (Manassas, VA). The S*almonella* strain used is in this

study is wild type *S.* Typhimurium SL1344, *S.* Typhimurium SL1344 ($_P$FPV25.1 GFP) and *S.* Typhimurium SL1344 ($_P$BR-RFP.1).

4.2.2 Cell culture, SILAC and *Salmonella* infection

HeLa cells were triple SILAC labeled as in section 2.2.2. We refer to the different labels as 0/0 for the normal isotopic abundance Lys and Arg, 4/6 for $^{2}H_4$-Lys and $^{13}C_6$-Arg, and 8/10 for $^{13}C_6{}^{15}N_2$-Lys and $^{13}C_6{}^{15}N_4$-Arg. To obtain enough material for effective proteomic analysis, five 15 cm plates of 70 – 80% confluent HeLa cells were used for *Salmonella* infection for each SILAC condition.

2 h before *Salmonella* infection, HeLa cells growing in normal SILAC medium were changed to antibiotic free SILAC medium. Overnight *Salmonella* culture of wild type *S.* Typhimurium SL1344 or *S.* Typhimurium SL1344 ($_P$FPV25.1 GFP) or *S.* Typhimurium SL1344 ($_P$BR-RFP.1) were subcultured 1:33 in LB broth for 3 h to reach the log phase. Then the bacteria was pelleted at 10,000 g for 2 min, resuspended in antibiotic free medium and infecting HeLa cells at multiplicity of infection (MOI) equal to 100 unless otherwise indicated and incubated at 37°C and 5% CO_2 for different times. In some cases like long infection (6, 8 and 16 h), *Salmonella* were infected for 20 min, followed by replacing with antibiotic free SILAC medium with 100 ug/ml gentamicin for 2 h, after that lower the gentamicin concentration to 15 ug/ml to the end of the infection.

4.2.3 Detergent-resistant membrane (DRM) preparation

After *Salmonella* infection, 0/0, 4/6 and 8/10 labeled HeLa cells were placed on ice and DRMs were isolated as described in section 2.2.5.

4.2.4 Cyclodextrin treatment, filipin III staining and immunofluorescence microscopy

HeLa cells were grown on coverslips in 24 well plates. In the cyclodextrin treatment experiment, HeLa cells were serum starved for 18 h before being treated with 10 mM MβCD for 1 h ([MβCD]max for HeLa determined in chapter 2), the control cells were left untreated. The cells were then infected with *Salmonella* for the indicated lengths of time and fixed with 4% paraformaldehyde. Non-specific binding sites were blocked with 10% NGS and cells were permeablized with 0.1% Triton X-100 before incubation with Mab to *Salmonella* (1:200) and rabbit anti-Cav1 (1:200) for 45 min for the control and treated HeLa cells. Cells were then stained with secondary anti-mouse 568 and anti-rabbit 488 (1:200) for another 45 min. The DNA dye DAPI was used to visualize the nucleus and then coverslips were mounted in ProGold for visualization on a Carl Zeiss Axio Vision microscope. For the filipin III straining, HeLa cells were infected for the indicated times and then fixed with PFA. The cells then incubated with 50 ug/ml filipin III for 2 h at RT, protected from light. Filipin staining was visualized using the DAPI filterset on a Carl Zeiss Axio Vision microscope.

4.2.5 Plasmid and siRNA transfection

A dominant negative (DN) Cav1 construct P132L (from Numata group at UBC) was transient transfected into HeLa cells growing on coverslips by using the calcium phosphate method to introduce 10 ug of plasmid for each 5 cm plate. Cells were then infected with *Salmonella* for different times and fixed with 4% PFA. After blocking and permeabilizing as above, the cells were stained with Mab to *Salmonella* and rabbit anti-Cav1.

Cells were then stained with secondary anti-mouse 568 and anti-rabbit 488 and DAPI before being mounted and visualized using the Carl Zeiss Axio Vision microscope. The HeLa cells were also plated and transfected with Cav1 siRNA or control siRNA using Lipofectamine 2000. Forty-eight hours after transfection, cells were infected with *Salmonella* and then incubated with Cav1 and *Salmonella* primary and secondary antibodies. Coverslips were mounted in ProGold for microscopy analysis.

4.2.6 High-content Cellomics screening assay

HeLa cells were seeded at 5000/well in 96 well plates one day before being infected with *S.* Typhimurium SL1344 ($_{P}$BR-RFP.1), a red fluorescent protein-expressing strain. After fixation, extracellular *Salmonella* were stained with Mab to *Salmonella* and then anti-mouse 488 (green), while DNA was stained with DAPI. Spot Detector BioApplication (version 2.0, Cellomics) software was used to determine the number of internalized *Salmonella*. Objects were identified by a positive DAPI stain, with a region of 99 pixels beyond the edge of the nucleus (99 pixels is the maximum the software can handle and we tried to maximize the covered region) being defined as the boundary to determine the total number of bacteria (red) and external number of bacteria (green). The number of internalized bacteria was calculated by subtracting the number of external bacteria from the total number of bacteria. In turn, the index of invasion was computed by dividing the number of internalized bacterial by the number of HeLa cells identified. In the intensity based calculation where the bacteria could not be completely resolved due to their density, the number of total or internalized bacteria equals the total *Salmonella* intensity, e.g., the total RFP signal, divided by the intensity of an

individual bacterium. Quantification of Filipin III staining of internal cholesterol was done by the Target Activation BioApplication (version 2.0, Cellomics). HeLa cells were infected with *S.* Typhimurium SL1344. Each cell was defined by Nuclear-ID Red DNA staining and the cell cytosol was defined by a region 6 pixels away from the edge of the nucleus and the amount of internal cholesterol was measured within this area.

4.2.7 LC-MS/MS, database searching and data clustering

The protein samples were digested and analyzed by liquid chromatography-tandem mass spectrometry (LC-MS/MS) on a LTQ-OrbitrapXL (ThermoFisher, Bremen, Germany) as described in section 3.2.7. In all experiments, digested peptides were also further fractionated by strong cation exchange chromatography into five fractions using 0, 20, 50, 100, and 500 mM of NH_4CH_3COO as described [237] and analyzed as above on an LTQ-OrbitrapXL.

Protein identification and quantification were done using MaxQuant (v 1.0.13.13) [238] by searching against the International Protein Index Human database + *S.* Typhimurium SL1344 (v3.73; 154,798 sequences) using the following criteria: minimum peptide length 6 amino acids; tryptic specificity with up to two missed cleavages; ±0.5 Da accuracy for MS/MS measurements; electrospray ionization-ion trap fragmentation characteristics; cysteine carbamidomethylation as a fixed modification; N-terminal protein acetylation, methionine oxidation, $^{2}H_4$-Lys, $^{13}C_6$-Arg, $^{13}C_6{}^{15}N_2$-Lys, and $^{13}C_6{}^{15}N_4$-Arg as variable modifications as necessary; 1% protein and peptide false discovery rate (FDR). Proteins were considered identified if we observed at least two unique peptides. Analytical

variability of SILAC data in the types of experiments performed here is typically < 23%. Biological variability was addressed in these experiments by performing three independent replicates of each experiment with variability < 17% between replicates. Fuzzy c-means (FCM) clustering was done using the MFuzz toolbox with c (number of clusters) and m (fuzzification parameter) values of 7 and 2 [274].

4.3 Results

4.3.1 Both cell surface and internal cholesterol are required for *Salmonella* infection

To test the importance of membrane cholesterol on *Salmonella*'s invasiveness, we treated HeLa cells with the cholesterol depleting drug methyl-β-cyclodextrin (MβCD) for 1 h prior to infecting the cells for 2 h (Figure 4.1). Control HeLa cells show very distinct clustering of membrane caveolin, whereas caveolin in the MβCD treated cells was more dispersed throughout the cells, presumably because MβCD disrupted the structure of lipid rafts/caveolae that cause the release of caveolin from the microdomain. The MβCD treated cells have many fewer bacteria inside after the 2 h infection compared to the untreated cells, suggesting that the lack of cholesterol is essentially blocking infection at the initial invasion stage.

Figure 4.1 Cell surface cholesterol is important for *Salmonella* invasion

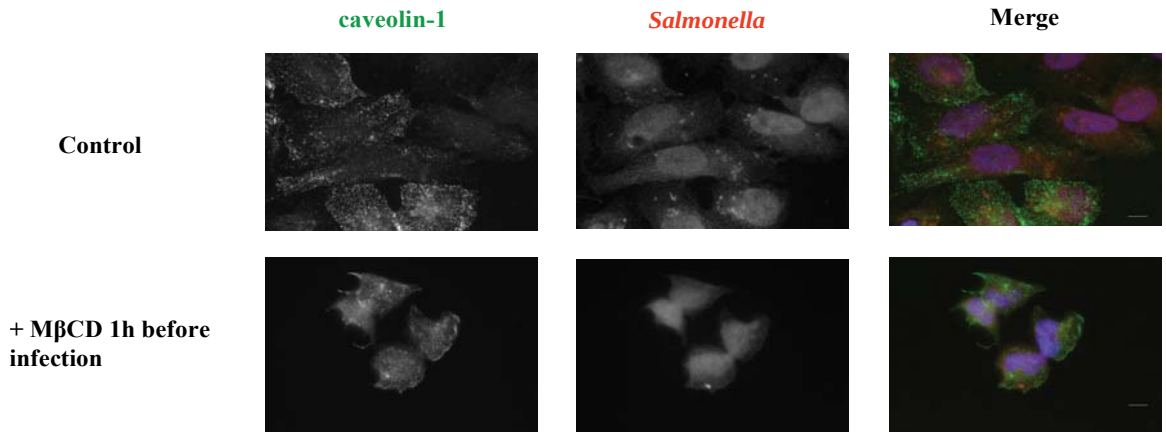

MβCD disrupt lipid rafts/caveolae by removing membrane cholesterol and that inhibited the *Salmonella* invasion on HeLa cells. Bar: 10 um.

As *Salmonella* enters its host, cholesterol remains associated with the SCVs. This can be visualized using filipin III staining of cellular cholesterol as we observed that the intracellular pool of cholesterol is markedly increased as the infection proceeds (Figure 4.2A). We further measured the change in the amount of intracellular cholesterol from no infection to 5 min, 2 h and 6 h at two different MOIs (Figure 4.2B). The intracellular cholesterol levels increase up to 2 h and then begin to decline. At 2 h post-infection, SCVs are interacting with late endosomal compartments and that internal cholesterol is at its highest level at this time suggests that the raft density on SCVs is very high. The intracellular cholesterol response curve is very similar for the two MOIs tested, meaning there is probably a basal level of cholesterol associated with the SCVs and that a single SCV might contain a few of the bacteria.

Figure 4.2 Intracellular cholesterol associated with *Salmonella* when they are in the host

A

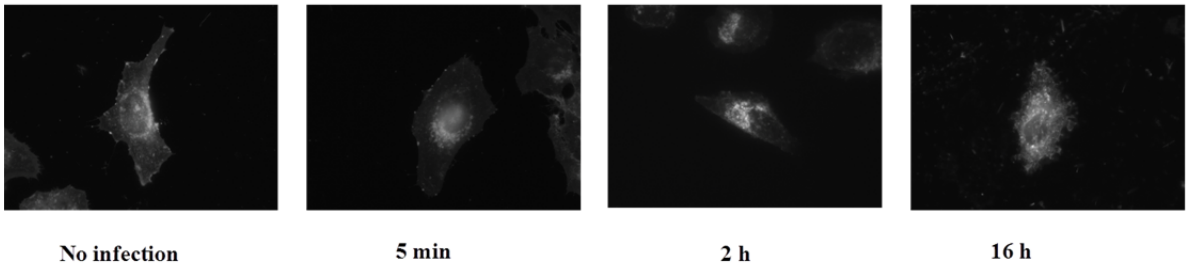

B

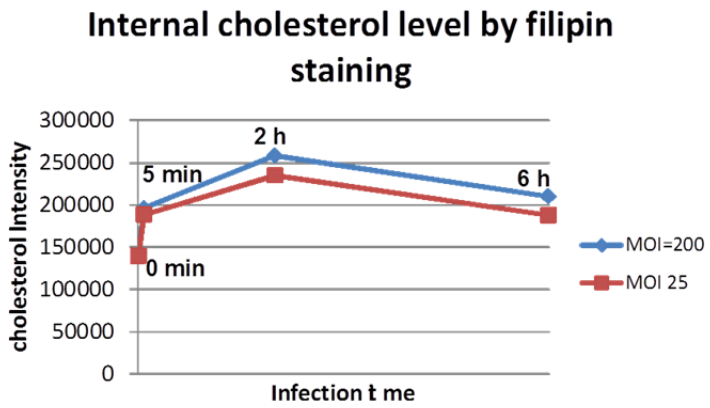

A. HeLa cells infected for different times were stained with filipin III for whole cell cholesterol. B. Amount of intracellular cholesterol was measured by Cellomics Arrayscan using filipin III staining for two MOIs.

4.3.2 The raft proteome changes as *Salmonella* infection proceeds

Many studies have shown the relationship between rafts/caveolae and *Salmonella* infection, e.g., by looking at the role of cell surface cholesterol on invasion [178], by knocking down host raft proteins and examine their role in infection [182] or by finding

Salmonella protein that bind cholesterol [181]. All of these studies, however, have ignored the bigger picture of what is happening in rafts during infection.

HeLa cells were triple SILAC encoded and then infected with *Salmonella* for different times: 0 (uninfected control), 5 min, 20 min, 1 h, 2 h, 8 h and 16 h, all at MOI=100. An equal amount of lysate protein from each sample was combined after harvesting and DRMs were subsequently purified and analyzed by mass spectrometry to identify proteins whose abundance in DRMs changes over the infection time (Figure 4.3). By searching a combined human and *Salmonella* protein database, 966 proteins were identified with at least 2 unique peptides, including 6 *Salmonella* proteins. To more clearly visualize the trend of DRMs/rafts protein abundance change, we clustered all 531 raft proteins for which we could measure ratios at all 7 time points tested (Figure 4.4). From this clustering plot alone, it is clear that infection has a dramatic effect on the raft proteome, which is consistent with the role of rafts as platforms for coordinating complex intracellular processes [47]. Amongst the clusters were groups (cluster 1 and 4) whose abundance increased at the initial invasion (bacteria intake and internalization) – 5 min. A group peak at 1 to 2 h of infection (cluster 5) (fusion with lysosome) and a group increases at late infection (cluster 2) (host lysis and *Salmonella* replication) – 8 and 16 h.

Figure 4.3 Proteomics workflow

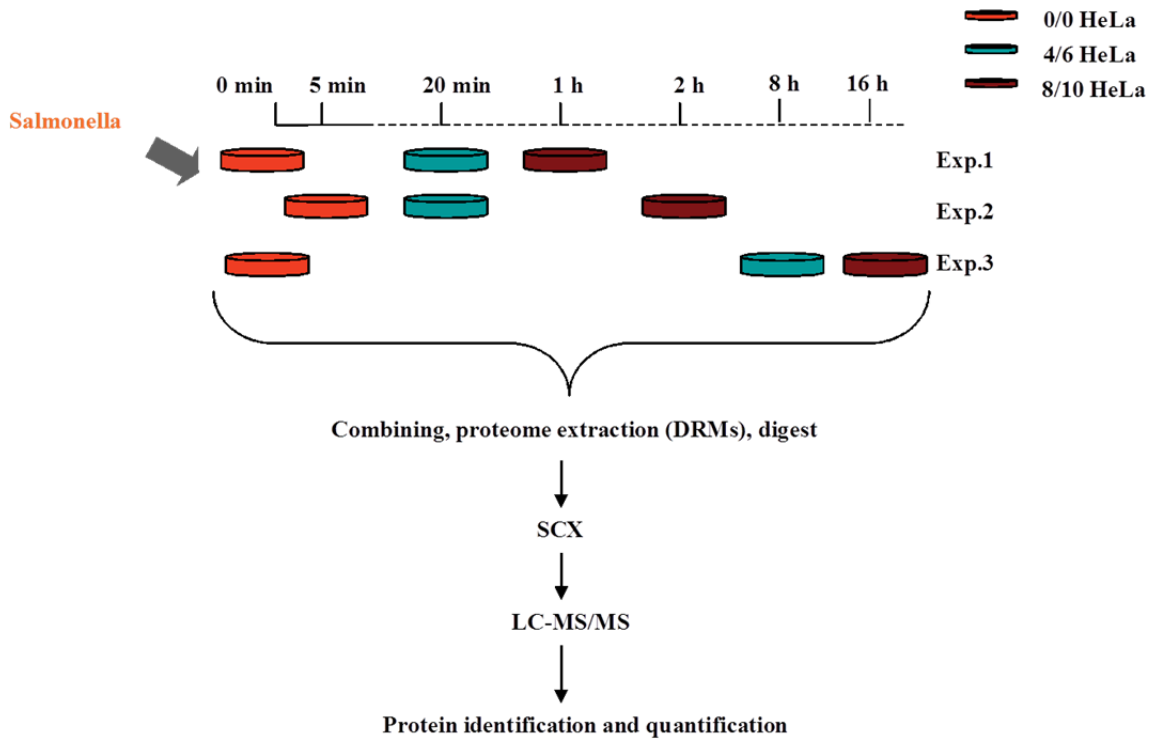

Triple SILAC labeled HeLa cells were infected with *Salmonella* for different times in three different experiments. Equal protein lysates were mixed and DRMs were extracted followed by LC-MS/MS and MaxQuant search. Biological triplicates were performed for each of the three experiments.

Figure 4.4 Clustering

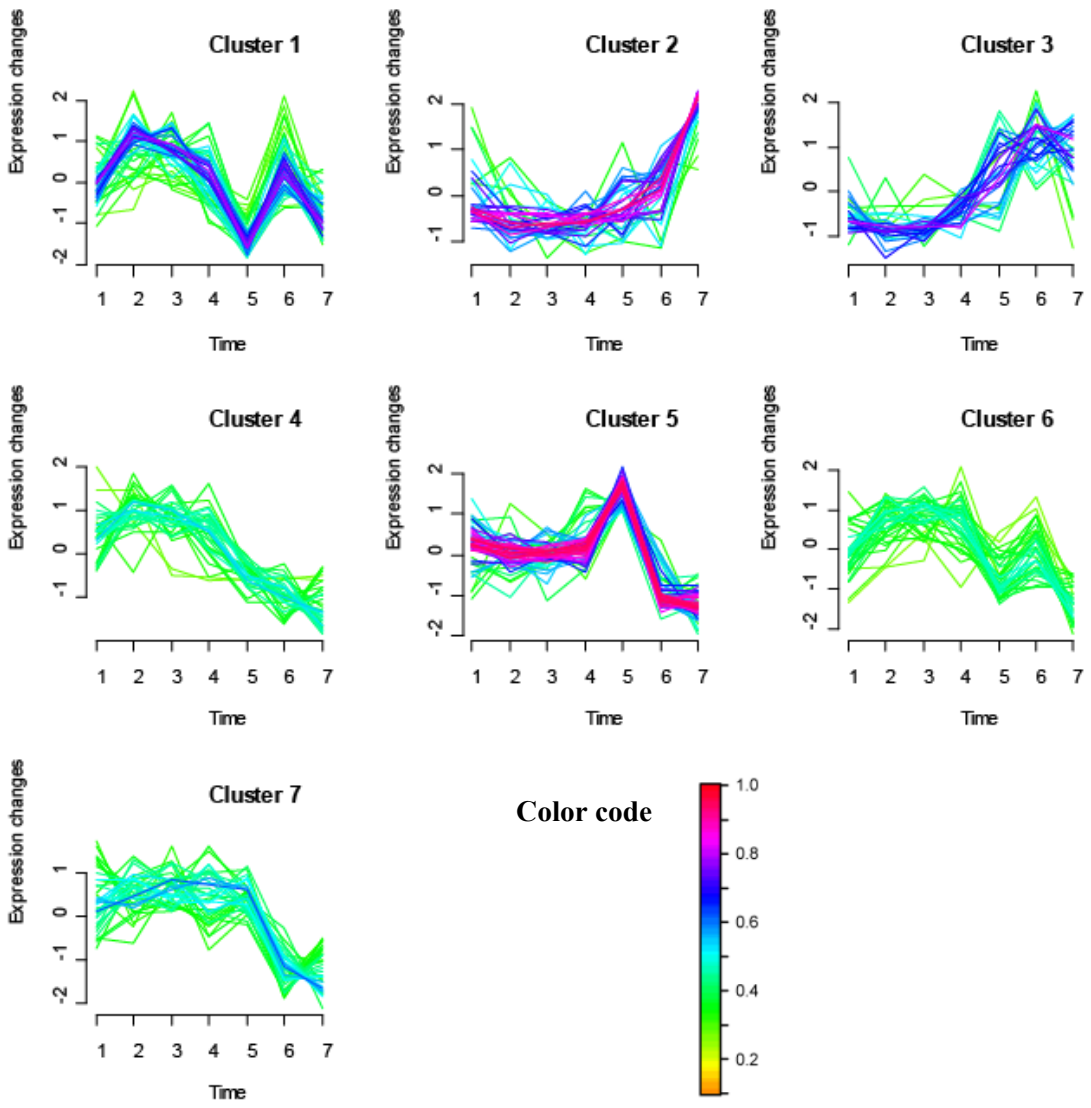

DRM proteins identified with ratios from all 7 time points were clustered together. Expression ratio change (log_{10} transformed) were on the y-axis, Time 1 to 7 on the x-axis corresponds to 0 min, 5 min, 20 min, 1 h, 2 h, 8 h and 16 h.

We counted the number of proteins recruited to and displaced from DRMs/rafts with cut off ratio of 2 ($\bar{x} + 4\sigma$ of the whole data set) at 5 min, 2 h and 16 h from the 966 quantified proteins (Figure 4.5). DRM/raft proteins were dynamic during infection, more proteins are entering and leaving rafts at 2 h and 16 h of infection than the initial infection of 5 min suggesting rafts are more dynamics at later infection stages like SCV maturation and *Salmonella* replication. Proteins recruited to DRMs at 5 min were typical previously identified rafts/caveolae proteins; others identified like actin binding proteins are probably responsible for cytoskeletal rearrangements, lipid binding proteins and lipopolysaccharide binding proteins are for bacteria attachment to the host. At 2 h, endosomal and lysosomal proteins like charged multivesicular body proteins were accumulated in DRMs indicating some connection of those degradtive compartments in SCV maturation. In the later stages of infection, caveolae structural proteins - caveolin and Ptrf were among the most enriched on DRMs. If this reflects enrichment on intracellular rafts, it might suggest that rafts/caveolae travel with the SCVs from the plasma membrane to cytoplasm. Many of the other proteins enriched at this time include those involved in amino acid transport, suggesting that *Salmonella* may be using these to collect nutrients from the host cytosol in order to fuel its intravacuolar replication. Interestingly, heterotrimeric G-proteins, which are typically a hallmark of rafts, are largely gone from DRMs from 2 h onwards.

Figure 4.5 Proteins recruited and displaced from DRMs/rafts

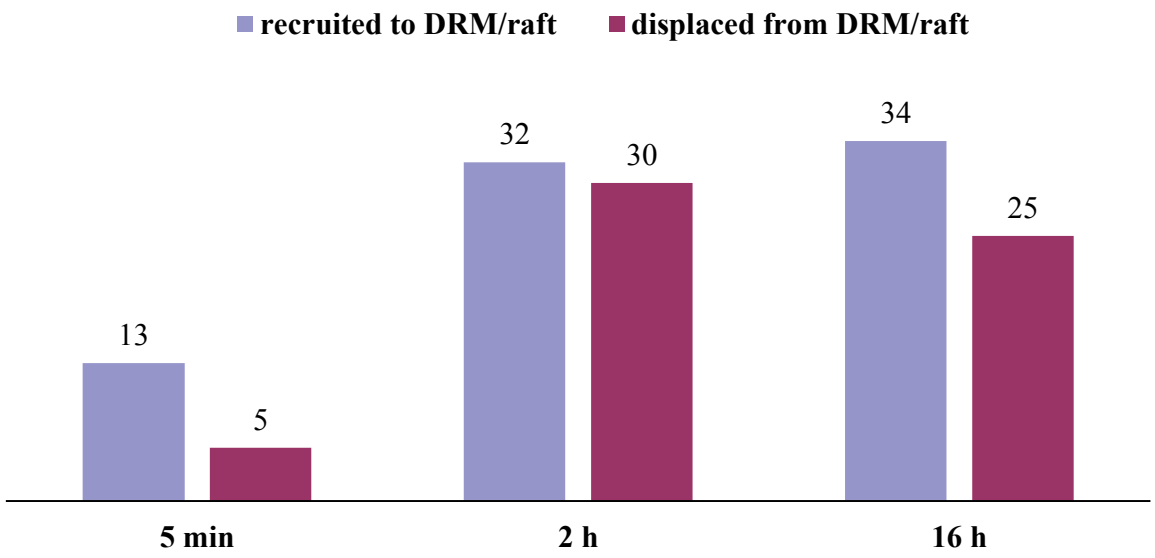

Number of proteins recruited to or displaced from DRM/raft at 5 min, 2 h and 16 h of infection with significant cut off value equals to 2.

Salmonella effector proteins were also identified in the DRM preparations with SILAC ratios. The bacteria were not labeled prior to infection so the incorporation of labeled amino acids could only have occurred once inside the host. Because of this though, any SILAC ratios measured will underestimate the levels of protein in the medium and heavy labels since there will have been significant levels of unlabeled protein still present. That any effectors were detected at all is remarkable, however, since it is generally assumed that relatively few copies of each protein are secreted into the host. While less complex than a whole cell lysate, DRM preparations still include hundreds of proteins, some of which are quite abundant so only 9 *Salmonella* proteins were identified with at least 2 unique peptides. These included 2 effector proteins, SopB and SipC, as well as other *Salmonella* outer

membrane proteins. The identification of effector proteins in the DRM suggested a strong interaction of DRMs/rafts and the effectors. To further explore the presence of effector proteins on DRMs, we designed SPI-1 *Salmonella* effector multiple reaction monitoring (MRM). Four effectors were identified by the MRM: SopB, SipC, SipB and SopE (data not shown).

4.3.3 Caveolin-1 is required for *Salmonella* invasion

Cav1 expression on the cell surface is required for caveolae to properly form [66] and it is involved in *Salmonella* invasion according to recent report on endothelial M cells [182], here we are testing if Cav1 is also involved in *Salmonella* invasion on epithelial HeLa cells. The proteomic survey data presented above, Cav1 was observed to increase in DRMs from the earliest time points. To test the role of Cav1 in invasion, HeLa cells were transiently transfected with a dominant negative Cav1 construct containing a point mutation (P132L) that mislocalizes Cav1 to an internal compartment [108] and dramatically suppressed *Salmonella* invasion (Figure 4.6A). In support of this, siRNA-mediated Cav1 knock down (compare Cav1 fluorescence intensities in Figure 4.6B) also reduced the number of intracellular *Salmonella*. All of the above suggests that *Salmonella* needs Cav1 at the inner leaflet of the plasma membrane in order to invade HeLa cells.

Figure 4.6 The expression and cell surface localization of caveolin-1 is required for *Salmonella* entrance

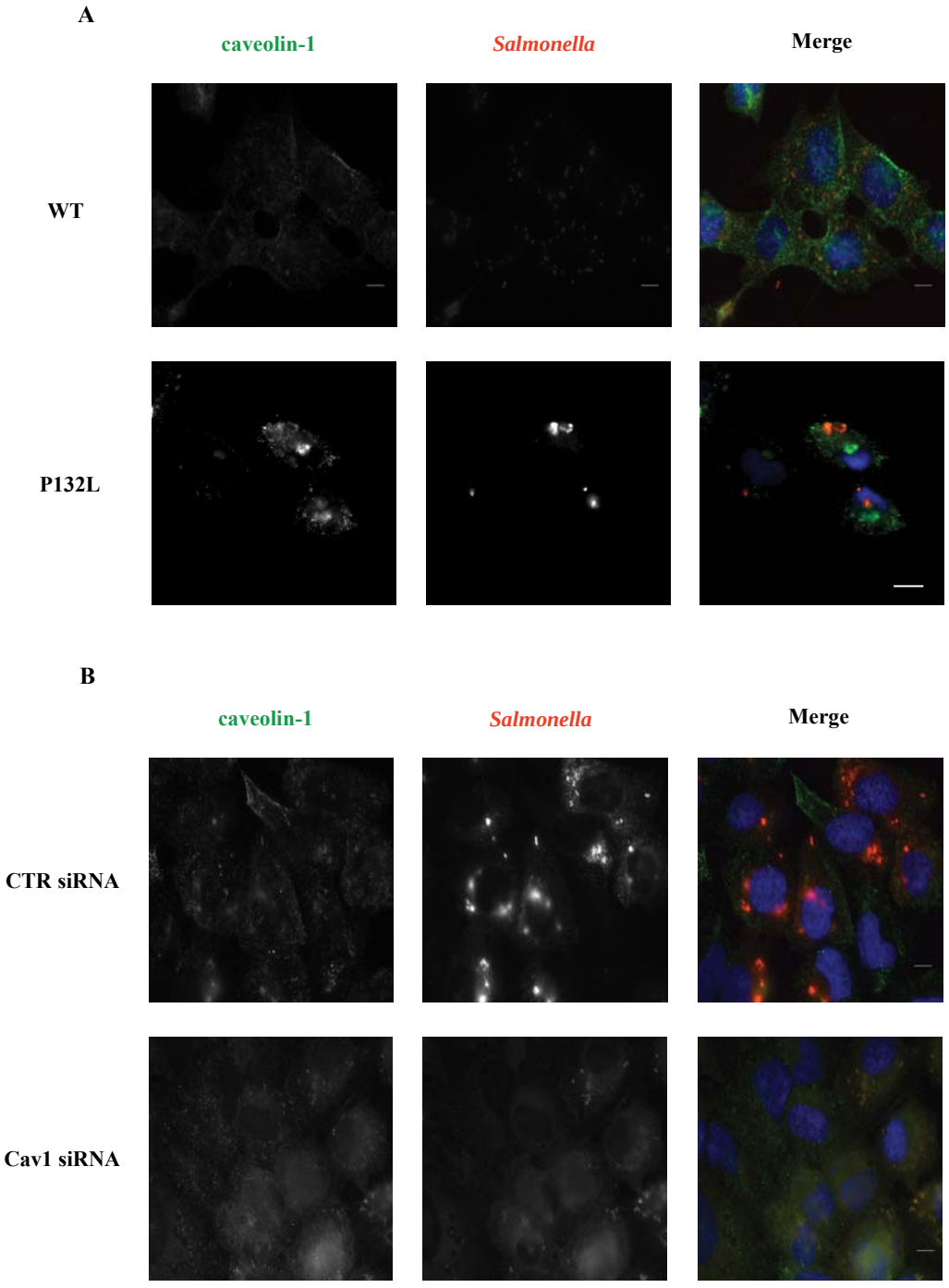

A. HeLa cells were transient transfected with DN P132L Cav1 construct. Both the control and the P132L cells were infected with *Salmonella* for 2 h. B. Cav1 knocking down HeLa cells and control siRNA cells were infected with *Salmonella* for 2 h. Bar: 10 um.

4.3.4 High-throughput assay for bacterial invasion and replication

Here we have identified dozens of interesting proteins that are candidates for having a functional role in *Salmonella*'s interactions with host cells since they are either recruited to or depleted from DRMs post-infection. These could be involved in the initial invasion process, SCV maturation or intracellular survival. As is typical for this type of experiment, far more candidates can be identified than can feasibly be pursued in the focused experiments that led to Figure 4.6. To overcome this limitation, we developed a cell-based high-content screen that would allow us to count or measure the number of bacteria able to invade host cells or surviving inside the cells after a given treatment.

Building from a previous study [275], an *Salmonella* strain engineered to express red fluorescent protein was first used to infect cells. After the desired infection time, extracellular bacteria (i.e., those that had not invaded and not been washed away) were stained another colour without permeabilizing the cells; in this way we can differentiate the extracellular bacteria (should display both colours) from those that have been internalized (should only be red, see section 4.2.6 in Experimental procedures). By using a 96 well format with automated microscopy and image processing, many screening tests can be done at a high-throughput manner (Figure 4.7A). One downside to this approach is the limited resolution of the microscopy system, meaning that high MOI levels or long infection periods cannot be used since there will be too many bacteria clustered together inside the HeLa cells to accurately resolve them. Thus, we tested the effective range of MOIs and incubation times, estimating the number of internalized bacteria by two methods (see section 4.2.6, Experimental procedures): 1) we counted the number of bacteria directly, where they could be resolved, or 2) we used an intensity-based calculation to estimate the bacteria number (i.e.,

total RFP intensity divided by the intensity of an individual bacteria. As might be expected, the intensity-based calculation had a higher dynamic range than counting individual bacteria (Figure 4.7B and C).

Figure 4.7 Cell-based high content screening assay

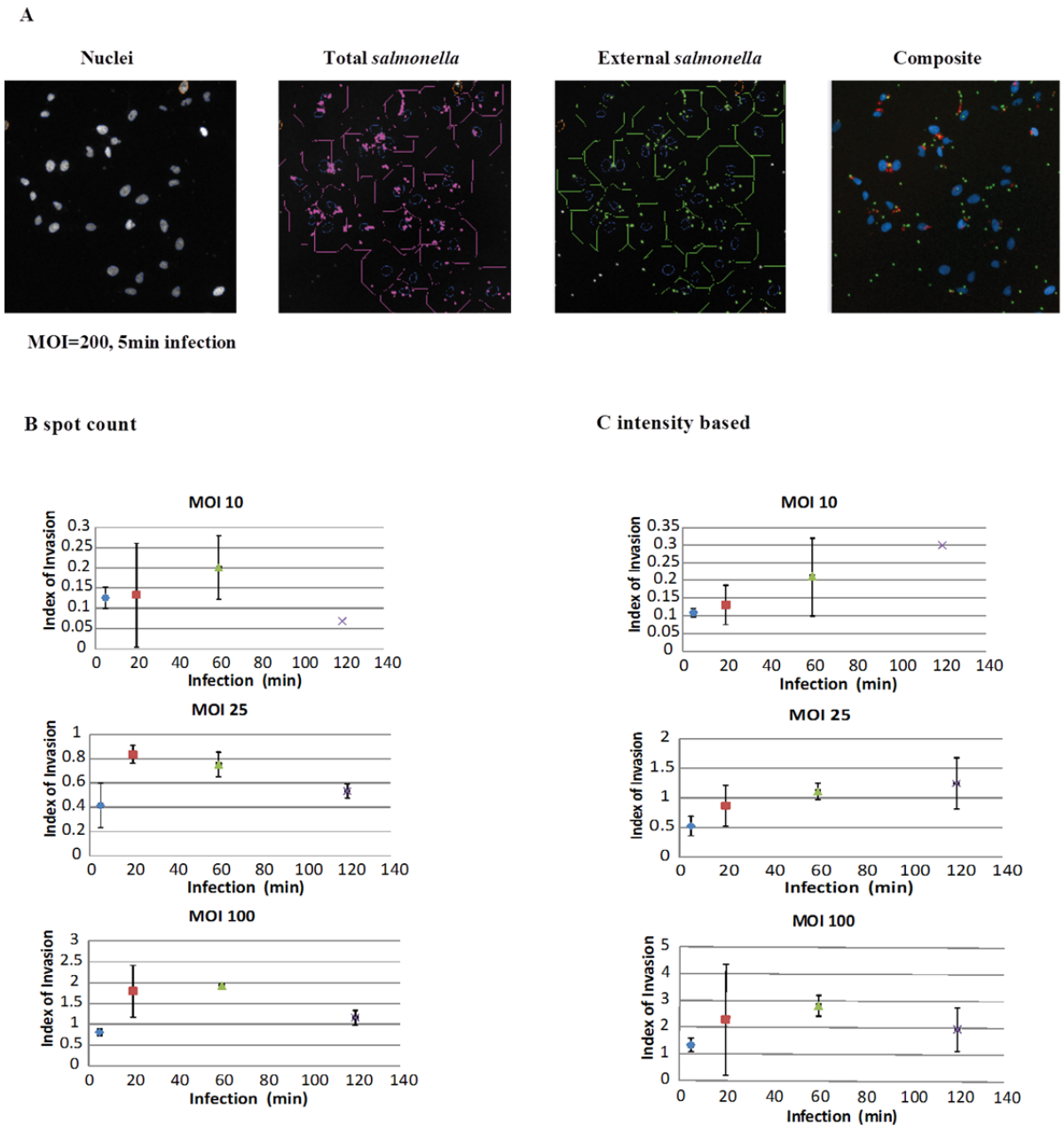

A. Nuclear staining was used to define each cell. All *Salmonella* are red while only external *Salmonella* are also green. Red dots on the composite are internalized *Salmonella*. B. index of invasion at different MOIs and times calculated use spot count. C. index of invasion at different MOIs and times calculated using the intensity based calculation.

4.4 Discussion

Lipid rafts, with their high concentration of signaling proteins, are likely targets for pathogens that need to subvert host cell processes. Rafts are highly dynamic microdomains/cellular reaction centres whose protein composition changes in response to altered cellular states or external signals [15, 16]. By attacking its host via lipid rafts, pathogens like *Salmonella* can use the endogenous raft proteins to regulate or manipulate host signaling events through its effector proteins, some of which are actually cholesterol binding proteins. In fact, cell surface rafts could even be considered a portal for *Salmonella* to communicate with host cells. Rafts have been a focus of a number of proteomics studies in recent years (see review [268]) [37, 276, 44] and the field has now moved to using technology to study how various stimuli alter the raft proteome in order to better understand the biology consequences of the stimuli. In this chapter, we used mass spectrometry-based proteomics to track changes in DRM preparations in response to *Salmonella* infection as a function of time, leading to the identification of dozens of proteins being up or down regulated at each of the infection time points (Figure 4.4).

Our knowledge that raft integrity is required for *Salmonella* invasion is based on previously studies where removal of cholesterol from the cell surface blocked invasion [178, 183]. Indeed, we found in this study too that disrupting rafts by depleting cholesterol from epithelial HeLa cells inhibited *Salmonella's* internalization. Additional evidence that rafts are likely involved in *Salmonella* pathogenesis is found in our proteomics data where many raft

proteins (i.e., those that are sensitive to cholesterol disruption) are recruited to DRMs upon *Salmonella* infection. One of the many proteins that were recruited in this way was the caveolae structural protein, Cav1. Knocking down Cav1 in the host cells reduces the infection rate (Figure 4.6B) and a dominant negative Cav1 that mislocalizes endogenous Cav1 to an internal compartment also blocked invasion (Figure 4.6A). These data suggest that caveolae specifically, not rafts more generally, are required for *Salmonella* uptake in HeLa. The involvement of Cav1 also helps validate our proteomics data. Intriguingly, however, the requirement for Cav1 in invasion seems to be cell type-dependent: Tumor cells from *Mgat5*$^{-/-}$ mice that are lack caveolae or caveolin are still susceptible to *Salmonella* infection (data not shown).

In support of there being substantial numbers of rafts/caveolae associated with SCVs, we also observed a massive intracellular accumulation of cholesterol once *Salmonella* had entered the cells. From our proteomics data (Figure 4.5), it seems that rafts start to accumulate at 1 or 2 h post infection. Our data suggests that rafts remain associated with SCVs and perhaps even concentrate on SCVs with time but their function there is open to speculation. One intriguing hypothesis is that *Salmonella* needs to remain associated with rafts as rafts are its link to the host's signaling pathways.

Omics technologies, including proteomics, can routinely identify hundreds or thousands of candidate genes/proteins but validation of such datasets is very challenging and full functional exploration of each candidate essentially impossible. In the current study, dozens of proteins recruited to or displaced from rafts during the infection are our highest priority candidates for exploring further. The cell-based high-content screening assay developed here now allows us to derive more value from the huge effort that goes into the

initial proteomics screens. With the application of 96 well formats, the current assay will allow us to screen siRNA libraries of candidate genes.

We have demonstrated here how the proteome of DRMs, as a proxy for lipid rafts, changes following *Salmonella* infection and confirmed the dynamic property of this membrane domain. Rafts are required for *Salmonella* invasion into the host through a caveolae-mediated process. Numerous other proteins were also identified that will feed future functional studies by siRNA library screens using cell-based high-content screening assays.

5 Conclusions

A primary challenge in any organelle proteomics study is to isolate a homogenous sample free of all nonspecific proteins or contaminants. In reality, it is effectively impossible to purify any organelle to homogeneity [236, 250], although many biochemical approaches have been developed in order to maximize the percentage of authentic organelle components in a sample (e.g., multi-step biochemical preparations or immunoenrichment) and to minimize the nonspecific contaminants [1]. Because the latter cannot be reduced to zero, however, there is always some doubt as to whether any protein identified in an organelle proteomics experiment is a real component of the enriched compartment or not. Several quantitative proteomics approaches have been designed to achieve much more accurate assignments of general subcellular localization (as reviewed in Ref. [277]). For lipid raft proteomics, quantitative proteomics combining a cholesterol dependence test has been employed to correctly identify true raft components [37].

In the research presented here, we used SILAC to encode the sensitivity to cholesterol disruption into proteomics analysis of DRMs from three different cell lines (chapter 2). DRM proteins showed different degrees of cholesterol dependence and that in turn classified them into raft proteins or non-raft DRM contaminants. Proteins in raft share some common components in the three cell lines tested but also contain their own subset. More importantly, this study demonstrated in an unbiased manner that lipid rafts are enriched in signaling proteins in the various different cell lines. In response to several claims that mitochondrial proteins are in rafts, we tested all the formal possibilities by examining the isolated mitochondria rafts, enrichment of mitochondrial proteins in the DRM relative to whole cell membrane and DRM protein co-migration on a linear density gradient. All of the

evidence supported our hypothesis that rafts are not on mitochondria and mitochondrial proteins are not in lipid rafts [38]; previously studies have incorrectly assigned mitochondrial proteins to rafts due to the lack of cyclodextrin test [233, 130].

Although only three cell lines have been tested, we feel the cholesterol sensitivity test should be effective to other cell models and should be used as a 'gold standard' for research on identifying proteins' localization on lipid rafts. The identified raft proteins were validated by other proteomics approaches confirmed their raft localization in the study, but orthogonal method like commonly used fluorescence microscopy could also be used to determine the mitochondrial proteins' localization and compared to a good raft marker protein. This method is good for validating a small number of proteins due to the cost, availability and specificity of antibodies required. With recent work on the Human Proteins Atlas [278], such protein localization information (like cell surface or cytoplasm localization) can be easily confirmed by a database search, thus providing a good validation tool for the protein identification. Further classifying those identified raft proteins could also be done by for example computational prediction of integral raft membrane proteins [279, 280] or use 'modification specific proteomics' to identify raft proteins that are anchored to the membrane through some sort of post-translational modifications [137, 138]. Furthermore, high resolution linear density gradient could help to resolve subclasses of rafts as we know that rafts are not homogenisis but contain domains with different structures, sizes and properties that result in different protein content and unique functions. By using current biochemical techniques, the identified microdomain proteomes are an average view of several subpopulations. Fine linear density gradient is also useful for looking at protein dynamics among different cellular compartments.

In a typical SILAC quantitative proteomics experiment, samples being compared are normalized at the cell lysate prior to fractionation (such as the control and MβCD treated cell lysates are combined before DRM isolation), thus reducing variability introduced during the often long process of subcellular fractionation, so the two populations are isolated and digested equally [37]. Chemical tagging and label-free approaches have also been applied in organelle proteomics [257, 232, 256] but most of the sample handling steps have to be conducted in parallel and normalization of sample occurs at the level of the prepared fraction. In fact, the differences in when this normalization step is applied can lead to apparent differences in the data (data not shown). For samples with minor proteome differences (like stimulated vs. unstimulated) normalization at which step will probably not make a big difference on the final comparison result; however, samples with big difference on the protein levels (some chemical treatment or protein knock down) normalize too late in the procedure will lead to unintended bias in the data. Therefore, potential differences in the relative abundance of the organelle/fraction between samples need to be considered during experimental design and data interpretation.

As stable invaginations of the plasma membrane, caveolae are intriguing structures. Our work here has taken advantage of a completely unique set of tools to probe the caveolae proteome. Various cell lines derived from *Magt5*$^{+/+}$ and *Mgat5*$^{-/-}$ mice display distinct states of caveolin and caveolae, allowing us to tease apart some of the finer details of caveolae composition (chapter 3). Other studies have used a similar strategy to compare DRMs from caveolae-containing and deficient cells, but due to the technique chosen, very few caveolae proteins were identified [73]. *Mgat5*$^{-/-}$ cells have no caveolae, despite still expressing Cav1, albeit at a reduced level. Tellingly, however, they also do not express another caveolae

structural protein, PTRF/Cavin1. This implies that 'normal' levels of PTRF and Cav1 are required for fully functional caveolae. One way to demonstrate this would be to reintroduce PTRF into *Mgat5*$^{-/-}$ cells and test whether this leads to caveolae reforming. Alternatively, knocking down PTRF in *Mgat5*$^{+/+}$ cells, which also contain normal Cav1, and checking caveolae would answer this question. If the above two knock in or knock down experiments fail, then it would suggest that there are other caveolae structural proteins that are missing due to the lack of Mgat5 in these cell lines that will require further examination. *Mgat5*$^{-/-}$ cells contain no caveolae but they do contain Cav1 scaffolds that can be visualized by electron microscopy. These scaffolds likely regulate cell signaling independent of caveolae, so their protein content is also of interest. The *Mgat5*$^{-/-}$ vs. *Mgat5*$^{-/-ESC}$ comparison identified the Cav1 scaffolds to be small with only a few proteins partitioned to them specifically. More experiments can be done is to validate the few identified scaffold proteins' localization by microscopy or immunoprecipitation. In contrast to caveolae, Cav1 scaffolds seem to segregate or deplete proteins from DRMs; the reasons for this are another potential avenue that could be explored.

Many membrane microdomain proteomics studies are now moving to look at the dynamic changes to the proteome upon various types of stimulations. In the thesis presented here, *Salmonella,* a facultative intracellular pathogen that utilizes rafts during invasion was used to examine the dynamic change of raft proteome (chapter 4). Out of more than 900 proteins identified and quantified were a few dozen whose abundance in DRMs is seen to change at various times after infection. This study has improved our understanding of lipid rafts as dynamic structures and the data contributes to our knowledge of the initial site of

host-pathogen interactions during *Salmonella* pathogenesis. The method could also be applied to other systems as well to look at how rafts respond.

Most of the validation work performed in chapter 4 focused on Cav1 but other proteins were identified that might also have significant consequences on *Salmonella* but those need to be explored further. My work here has focused on measuring changes in protein expression, which gets directly at the function of the microdomain, but there is much more that could be going on at the protein level but that would not be reflected in the approaches I have used here. For example, post-translational modifications are particularly important for the function of many proteins and there are now proteomic techniques available to probe some such modifications, e.g., the highly dynamic ones such as phosphorylation and microdomain-targeting ones such as glycosyphosphatidylinositol [137, 138]. With the development of mass spectrometers and proteomics techniques, proteins and proteins' PTM change can be determined simultaneously and the two aspects can compensate or complement one another, giving a more complete view of the changes to rafts.

One limitation of the work performed in chapter 4 was that, while we could detect several *Salmonella* proteins, the ratios we were able to measure for them were meaningless since they did not start out fully labeled. Thus, in future experiments, bacteria could be pre-labeled prior to infection of host cells. Matching the labels used for a particular culture with the labels in a particular host cell would then allow accurate quantitation of *Salmonella* proteins as well. Such an approach would not be limited just to the DRM proteomics I have done here but could be used in other studies too [281].

As I and all my colleagues constantly find, however, it is very difficult to effectively follow up on all the proteins one can find in a proteomics experiment. To this end, I feel that

my biggest technical contribution to my field from my doctoral work will turn out to be my development of a high-content screening assay to measure *Salmonella*'s invasiveness and intracellular replication.

The research presented in this thesis has contributed to the membrane microdomain field in several ways: We have demonstrated unequivocally which membrane compartments do and do not contain rafts, where some of the proteins seen in DRMs likely come from, if not from rafts, and the differential composition of rafts and caveolae. My hope is that the field can move past trying to explore a role in rafts for proteins that are mistakenly assigned to this subdomain and focus on those correctly identified rafts/caveolae proteins to further test their functional roles. With regards to the specific system of *Salmonella*-host interactions, we have identified several proteins here that appear to be involved in either invasion or maturation of the SCV. These high quality targets will provide a starting point for future cell biological and biochemical study of this intriguing system.

References

1. Zheng, Y.Z. and L.J. Foster, *Biochemical and proteomic approaches for the study of membrane microdomains.* J Proteomics, 2009. 72(1): p. 12-22.
2. De Weer, P., *A century of thinking about cell membranes.* Annu Rev Physiol, 2000. 62: p. 919-26.
3. Zachowski, A. and P.F. Devaux, *Transmembrane movements of lipids.* Experientia, 1990. 46(6): p. 644-56.
4. Wallin, E. and G. von Heijne, *Genome-wide analysis of integral membrane proteins from eubacterial, archaean, and eukaryotic organisms.* Protein Sci, 1998. 7(4): p. 1029-38.
5. Lipowsky, R., *The conformation of membranes.* Nature, 1991. 349(6309): p. 475-81.
6. Singer, S.J. and G.L. Nicolson, *The fluid mosaic model of the structure of cell membranes.* Science, 1972. 175(23): p. 720-31.
7. Anderson, R.G. and K. Jacobson, *A role for lipid shells in targeting proteins to caveolae, rafts, and other lipid domains.* Science, 2002. 296(5574): p. 1821-5.
8. Bhattacharyya, R.P., et al., *Domains, motifs, and scaffolds: the role of modular interactions in the evolution and wiring of cell signaling circuits.* Annu Rev Biochem, 2006. 75: p. 655-80.
9. Brown, D.A. and J.K. Rose, *Sorting of GPI-anchored proteins to glycolipid-enriched membrane subdomains during transport to the apical cell surface.* Cell, 1992. 68(3): p. 533-44.
10. Charrin, S., et al., *A physical and functional link between cholesterol and tetraspanins.* Eur J Immunol, 2003. 33(9): p. 2479-89.
11. Harder, T. and K. Simons, *Caveolae, DIGs, and the dynamics of sphingolipid-cholesterol microdomains.* Curr Opin Cell Biol, 1997. 9(4): p. 534-42.
12. Dietrich, C., et al., *Lipid rafts reconstituted in model membranes.* Biophys J, 2001. 80(3): p. 1417-28.
13. Dietrich, C., et al., *Partitioning of Thy-1, GM1, and cross-linked phospholipid analogs into lipid rafts reconstituted in supported model membrane monolayers.* Proc Natl Acad Sci U S A, 2001. 98(19): p. 10642-7.
14. Renkonen, O., et al., *The lipid class composition of Semliki forest virus and plasma membranes of the host cells.* Virology, 1971. 46(2): p. 318-26.
15. Bini, L., et al., *Extensive temporally regulated reorganization of the lipid raft proteome following T-cell antigen receptor triggering.* Biochem J, 2003. 369(Pt 2): p. 301-9.
16. Gupta, N., et al., *Quantitative proteomic analysis of B cell lipid rafts reveals that ezrin regulates antigen receptor-mediated lipid raft dynamics.* Nat Immunol, 2006. 7(6): p. 625-33.
17. Simons, K. and E. Ikonen, *Functional rafts in cell membranes.* Nature, 1997. 387(6633): p. 569-72.
18. Li, N., et al., *Monocyte lipid rafts contain proteins implicated in vesicular trafficking and phagosome formation.* Proteomics, 2003. 3(4): p. 536-48.
19. Brown, D.A. and E. London, *Structure and origin of ordered lipid domains in biological membranes.* J Membr Biol, 1998. 164(2): p. 103-14.

20. Schroeder, R., E. London, and D. Brown, *Interactions between saturated acyl chains confer detergent resistance on lipids and glycosylphosphatidylinositol (GPI)-anchored proteins: GPI-anchored proteins in liposomes and cells show similar behavior.* Proc Natl Acad Sci U S A, 1994. 91(25): p. 12130-4.
21. Schroeder, R.J., et al., *Cholesterol and sphingolipid enhance the Triton X-100 insolubility of glycosylphosphatidylinositol-anchored proteins by promoting the formation of detergent-insoluble ordered membrane domains.* J Biol Chem, 1998. 273(2): p. 1150-7.
22. Simons, K. and G. van Meer, *Lipid sorting in epithelial cells.* Biochemistry, 1988. 27(17): p. 6197-202.
23. van Meer, G. and Q. Lisman, *Sphingolipid transport: rafts and translocators.* J Biol Chem, 2002. 277(29): p. 25855-8.
24. Pike, L.J., *Rafts defined: a report on the Keystone Symposium on Lipid Rafts and Cell Function.* J Lipid Res, 2006. 47(7): p. 1597-8.
25. Vereb, G., et al., *Dynamic, yet structured: The cell membrane three decades after the Singer-Nicolson model.* Proc Natl Acad Sci U S A, 2003. 100(14): p. 8053-8.
26. Heerklotz, H., *Triton promotes domain formation in lipid raft mixtures.* Biophys J, 2002. 83(5): p. 2693-701.
27. Heerklotz, H., et al., *The sensitivity of lipid domains to small perturbations demonstrated by the effect of Triton.* J Mol Biol, 2003. 329(4): p. 793-9.
28. Heffer-Lauc, M., et al., *Membrane redistribution of gangliosides and glycosylphosphatidylinositol-anchored proteins in brain tissue sections under conditions of lipid raft isolation.* Biochim Biophys Acta, 2005. 1686 3: p. 200-8.
29. Ahmed, S.N., D.A. Brown, and E. London, *On the origin of sphingolipid/cholesterol-rich detergent-insoluble cell membranes: physiological concentrations of cholesterol and sphingolipid induce formation of a detergent-insoluble, liquid-ordered lipid phase in model membranes.* Biochemistry, 1997. 36(36): p. 10944-53.
30. Friedrichson, T. and T.V. Kurzchalia, *Microdomains of GPI-anchored proteins in living cells revealed by crosslinking.* Nature, 1998. 394(6695): p. 802-5.
31. Garner, A.E., D.A. Smith, and N.M. Hooper, *Visualization of detergent solubilization of membranes: implications for the isolation of rafts.* Biophys J, 2008. 94(4): p. 1326-40.
32. Harder, T., et al., *Lipid domain structure of the plasma membrane revealed by patching of membrane components.* J Cell Biol, 1998. 141(4): p. 929-42.
33. Pralle, A., et al., *Sphingolipid-cholesterol rafts diffuse as small entities in the plasma membrane of mammalian cells.* J Cell Biol, 2000. 148(5): p. 997-1008.
34. Varma, R. and S. Mayor, *GPI-anchored proteins are organized in submicron domains at the cell surface.* Nature, 1998. 394(6695): p. 798-801.
35. Browman, D.T., et al., *Erlin-1 and erlin-2 are novel members of the prohibitin family of proteins that define lipid-raft-like domains of the ER.* J Cell Sci, 2006. 119(Pt 15): p. 3149-60.
36. Hayashi, T. and T.P. Su, *Sigma-1 receptors (sigma(1) binding sites) form raft-like microdomains and target lipid droplets on the endoplasmic reticulum: roles in endoplasmic reticulum lipid compartmentalization and export.* J Pharmacol Exp Ther, 2003. 306(2): p. 718-25.

37. Foster, L.J., C.L. De Hoog, and M. Mann, *Unbiased quantitative proteomics of lipid rafts reveals high specificity for signaling factors.* Proc Natl Acad Sci U S A, 2003. 100(10): p. 5813-8.
38. Zheng, Y.Z., K.B. Berg, and L.J. Foster, *Mitochondria do not contain lipid rafts, and lipid rafts do not contain mitochondrial proteins.* J Lipid Res, 2009. 50(5): p. 988-98.
39. Eberle, H.B., et al., *Identification and characterization of a novel human plant pathogenesis-related protein that localizes to lipid-enriched microdomains in the Golgi complex.* J Cell Sci, 2002. 115(Pt 4): p. 827-38.
40. Dermine, J.F., et al., *Flotillin-1-enriched lipid raft domains accumulate on maturing phagosomes.* J Biol Chem, 2001. 276(21): p. 18507-12.
41. Gagescu, R., J. Gruenberg, and E. Smythe, *Membrane dynamics in endocytosis: structure--function relationship.* Traffic, 2000. 1(1): p. 84-8.
42. Sobo, K., et al., *Diversity of raft-like domains in late endosomes.* PLoS One, 2007. 2(4): p. e391.
43. Pike, L.J., *Lipid rafts: heterogeneity on the high seas.* Biochem J, 2004. 378(Pt 2): p. 281-92.
44. Zheng, Y.Z., et al., *Differential impact of caveolae and caveolin-1 scaffolds on the membrane raft proteome.* Mol Cell Proteomics. 10(10): p. M110 007146.
45. Palade, G.E., *An electron microscope study of the mitochondrial structure.* J Histochem Cytochem, 1953. 1(4): p. 188-211.
46. Lo, W.K., C.J. Zhou, and J. Reddan, *Identification of caveolae and their signature proteins caveolin 1 and 2 in the lens.* Exp Eye Res, 2004. 79(4): p. 487-98.
47. Simons, K. and D. Toomre, *Lipid rafts and signal transduction.* Nat Rev Mol Cell Biol, 2000. 1(1): p. 31-9.
48. Irwin, M.E., et al., *Lipid raft localization of EGFR alters the response of cancer cells to the EGFR tyrosine kinase inhibitor gefitinib.* J Cell Physiol. 226(9): p. 2316-28.
49. Kumari, R. and A. Francesconi, *Identification of GPCR localization in detergent resistant membranes.* Methods Mol Biol. 746: p. 411-23.
50. Rajala, R.V., et al., *Localization of the insulin receptor and phosphoinositide 3-kinase in detergent-resistant membrane rafts of rod photoreceptor outer segments.* Adv Exp Med Biol, 2006. 572: p. 491-7.
51. Mineo, C., G.N. Gill, and R.G. Anderson, *Regulated migration of epidermal growth factor receptor from caveolae.* J Biol Chem, 1999. 274(43): p. 30636-43.
52. Wary, K.K., et al., *A requirement for caveolin-1 and associated kinase Fyn in integrin signaling and anchorage-dependent cell growth.* Cell, 1998. 94(5): p. 625-34.
53. Janes, P.W., et al., *The role of lipid rafts in T cell antigen receptor (TCR) signalling.* Semin Immunol, 2000. 12(1): p. 23-34.
54. Kroczek, C., et al., *Swiprosin-1/EFhd2 controls B cell receptor signaling through the assembly of the B cell receptor, Syk, and phospholipase C gamma2 in membrane rafts.* J Immunol. 184(7): p. 3665-76.
55. Stan, R.V., *Structure of caveolae.* Biochim Biophys Acta, 2005. 1746(3): p. 334-48.
56. Fan, J.Y., et al., *Morphological changes of the 3T3-L1 fibroblast plasma membrane upon differentiation to the adipocyte form.* J Cell Sci, 1983. 61: p. 219-30.
57. Mellgren, R.L., *Detergent-resistant membrane subfractions containing proteins of plasma membrane, mitochondrial, and internal membrane origins.* J Biochem Biophys Methods, 2008. 70(6): p. 1029-36.

58. Murata, M., et al., *VIP21/caveolin is a cholesterol-binding protein.* Proc Natl Acad Sci U S A, 1995. 92(22): p. 10339-43.
59. Smart, E.J., et al., *A role for caveolin in transport of cholesterol from endoplasmic reticulum to plasma membrane.* J Biol Chem, 1996. 271(46): p. 29427-35.
60. Drab, M., et al., *Loss of caveolae, vascular dysfunction, and pulmonary defects in caveolin-1 gene-disrupted mice.* Science, 2001. 293(5539): p. 2449-52.
61. Galbiati, F., et al., *Caveolin-3 null mice show a loss of caveolae, changes in the microdomain distribution of the dystrophin-glycoprotein complex, and t-tubule abnormalities.* J Biol Chem, 2001. 276(24): p. 21425-33.
62. Couet, J., et al., *Cell biology of caveolae and caveolin.* Adv Drug Deliv Rev, 2001. 49(3): p. 223-35.
63. Okamoto, T., et al., *Caveolins, a family of scaffolding proteins for organizing "preassembled signaling complexes" at the plasma membrane.* J Biol Chem, 1998. 273(10): p. 5419-22.
64. Parton, R.G., *Caveolae and caveolins.* Curr Opin Cell Biol, 1996. 8(4): p. 542-8.
65. Monier, S., et al., *VIP21-caveolin, a membrane protein constituent of the caveolar coat, oligomerizes in vivo and in vitro.* Mol Biol Cell, 1995. 6(7): p. 911-27.
66. Rothberg, K.G., et al., *Caveolin, a protein component of caveolae membrane coats.* Cell, 1992. 68(4): p. 673-82.
67. Scherer, P.E., et al., *Cell-type and tissue-specific expression of caveolin-2. Caveolins 1 and 2 co-localize and form a stable hetero-oligomeric complex in vivo.* J Biol Chem, 1997. 272(46): p. 29337-46.
68. Song, K.S., et al., *Expression of caveolin-3 in skeletal, cardiac, and smooth muscle cells. Caveolin-3 is a component of the sarcolemma and co-fractionates with dystrophin and dystrophin-associated glycoproteins.* J Biol Chem, 1996. 271(25): p. 15160-5.
69. Couet, J., et al., *Identification of peptide and protein ligands for the caveolin-scaffolding domain. Implications for the interaction of caveolin with caveolae-associated proteins.* J Biol Chem, 1997. 272(10): p. 6525-33.
70. Sargiacomo, M., et al., *Oligomeric structure of caveolin: implications for caveolae membrane organization.* Proc Natl Acad Sci U S A, 1995. 92(20): p. 9407-11.
71. Schlegel, A. and M.P. Lisanti, *A molecular dissection of caveolin-1 membrane attachment and oligomerization. Two separate regions of the caveolin-1 C-terminal domain mediate membrane binding and oligomer/oligomer interactions in vivo.* J Biol Chem, 2000. 275(28): p. 21605-17.
72. Schlegel, A., et al., *A role for the caveolin scaffolding domain in mediating the membrane attachment of caveolin-1. The caveolin scaffolding domain is both necessary and sufficient for membrane binding in vitro.* J Biol Chem, 1999. 274(32): p. 22660-7.
73. Hill, M.M., et al., *PTRF-Cavin, a conserved cytoplasmic protein required for caveola formation and function.* Cell, 2008. 132(1): p. 113-24.
74. Bastiani, M., et al., *MURC/Cavin-4 and cavin family members form tissue-specific caveolar complexes.* J Cell Biol, 2009. 185(7): p. 1259-73.
75. Hansen, C.G., et al., *SDPR induces membrane curvature and functions in the formation of caveolae.* Nat Cell Biol, 2009. 11(7): p. 807-14.

76. McMahon, K.A., et al., *SRBC/cavin-3 is a caveolin adapter protein that regulates caveolae function.* Embo J, 2009. 28(8): p. 1001-15.
77. Lisanti, M.P., et al., *Characterization of caveolin-rich membrane domains isolated from an endothelial-rich source: implications for human disease.* J Cell Biol, 1994. 126(1): p. 111-26.
78. Sargiacomo, M., et al., *Signal transducing molecules and glycosyl-phosphatidylinositol-linked proteins form a caveolin-rich insoluble complex in MDCK cells.* J Cell Biol, 1993. 122(4): p. 789-807.
79. Hino, M., et al., *Caveolin-1 as tumor suppressor gene in breast cancer.* Surg Today, 2003. 33(7): p. 486-90.
80. Parton, R.G. and K. Simons, *The multiple faces of caveolae.* Nat Rev Mol Cell Biol, 2007. 8(3): p. 185-94.
81. Chen, J., et al., *Regulation of insulin receptor substrate-1 expression levels by caveolin-1.* J Cell Physiol, 2008.
82. Cohen, A.W., et al., *Caveolin-1-deficient mice show insulin resistance and defective insulin receptor protein expression in adipose tissue.* Am J Physiol Cell Physiol, 2003. 285(1): p. C222-35.
83. Nystrom, F.H., et al., *Caveolin-1 interacts with the insulin receptor and can differentially modulate insulin signaling in transfected Cos-7 cells and rat adipose cells.* Mol Endocrinol, 1999. 13(12): p. 2013-24.
84. Yamamoto, M., et al., *Caveolin is an activator of insulin receptor signaling.* J Biol Chem, 1998. 273(41): p. 26962-8.
85. Nabi, I.R. and P.U. Le, *Caveolae/raft-dependent endocytosis.* J Cell Biol, 2003. 161(4): p. 673-7.
86. Lajoie, P. and I.R. Nabi, *Regulation of raft-dependent endocytosis.* J Cell Mol Med, 2007. 11(4): p. 644-53.
87. Lajoie, P., et al., *Caveolin-1 regulation of dynamin-dependent, raft-mediated endocytosis of cholera toxin-B sub-unit occurs independently of caveolae.* J Cell Mol Med, 2009. 13(9B): p. 3218-25.
88. Mundy, D.I., et al., *Dual control of caveolar membrane traffic by microtubules and the actin cytoskeleton.* J Cell Sci, 2002. 115(Pt 22): p. 4327-39.
89. Pelkmans, L., D. Puntener, and A. Helenius, *Local actin polymerization and dynamin recruitment in SV40-induced internalization of caveolae.* Science, 2002. 296(5567): p. 535-9.
90. Hailstones, D., et al., *Regulation of caveolin and caveolae by cholesterol in MDCK cells.* J Lipid Res, 1998. 39(2): p. 369-79.
91. Schnitzer, J.E., et al., *Filipin-sensitive caveolae-mediated transport in endothelium: reduced transcytosis, scavenger endocytosis, and capillary permeability of select macromolecules.* J Cell Biol, 1994. 127(5): p. 1217-32.
92. Sharma, D.K., et al., *Selective stimulation of caveolar endocytosis by glycosphingolipids and cholesterol.* Mol Biol Cell, 2004. 15(7): p. 3114-22.
93. Oh, P., D.P. McIntosh, and J.E. Schnitzer, *Dynamin at the neck of caveolae mediates their budding to form transport vesicles by GTP-driven fission from the plasma membrane of endothelium.* J Cell Biol, 1998. 141(1): p. 101-14.
94. Glenney, J.R., Jr., *Tyrosine phosphorylation of a 22-kDa protein is correlated with transformation by Rous sarcoma virus.* J Biol Chem, 1989. 264(34): p. 20163-6.

95. Chen, Y. and L.C. Norkin, *Extracellular simian virus 40 transmits a signal that promotes virus enclosure within caveolae.* Exp Cell Res, 1999. 246(1): p. 83-90.
96. Pelkmans, L., J. Kartenbeck, and A. Helenius, *Caveolar endocytosis of simian virus 40 reveals a new two-step vesicular-transport pathway to the ER.* Nat Cell Biol, 2001. 3(5): p. 473-83.
97. Fittipaldi, A., et al., *Cell membrane lipid rafts mediate caveolar endocytosis of HIV-1 Tat fusion proteins.* J Biol Chem, 2003. 278(36): p. 34141-9.
98. Minshall, R.D., et al., *Endothelial cell-surface gp60 activates vesicle formation and trafficking via G(i)-coupled Src kinase signaling pathway.* J Cell Biol, 2000. 150(5): p. 1057-70.
99. Nichols, B.J., *A distinct class of endosome mediates clathrin-independent endocytosis to the Golgi complex.* Nat Cell Biol, 2002. 4(5): p. 374-8.
100. Damm, E.M., et al., *Clathrin- and caveolin-1-independent endocytosis: entry of simian virus 40 into cells devoid of caveolae.* J Cell Biol, 2005. 168(3): p. 477-88.
101. Glebov, O.O., N.A. Bright, and B.J. Nichols, *Flotillin-1 defines a clathrin-independent endocytic pathway in mammalian cells.* Nat Cell Biol, 2006. 8(1): p. 46-54.
102. Duncan, M.J., J.S. Shin, and S.N. Abraham, *Microbial entry through caveolae: variations on a theme.* Cell Microbiol, 2002. 4(12): p. 783-91.
103. Koleske, A.J., D. Baltimore, and M.P. Lisanti, *Reduction of caveolin and caveolae in oncogenically transformed cells.* Proc Natl Acad Sci U S A, 1995. 92(5): p. 1381-5.
104. Lee, S.W., et al., *Tumor cell growth inhibition by caveolin re-expression in human breast cancer cells.* Oncogene, 1998. 16(11): p. 1391-7.
105. Capozza, F., et al., *Absence of caveolin-1 sensitizes mouse skin to carcinogen-induced epidermal hyperplasia and tumor formation.* Am J Pathol, 2003. 162(6): p. 2029-39.
106. Sunaga, N., et al., *Different roles for caveolin-1 in the development of non-small cell lung cancer versus small cell lung cancer.* Cancer Res, 2004. 64(12): p. 4277-85.
107. Hayashi, K., et al., *Invasion activating caveolin-1 mutation in human scirrhous breast cancers.* Cancer Res, 2001. 61(6): p. 2361-4.
108. Lee, H., et al., *Caveolin-1 mutations (P132L and null) and the pathogenesis of breast cancer: caveolin-1 (P132L) behaves in a dominant-negative manner and caveolin-1 (-/-) null mice show mammary epithelial cell hyperplasia.* Am J Pathol, 2002. 161(4): p. 1357-69.
109. Galbiati, F., B. Razani, and M.P. Lisanti, *Caveolae and caveolin-3 in muscular dystrophy.* Trends Mol Med, 2001. 7(10): p. 435-41.
110. Hernandez-Deviez, D.J., et al., *Aberrant dysferlin trafficking in cells lacking caveolin or expressing dystrophy mutants of caveolin-3.* Hum Mol Genet, 2006. 15(1): p. 129-42.
111. Boucheix, C. and E. Rubinstein, *Tetraspanins.* Cell Mol Life Sci, 2001. 58(9): p. 1189-205.
112. Maecker, H.T., S.C. Todd, and S. Levy, *The tetraspanin superfamily: molecular facilitators.* Faseb J, 1997. 11(6): p. 428-42.
113. Levy, S. and T. Shoham, *The tetraspanin web modulates immune-signalling complexes.* Nat Rev Immunol, 2005. 5(2): p. 136-48.
114. Berditchevski, F., *Complexes of tetraspanins with integrins: more than meets the eye.* J Cell Sci, 2001. 114(Pt 23): p. 4143-51.

115. Levy, S., S.C. Todd, and H.T. Maecker, *CD81 (TAPA-1): a molecule involved in signal transduction and cell adhesion in the immune system.* Annu Rev Immunol, 1998. 16: p. 89-109.
116. Silvie, O., et al., *Hepatocyte CD81 is required for Plasmodium falciparum and Plasmodium yoelii sporozoite infectivity.* Nat Med, 2003. 9(1): p. 93-6.
117. Zemni, R., et al., *A new gene involved in X-linked mental retardation identified by analysis of an X;2 balanced translocation.* Nat Genet, 2000. 24(2): p. 167-70.
118. Claas, C., C.S. Stipp, and M.E. Hemler, *Evaluation of prototype transmembrane 4 superfamily protein complexes and their relation to lipid rafts.* J Biol Chem, 2001. 276(11): p. 7974-84.
119. Israels, S.J. and E.M. McMillan-Ward, *Platelet tetraspanin complexes and their association with lipid rafts.* Thromb Haemost, 2007. 98(5): p. 1081-7.
120. Berditchevski, F., M.M. Zutter, and M.E. Hemler, *Characterization of novel complexes on the cell surface between integrins and proteins with 4 transmembrane domains (TM4 proteins).* Mol Biol Cell, 1996. 7(2): p. 193-207.
121. Rubinstein, E., et al., *CD9, CD63, CD81, and CD82 are components of a surface tetraspan network connected to HLA-DR and VLA integrins.* Eur J Immunol, 1996. 26(11): p. 2657-65.
122. Blonder, J., et al., *Combined chemical and enzymatic stable isotope labeling for quantitative profiling of detergent-insoluble membrane proteins isolated using Triton X-100 and Brij-96.* J Proteome Res, 2006. 5(2): p. 349-60.
123. Man, P., et al., *Mass spectrometric analysis of the glycosphingolipid-enriched microdomains of rat natural killer cells.* Proteomics, 2005. 5(1): p. 113-22.
124. Schuck, S., et al., *Resistance of cell membranes to different detergents.* Proc Natl Acad Sci U S A, 2003. 100(10): p. 5795-800.
125. Macdonald, J.L. and L.J. Pike, *A simplified method for the preparation of detergent-free lipid rafts.* J Lipid Res, 2005. 46(5): p. 1061-7.
126. Smart, E.J., et al., *A detergent-free method for purifying caveolae membrane from tissue culture cells.* Proc Natl Acad Sci U S A, 1995. 92(22): p. 10104-8.
127. Chang, W.J., et al., *Purification and characterization of smooth muscle cell caveolae.* J Cell Biol, 1994. 126(1): p. 127-38.
128. Schnitzer, J.E., et al., *Caveolae from luminal plasmalemma of rat lung endothelium: microdomains enriched in caveolin, Ca(2+)-ATPase, and inositol trisphosphate receptor.* Proc Natl Acad Sci U S A, 1995. 92(5): p. 1759-63.
129. Calaghan, S., L. Kozera, and E. White, *Compartmentalisation of cAMP-dependent signalling by caveolae in the adult cardiac myocyte.* J Mol Cell Cardiol, 2008.
130. McMahon, K.A., et al., *Detergent-free caveolae proteome suggests an interaction with ER and mitochondria.* Proteomics, 2006. 6(1): p. 143-52.
131. Oh, P. and J.E. Schnitzer, *Immunoisolation of caveolae with high affinity antibody binding to the oligomeric caveolin cage. Toward understanding the basis of purification.* J Biol Chem, 1999. 274(33): p. 23144-54.
132. Stan, R.V., et al., *Immunoisolation and partial characterization of endothelial plasmalemmal vesicles (caveolae).* Mol Biol Cell, 1997. 8(4): p. 595-605.
133. Clark, K.L., et al., *PGRL is a major CD81-associated protein on lymphocytes and distinguishes a new family of cell surface proteins.* J Immunol, 2001. 167(9): p. 5115-21.

134. Le Naour, F., et al., *Tetraspanins connect several types of Ig proteins: IgM is a novel component of the tetraspanin web on B-lymphoid cells.* Cancer Immunol Immunother, 2004. 53(3): p. 148-52.
135. Stipp, C.S., D. Orlicky, and M.E. Hemler, *FPRP, a major, highly stoichiometric, highly specific CD81- and CD9-associated protein.* J Biol Chem, 2001. 276(7): p. 4853-62.
136. Bordier, C., *Phase separation of integral membrane proteins in Triton X-114 solution.* J Biol Chem, 1981. 256(4): p. 1604-7.
137. Elortza, F., et al., *Modification-specific proteomics of plasma membrane proteins: identification and characterization of glycosylphosphatidylinositol-anchored proteins released upon phospholipase D treatment.* J Proteome Res, 2006. 5(4): p. 935-43.
138. Elortza, F., et al., *Proteomic analysis of glycosylphosphatidylinositol-anchored membrane proteins.* Mol Cell Proteomics, 2003. 2(12): p. 1261-70.
139. McNall, R.J. and M.J. Adang, *Identification of novel Bacillus thuringiensis Cry1Ac binding proteins in Manduca sexta midgut through proteomic analysis.* Insect Biochem Mol Biol, 2003. 33(10): p. 999-1010.
140. Parkin, E.T., A.J. Turner, and N.M. Hooper, *Isolation and characterization of two distinct low-density, Triton-insoluble, complexes from porcine lung membranes.* Biochem J, 1996. 319 (Pt 3): p. 887-96.
141. Taylor, C.M. and S.E. Pfeiffer, *Enhanced resolution of glycosylphosphatidylinositol-anchored and transmembrane proteins from the lipid-rich myelin membrane by two-dimensional gel electrophoresis.* Proteomics, 2003. 3(7): p. 1303-12.
142. Ferguson, M.A., et al., *Glycosyl-phosphatidylinositol moiety that anchors Trypanosoma brucei variant surface glycoprotein to the membrane.* Science, 1988. 239(4841 Pt 1): p. 753-9.
143. Hooper, N.M., *Determination of glycosyl-phosphatidylinositol membrane protein anchorage.* Proteomics, 2001. 1(6): p. 748-55.
144. Metzner, C., et al., *Association of glycosylphosphatidylinositol-anchored protein with retroviral particles.* Faseb J, 2008.
145. Paratcha, G., et al., *Released GFRalpha1 potentiates downstream signaling, neuronal survival, and differentiation via a novel mechanism of recruitment of c-Ret to lipid rafts.* Neuron, 2001. 29(1): p. 171-84.
146. Triantafilou, M. and K. Triantafilou, *Lipopolysaccharide recognition: CD14, TLRs and the LPS-activation cluster.* Trends Immunol, 2002. 23(6): p. 301-4.
147. Taylor, D.R. and N.M. Hooper, *The prion protein and lipid rafts.* Mol Membr Biol, 2006. 23(1): p. 89-99.
148. Naik, R.S., G. Krishnegowda, and D.C. Gowda, *Glucosamine inhibits inositol acylation of the glycosylphosphatidylinositol anchors in intraerythrocytic Plasmodium falciparum.* J Biol Chem, 2003. 278(3): p. 2036-42.
149. Nakatsura, T., et al., *Glypican-3, overexpressed specifically in human hepatocellular carcinoma, is a novel tumor marker.* Biochem Biophys Res Commun, 2003. 306(1): p. 16-25.
150. Swierczynski, S.L., et al., *Analysis of novel tumor markers in pancreatic and biliary carcinomas using tissue microarrays.* Hum Pathol, 2004. 35(3): p. 357-66.
151. Zhao, X., H. Li, and R.J. Lee, *Targeted drug delivery via folate receptors.* Expert Opin Drug Deliv, 2008. 5(3): p. 309-19.

152. Eisenhaber, B., P. Bork, and F. Eisenhaber, *Post-translational GPI lipid anchor modification of proteins in kingdoms of life: analysis of protein sequence data from complete genomes.* Protein Eng, 2001. 14(1): p. 17-25.
153. Fankhauser, N. and P. Maser, *Identification of GPI anchor attachment signals by a Kohonen self-organizing map.* Bioinformatics, 2005. 21(9): p. 1846-52.
154. Kronegg, D.B., D. , *http://www.expasy.ch/tools*. 1999. Accessed on 6/Dec./2008
155. Omaetxebarria, M.J., et al., *Computational approach for identification and characterization of GPI-anchored peptides in proteomics experiments.* Proteomics, 2007. 7(12): p. 1951-60.
156. Hooper, N.M., M.G. Low, and A.J. Turner, *Renal dipeptidase is one of the membrane proteins released by phosphatidylinositol-specific phospholipase C.* Biochem J, 1987. 244(2): p. 465-9.
157. Seelenmeyer, C., C. Stegmayer, and W. Nickel, *Unconventional secretion of fibroblast growth factor 2 and galectin-1 does not require shedding of plasma membrane-derived vesicles.* FEBS Lett, 2008. 582(9): p. 1362-8.
158. Ahmad, N., et al., *Galectin-3 precipitates as a pentamer with synthetic multivalent carbohydrates and forms heterogeneous cross-linked complexes.* J Biol Chem, 2004. 279(12): p. 10841-7.
159. Mehul, B., S. Bawumia, and R.C. Hughes, *Cross-linking of galectin 3, a galactose-binding protein of mammalian cells, by tissue-type transglutaminase.* FEBS Lett, 1995. 360(2): p. 160-4.
160. Nieminen, J., et al., *Visualization of galectin-3 oligomerization on the surface of neutrophils and endothelial cells using fluorescence resonance energy transfer.* J Biol Chem, 2007. 282(2): p. 1374-83.
161. Collins, B.E. and J.C. Paulson, *Cell surface biology mediated by low affinity multivalent protein-glycan interactions.* Curr Opin Chem Biol, 2004. 8(6): p. 617-25.
162. Garner, O.B. and L.G. Baum, *Galectin-glycan lattices regulate cell-surface glycoprotein organization and signalling.* Biochem Soc Trans, 2008. 36(Pt 6): p. 1472-7.
163. Brewer, C.F., M.C. Miceli, and L.G. Baum, *Clusters, bundles, arrays and lattices: novel mechanisms for lectin-saccharide-mediated cellular interactions.* Curr Opin Struct Biol, 2002. 12(5): p. 616-23.
164. Paulson, J.C., O. Blixt, and B.E. Collins, *Sweet spots in functional glycomics.* Nat Chem Biol, 2006. 2(5): p. 238-48.
165. Braccia, A., et al., *Microvillar membrane microdomains exist at physiological temperature. Role of galectin-4 as lipid raft stabilizer revealed by "superrafts".* J Biol Chem, 2003. 278(18): p. 15679-84.
166. Tanikawa, R., et al., *Interaction of galectin-9 with lipid rafts induces osteoblast proliferation through the c-Src/ERK signaling pathway.* J Bone Miner Res, 2008. 23(2): p. 278-86.
167. Groisman, E.A. and H. Ochman, *How to become a pathogen.* Trends Microbiol, 1994. 2(8): p. 289-94.
168. Becker, D., et al., *Robust Salmonella metabolism limits possibilities for new antimicrobials.* Nature, 2006. 440(7082): p. 303-7.

169. Salcedo, S.P., et al., *Intracellular replication of Salmonella typhimurium strains in specific subsets of splenic macrophages in vivo.* Cell Microbiol, 2001. 3(9): p. 587-97.
170. McGhie, E.J., et al., *Salmonella takes control: effector-driven manipulation of the host.* Curr Opin Microbiol, 2009. 12(1): p. 117-24.
171. McGhie, E.J., R.D. Hayward, and V. Koronakis, *Cooperation between actin-binding proteins of invasive Salmonella: SipA potentiates SipC nucleation and bundling of actin.* Embo J, 2001. 20(9): p. 2131-9.
172. Steele-Mortimer, O., et al., *Biogenesis of Salmonella typhimurium-containing vacuoles in epithelial cells involves interactions with the early endocytic pathway.* Cell Microbiol, 1999. 1(1): p. 33-49.
173. Bakowski, M.A., et al., *The phosphoinositide phosphatase SopB manipulates membrane surface charge and trafficking of the Salmonella-containing vacuole.* Cell Host Microbe. 7(6): p. 453-62.
174. Drecktrah, D., et al., *Dynamic behavior of Salmonella-induced membrane tubules in epithelial cells.* Traffic, 2008. 9(12): p. 2117-29.
175. Ramsden, A.E., et al., *The SPI-2 type III secretion system restricts motility of Salmonella-containing vacuoles.* Cell Microbiol, 2007. 9(10): p. 2517-29.
176. Waterman, S.R. and D.W. Holden, *Functions and effectors of the Salmonella pathogenicity island 2 type III secretion system.* Cell Microbiol, 2003. 5(8): p. 501-11.
177. Manes, S., G. del Real, and A.C. Martinez, *Pathogens: raft hijackers.* Nat Rev Immunol, 2003. 3(7): p. 557-68.
178. Garner, M.J., R.D. Hayward, and V. Koronakis, *The Salmonella pathogenicity island 1 secretion system directs cellular cholesterol redistribution during mammalian cell entry and intracellular trafficking.* Cell Microbiol, 2002. 4(3): p. 153-65.
179. Garcia-del Portillo, F., et al., *Salmonella typhimurium induces selective aggregation and internalization of host cell surface proteins during invasion of epithelial cells.* J Cell Sci, 1994. 107 (Pt 7): p. 2005-20.
180. Triantafilou, M., et al., *Mediators of innate immune recognition of bacteria concentrate in lipid rafts and facilitate lipopolysaccharide-induced cell activation.* J Cell Sci, 2002. 115(Pt 12): p. 2603-11.
181. Hayward, R.D., et al., *Cholesterol binding by the bacterial type III translocon is essential for virulence effector delivery into mammalian cells.* Mol Microbiol, 2005. 56(3): p. 590-603.
182. Lim, J.S., et al., *Caveolae-mediated entry of Salmonella typhimurium in a human M-cell model.* Biochem Biophys Res Commun, 2009. 390(4): p. 1322-7.
183. Lim, J.S., et al., *Caveolae-mediated entry of Salmonella typhimurium into senescent nonphagocytotic host cells.* Aging Cell. 9(2): p. 243-51.
184. Catron, D.M., et al., *The Salmonella-containing vacuole is a major site of intracellular cholesterol accumulation and recruits the GPI-anchored protein CD55.* Cell Microbiol, 2002. 4(6): p. 315-28.
185. Lange, Y., et al., *Plasma membranes contain half the phospholipid and 90% of the cholesterol and sphingomyelin in cultured human fibroblasts.* J Biol Chem, 1989. 264(7): p. 3786-93.
186. Knodler, L.A., et al., *Salmonella type III effectors PipB and PipB2 are targeted to detergent-resistant microdomains on internal host cell membranes.* Mol Microbiol, 2003. 49(3): p. 685-704.

187. Nawabi, P., D.M. Catron, and K. Haldar, *Esterification of cholesterol by a type III secretion effector during intracellular Salmonella infection.* Mol Microbiol, 2008. 68(1): p. 173-85.
188. Catron, D.M., et al., *Salmonella enterica serovar Typhimurium requires nonsterol precursors of the cholesterol biosynthetic pathway for intracellular proliferation.* Infect Immun, 2004. 72(2): p. 1036-42.
189. de Hoog, C.L. and M. Mann, *Proteomics.* Annu Rev Genomics Hum Genet, 2004. 5: p. 267-93.
190. Berglund, L., et al., *A genecentric Human Protein Atlas for expression profiles based on antibodies.* Mol Cell Proteomics, 2008. 7(10): p. 2019-27.
191. Aebersold, R. and M. Mann, *Mass spectrometry-based proteomics.* Nature, 2003. 422(6928): p. 198-207.
192. Fenn, J.B., et al., *Electrospray ionization for mass spectrometry of large biomolecules.* Science, 1989. 246(4926): p. 64-71.
193. Choi, E., et al., *High-throughput lectin magnetic bead array-coupled tandem mass spectrometry for glycoprotein biomarker discovery.* Electrophoresis. 32(24): p. 3564-75.
194. Rogers, L.D., Y. Fang, and L.J. Foster, *An integrated global strategy for cell lysis, fractionation, enrichment and mass spectrometric analysis of phosphorylated peptides.* Mol Biosyst. 6(5): p. 822-9.
195. Perry, R.H., R.G. Cooks, and R.J. Noll, *Orbitrap mass spectrometry: instrumentation, ion motion and applications.* Mass Spectrom Rev, 2008. 27(6): p. 661-99.
196. Makarov, A. and M. Scigelova, *Coupling liquid chromatography to Orbitrap mass spectrometry.* J Chromatogr A. 1217(25): p. 3938-45.
197. Lacorte, S. and A.R. Fernandez-Alba, *Time of flight mass spectrometry applied to the liquid chromatographic analysis of pesticides in water and food.* Mass Spectrom Rev, 2006. 25(6): p. 866-80.
198. Schuchardt, S. and A. Sickmann, *Protein identification using mass spectrometry: a method overview.* Exs, 2007. 97: p. 141-70.
199. Steen, H. and M. Mann, *The ABC's (and XYZ's) of peptide sequencing.* Nat Rev Mol Cell Biol, 2004. 5(9): p. 699-711.
200. Ong, S.E. and M. Mann, *Mass spectrometry-based proteomics turns quantitative.* Nat Chem Biol, 2005. 1(5): p. 252-62.
201. Gerber, S.A., et al., *Absolute quantification of proteins and phosphoproteins from cell lysates by tandem MS.* Proc Natl Acad Sci U S A, 2003. 100(12): p. 6940-5.
202. Bachi, A. and T. Bonaldi, *Quantitative proteomics as a new piece of the systems biology puzzle.* J Proteomics, 2008. 71(3): p. 357-67.
203. Ong, S.E., L.J. Foster, and M. Mann, *Mass spectrometric-based approaches in quantitative proteomics.* Methods, 2003. 29(2): p. 124-30.
204. Yang, W., H. Steen, and M.R. Freeman, *Proteomic approaches to the analysis of multiprotein signaling complexes.* Proteomics, 2008. 8(4): p. 832-51.
205. Liu, H., R.G. Sadygov, and J.R. Yates, 3rd, *A model for random sampling and estimation of relative protein abundance in shotgun proteomics.* Anal Chem, 2004. 76(14): p. 4193-201.
206. Gygi, S.P., et al., *Quantitative analysis of complex protein mixtures using isotope-coded affinity tags.* Nat Biotechnol, 1999. 17(10): p. 994-9.

207. Ow, S.Y., et al., *Quantitative shotgun proteomics of enriched heterocysts from Nostoc sp. PCC 7120 using 8-plex isobaric peptide tags.* J Proteome Res, 2008. 7(4): p. 1615-28.
208. Ross, P.L., et al., *Multiplexed protein quantitation in Saccharomyces cerevisiae using amine-reactive isobaric tagging reagents.* Mol Cell Proteomics, 2004. 3(12): p. 1154-69.
209. Zanivan, S., M. Krueger, and M. Mann, *In vivo quantitative proteomics: the SILAC mouse.* Methods Mol Biol. 757: p. 435-50.
210. Gouw, J.W., B.B. Tops, and J. Krijgsveld, *Metabolic labeling of model organisms using heavy nitrogen (15N).* Methods Mol Biol. 753: p. 29-42.
211. Ong, S.E., et al., *Stable isotope labeling by amino acids in cell culture, SILAC, as a simple and accurate approach to expression proteomics.* Mol Cell Proteomics, 2002. 1(5): p. 376-86.
212. Banfi, C., et al., *Proteomic analysis of membrane microdomains derived from both failing and non-failing human hearts.* Proteomics, 2006. 6(6): p. 1976-88.
213. Huang, P., et al., *Cholesterol reduction by methyl-beta-cyclodextrin attenuates the delta opioid receptor-mediated signaling in neuronal cells but enhances it in non-neuronal cells.* Biochem Pharmacol, 2007. 73(4): p. 534-49.
214. Yao, Y., et al., *The differential protein and lipid compositions of noncaveolar lipid microdomains and caveolae.* Cell Res, 2009. 19(4): p. 497-506.
215. Chaney, L.K. and B.S. Jacobson, *Coating cells with colloidal silica for high yield isolation of plasma membrane sheets and identification of transmembrane proteins.* J Biol Chem, 1983. 258(16): p. 10062-72.
216. Christian, A.E., et al., *Use of cyclodextrins for manipulating cellular cholesterol content.* J Lipid Res, 1997. 38(11): p. 2264-72.
217. Ilangumaran, S. and D.C. Hoessli, *Effects of cholesterol depletion by cyclodextrin on the sphingolipid microdomains of the plasma membrane.* Biochem J, 1998. 335 (Pt 2): p. 433-40.
218. Kierszniowska, S., B. Seiwert, and W.X. Schulze, *Definition of Arabidopsis sterol-rich membrane microdomains by differential treatment with methyl-beta-cyclodextrin and quantitative proteomics.* Mol Cell Proteomics, 2009. 8(4): p. 612-23.
219. Yu, C., M. Alterman, and R.T. Dobrowsky, *Ceramide displaces cholesterol from lipid rafts and decreases the association of the cholesterol binding protein caveolin-1.* J Lipid Res, 2005. 46(8): p. 1678-91.
220. Ledesma, M.D., et al., *Proteomic characterisation of neuronal sphingolipid-cholesterol microdomains: role in plasminogen activation.* Brain Res, 2003. 987(1): p. 107-16.
221. Oh, P., et al., *Live dynamic imaging of caveolae pumping targeted antibody rapidly and specifically across endothelium in the lung.* Nat Biotechnol, 2007. 25(3): p. 327-37.
222. Montixi, C., et al., *Engagement of T cell receptor triggers its recruitment to low-density detergent-insoluble membrane domains.* Embo J, 1998. 17(18): p. 5334-48.
223. Pizzo, P., et al., *Physiological T cell activation starts and propagates in lipid rafts.* Immunol Lett, 2004. 91(1): p. 3-9.
224. Xavier, R., et al., *Membrane compartmentation is required for efficient T cell activation.* Immunity, 1998. 8(6): p. 723-32.

225. Tu, X., et al., *Proteome analysis of lipid rafts in Jurkat cells characterizes a raft subset that is involved in NF-kappaB activation.* J Proteome Res, 2004. 3(3): p. 445-54.
226. von Haller, P.D., et al., *The application of new software tools to quantitative protein profiling via isotope-coded affinity tag (ICAT) and tandem mass spectrometry: I. Statistically annotated datasets for peptide sequences and proteins identified via the application of ICAT and tandem mass spectrometry to proteins copurifying with T cell lipid rafts.* Mol Cell Proteomics, 2003. 2(7): p. 426-7.
227. von Haller, P.D., et al., *The application of new software tools to quantitative protein profiling via isotope-coded affinity tag (ICAT) and tandem mass spectrometry: II. Evaluation of tandem mass spectrometry methodologies for large-scale protein analysis, and the application of statistical tools for data analysis and interpretation.* Mol Cell Proteomics, 2003. 2(7): p. 428-42.
228. Yanagida, M., et al., *Proteomic analysis of plasma membrane lipid rafts of HL-60 cells.* Proteomics, 2007. 7(14): p. 2398-409.
229. Blonder, J., et al., *Quantitative profiling of the detergent-resistant membrane proteome of iota-b toxin induced vero cells.* J Proteome Res, 2005. 4(2): p. 523-31.
230. MacLellan, D.L., et al., *A quantitative proteomic analysis of growth factor-induced compositional changes in lipid rafts of human smooth muscle cells.* Proteomics, 2005. 5(18): p. 4733-42.
231. Pike, L.J., *The challenge of lipid rafts.* J Lipid Res, 2009. 50 Suppl: p. S323-8.
232. Foster, L.J. and Q.W. Chan, *Lipid raft proteomics: more than just detergent-resistant membranes.* Subcell Biochem, 2007. 43: p. 35-47.
233. Bae, T.J., et al., *Lipid raft proteome reveals ATP synthase complex in the cell surface.* Proteomics, 2004. 4(11): p. 3536-48.
234. Rogers, L.D. and L.J. Foster, *The dynamic phagosomal proteome and the contribution of the endoplasmic reticulum.* Proc Natl Acad Sci U S A, 2007. 104(47): p. 18520-5.
235. Mickelson, J.R., M.L. Greaser, and B.B. Marsh, *Purification of skeletal-muscle mitochondria by density-gradient centrifugation with Percoll.* Anal Biochem, 1980. 109(2): p. 255-60.
236. Andersen, J.S. and M. Mann, *Organellar proteomics: turning inventories into insights.* EMBO Rep, 2006. 7(9): p. 874-9.
237. Saito, H., et al., *Multiplexed two-dimensional liquid chromatography for MALDI and nanoelectrospray ionization mass spectrometry in proteomics.* J Proteome Res, 2006. 5(7): p. 1803-7.
238. Cox, J. and M. Mann, *MaxQuant enables high peptide identification rates, individualized p.p.b.-range mass accuracies and proteome-wide protein quantification.* Nat Biotechnol, 2008. 26(12): p. 1367-72.
239. Eisen, M.B., et al., *Cluster analysis and display of genome-wide expression patterns.* Proc Natl Acad Sci U S A, 1998. 95(25): p. 14863-8.
240. Blonder, J., et al., *A proteomic characterization of the plasma membrane of human epidermis by high-throughput mass spectrometry.* J Invest Dermatol, 2004. 123(4): p. 691-9.
241. Borner, G.H., et al., *Analysis of detergent-resistant membranes in Arabidopsis. Evidence for plasma membrane lipid rafts.* Plant Physiol, 2005. 137(1): p. 104-16.

242. Karsan, A., et al., *Proteomic analysis of lipid microdomains from lipopolysaccharide-activated human endothelial cells.* J Proteome Res, 2005. 4(2): p. 349-57.
243. Li, N., et al., *Lipid raft proteomics: analysis of in-solution digest of sodium dodecyl sulfate-solubilized lipid raft proteins by liquid chromatography-matrix-assisted laser desorption/ionization tandem mass spectrometry.* Proteomics, 2004. 4(10): p. 3156-66.
244. Nebl, T., et al., *Proteomic analysis of a detergent-resistant membrane skeleton from neutrophil plasma membranes.* J Biol Chem, 2002. 277(45): p. 43399-409.
245. Nguyen, H.T., et al., *Proteomic characterization of lipid rafts markers from the rat intestinal brush border.* Biochem Biophys Res Commun, 2006. 342(1): p. 236-44.
246. Paradela, A., et al., *Proteomic analysis of apical microvillous membranes of syncytiotrophoblast cells reveals a high degree of similarity with lipid rafts.* J Proteome Res, 2005. 4(6): p. 2435-41.
247. Sanders, P.R., et al., *Distinct protein classes including novel merozoite surface antigens in Raft-like membranes of Plasmodium falciparum.* J Biol Chem, 2005. 280(48): p. 40169-76.
248. Sprenger, R.R., et al., *Comparative proteomics of human endothelial cell caveolae and rafts using two-dimensional gel electrophoresis and mass spectrometry.* Electrophoresis, 2004. 25(1): p. 156-72.
249. von Haller, P.D., et al., *Mass spectrometric characterization of proteins extracted from Jurkat T cell detergent-resistant membrane domains.* Proteomics, 2001. 1(8): p. 1010-21.
250. Foster, L., *Mass spectrometry outgrows simple biochemistry: new approaches to organelle proteomics.* Biophys. Rev. Lett., 2006. 1(2): p. 163-175.
251. Hess, S.T., et al., *Dynamic clustered distribution of hemagglutinin resolved at 40 nm in living cell membranes discriminates between raft theories.* Proc Natl Acad Sci U S A, 2007. 104(44): p. 17370-5.
252. Andersen, J.S., et al., *Proteomic characterization of the human centrosome by protein correlation profiling.* Nature, 2003. 426(6966): p. 570-4.
253. Dunkley, T.P., et al., *Localization of organelle proteins by isotope tagging (LOPIT).* Mol Cell Proteomics, 2004. 3(11): p. 1128-34.
254. Prokisch, H., et al., *MitoP2: the mitochondrial proteome database--now including mouse data.* Nucleic Acids Res, 2006. 34(Database issue): p. D705-11.
255. Rogers, L.D. and L.J. Foster, *Contributions of proteomics to understanding phagosome maturation.* Cell Microbiol, 2008.
256. Foster, L.J., et al., *A mammalian organelle map by protein correlation profiling.* Cell, 2006. 125(1): p. 187-99.
257. Forner, F., et al., *Quantitative proteomic comparison of rat mitochondria from muscle, heart, and liver.* Mol Cell Proteomics, 2006. 5(4): p. 608-19.
258. Lajoie, P. and I.R. Nabi, *Lipid rafts, caveolae, and their endocytosis.* Int Rev Cell Mol Biol. 282: p. 135-63.
259. Allen, J.A., et al., *Beta-adrenergic receptor stimulation promotes G alpha s internalization through lipid rafts: a study in living cells.* Mol Pharmacol, 2005. 67(5): p. 1493-504.
260. Head, B.P. and P.A. Insel, *Do caveolins regulate cells by actions outside of caveolae?* Trends Cell Biol, 2007. 17(2): p. 51-7.
261. Nabi, I.R., *Cavin fever: regulating caveolae.* Nat Cell Biol, 2009. 11(7): p. 789-91.

262. Lajoie, P., et al., *Lattices, rafts, and scaffolds: domain regulation of receptor signaling at the plasma membrane.* J Cell Biol, 2009. 185(3): p. 381-5.
263. Dennis, J.W., et al., *Adaptive regulation at the cell surface by N-glycosylation.* Traffic, 2009. 10(11): p. 1569-78.
264. Granovsky, M., et al., *Suppression of tumor growth and metastasis in Mgat5-deficient mice.* Nat Med, 2000. 6(3): p. 306-12.
265. Lajoie, P., et al., *Plasma membrane domain organization regulates EGFR signaling in tumor cells.* J Cell Biol, 2007. 179(2): p. 341-56.
266. Liu, L., et al., *Deletion of Cavin/PTRF causes global loss of caveolae, dyslipidemia, and glucose intolerance.* Cell Metab, 2008. 8(4): p. 310-7.
267. Davalos, A., et al., *Quantitative proteomics of caveolin-1-regulated proteins: characterization of polymerase i and transcript release factor/CAVIN-1 IN endothelial cells.* Mol Cell Proteomics. 9(10): p. 2109-24.
268. Zheng, Y.Z. and L.J. Foster, *Contributions of quantitative proteomics to understanding membrane microdomains.* J Lipid Res, 2009. 50(10): p. 1976-85.
269. Allen, J.A., et al., *Caveolin-1 and lipid microdomains regulate Gs trafficking and attenuate Gs/adenylyl cyclase signaling.* Mol Pharmacol, 2009. 76(5): p. 1082-93.
270. Bauer, P.M., et al., *Endothelial-specific expression of caveolin-1 impairs microvascular permeability and angiogenesis.* Proc Natl Acad Sci U S A, 2005. 102(1): p. 204-9.
271. Pelkmans, L. and M. Zerial, *Kinase-regulated quantal assemblies and kiss-and-run recycling of caveolae.* Nature, 2005. 436(7047): p. 128-33.
272. Vogels, M.W., et al., *Quantitative proteomic identification of host factors involved in the Salmonella typhimurium infection cycle.* Proteomics. 11(23): p. 4477-91.
273. Auweter, S.D., et al., *Quantitative mass spectrometry catalogues Salmonella pathogenicity island-2 effectors and identifies their cognate host binding partners.* J Biol Chem. 286(27): p. 24023-35.
274. Futschik, M.E. and B. Carlisle, *Noise-robust soft clustering of gene expression time-course data.* J Bioinform Comput Biol, 2005. 3(4): p. 965-88.
275. Steinberg, B.E., C.C. Scott, and S. Grinstein, *High-throughput assays of phagocytosis, phagosome maturation, and bacterial invasion.* Am J Physiol Cell Physiol, 2007. 292(2): p. C945-52.
276. Inder, K.L., et al., *Expression of PTRF in PC-3 Cells modulates cholesterol dynamics and the actin cytoskeleton impacting secretion pathways.* Mol Cell Proteomics. 11(2): p. M111 012245.
277. Foster, L.J., *Large-scale subcellular localization of proteins by protein correlation profiling.* Elsevier Science, 2008. 52(Mass spectrometry of proteins): p. 467 - 478.
278. Lundberg, E. and M. Uhlen, *Creation of an antibody-based subcellular protein atlas.* Proteomics. 10(22): p. 3984-96.
279. Krogh, A., et al., *Predicting transmembrane protein topology with a hidden Markov model: application to complete genomes.* J Mol Biol, 2001. 305(3): p. 567-80.
280. Kyte, J. and R.F. Doolittle, *A simple method for displaying the hydropathic character of a protein.* J Mol Biol, 1982. 157(1): p. 105-32.
281. Rogers, L.D., et al., *Phosphoproteomic analysis of Salmonella-infected cells identifies key kinase regulators and SopB-dependent host phosphorylation events.* Sci Signal. 4(191): p. rs9.

Appendix

Appendix: Supplemental figures

Figure A. 1 Label-free workflow

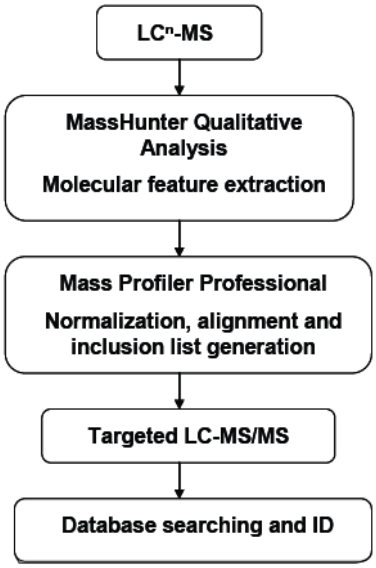

Figure A. 2 Testing the run reproducibility of Chip-Cube Q-TOF and the performance of 40 nl and 160 nl trap chip

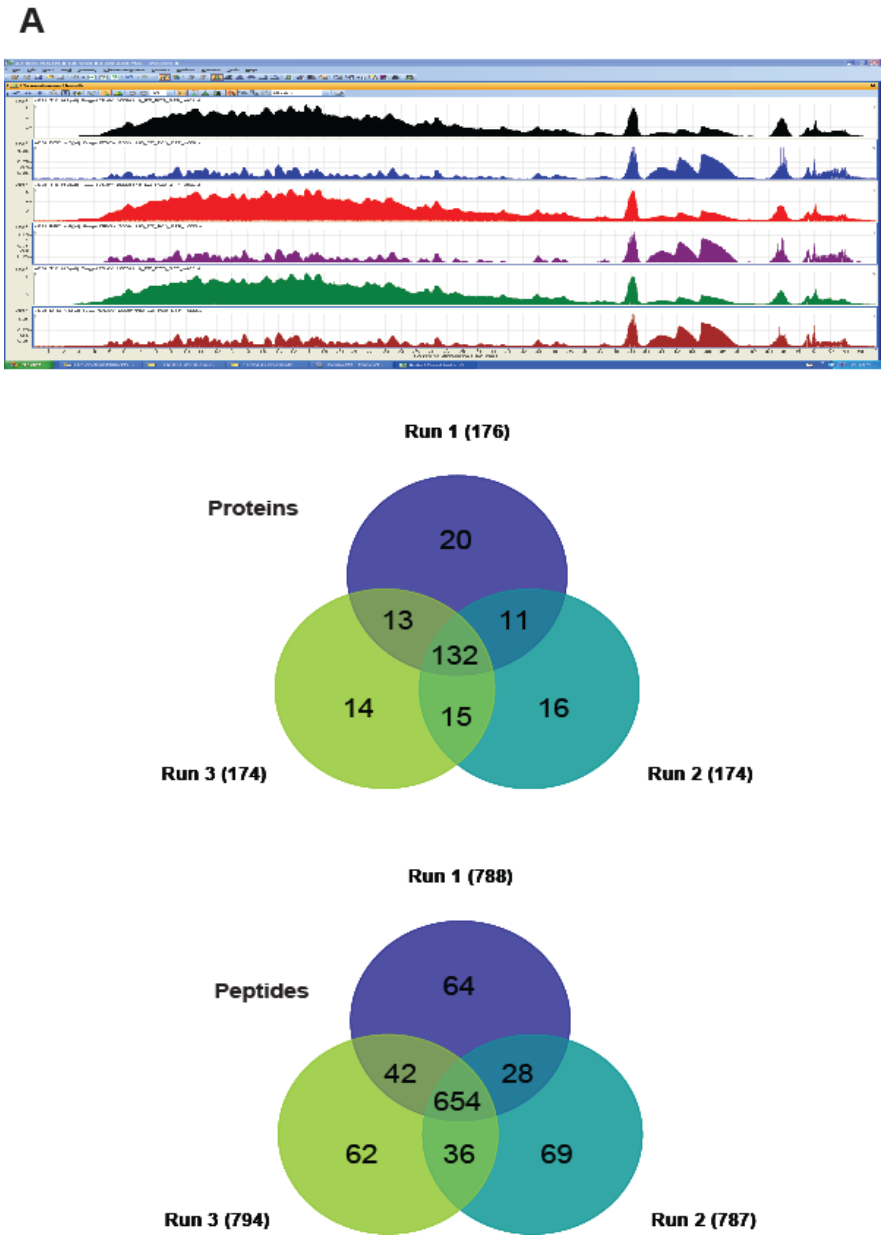

B

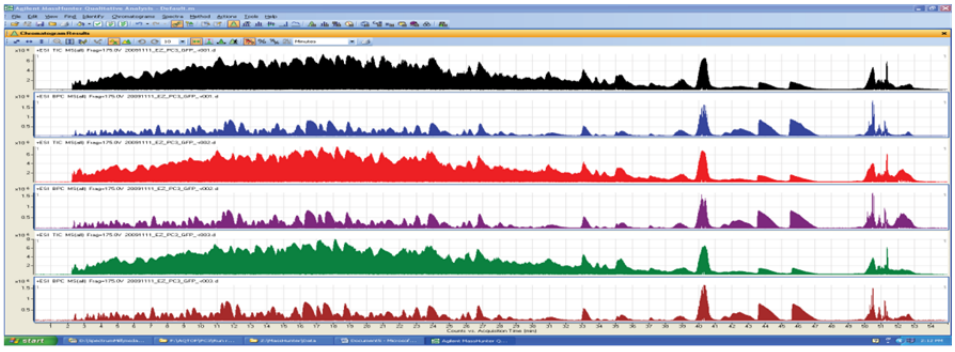

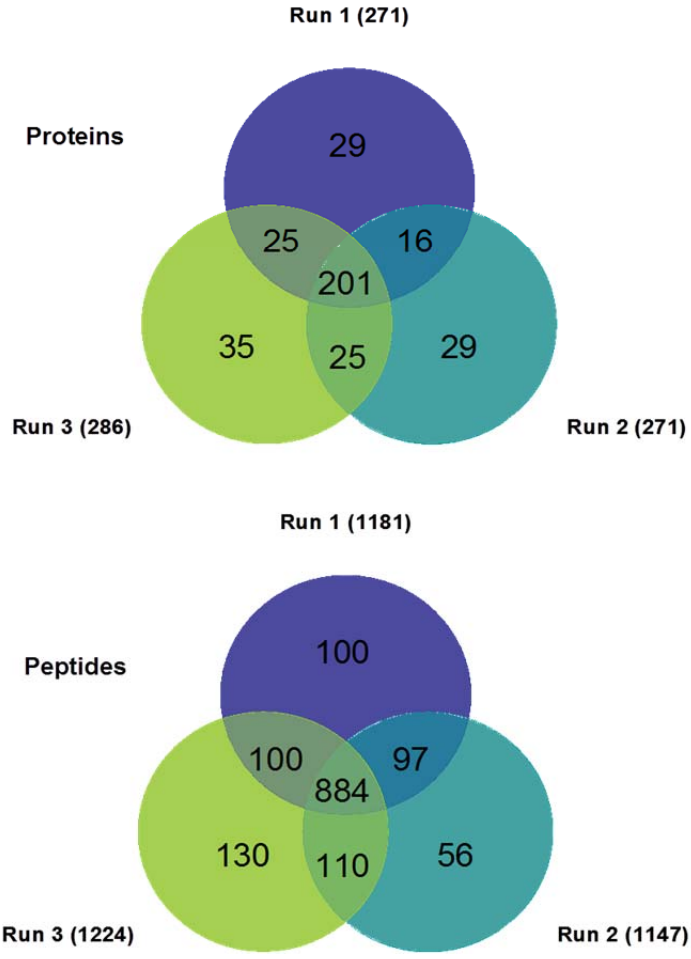

A. PC3 DRMs repeated three analyses using 40 nl trap chip (1 µg of protein injected) both TIC and BPC are shown. Number of proteins and peptides identified in each run and their overlap. B. PC3 DRMs repeated three analyses using 160 nl trap chip (4 µg of protein injected) both TIC and BPC are shown. Number of proteins and peptides identified in each run and their overlap.

Figure A. 3 Ingenuity Pathway Analysis

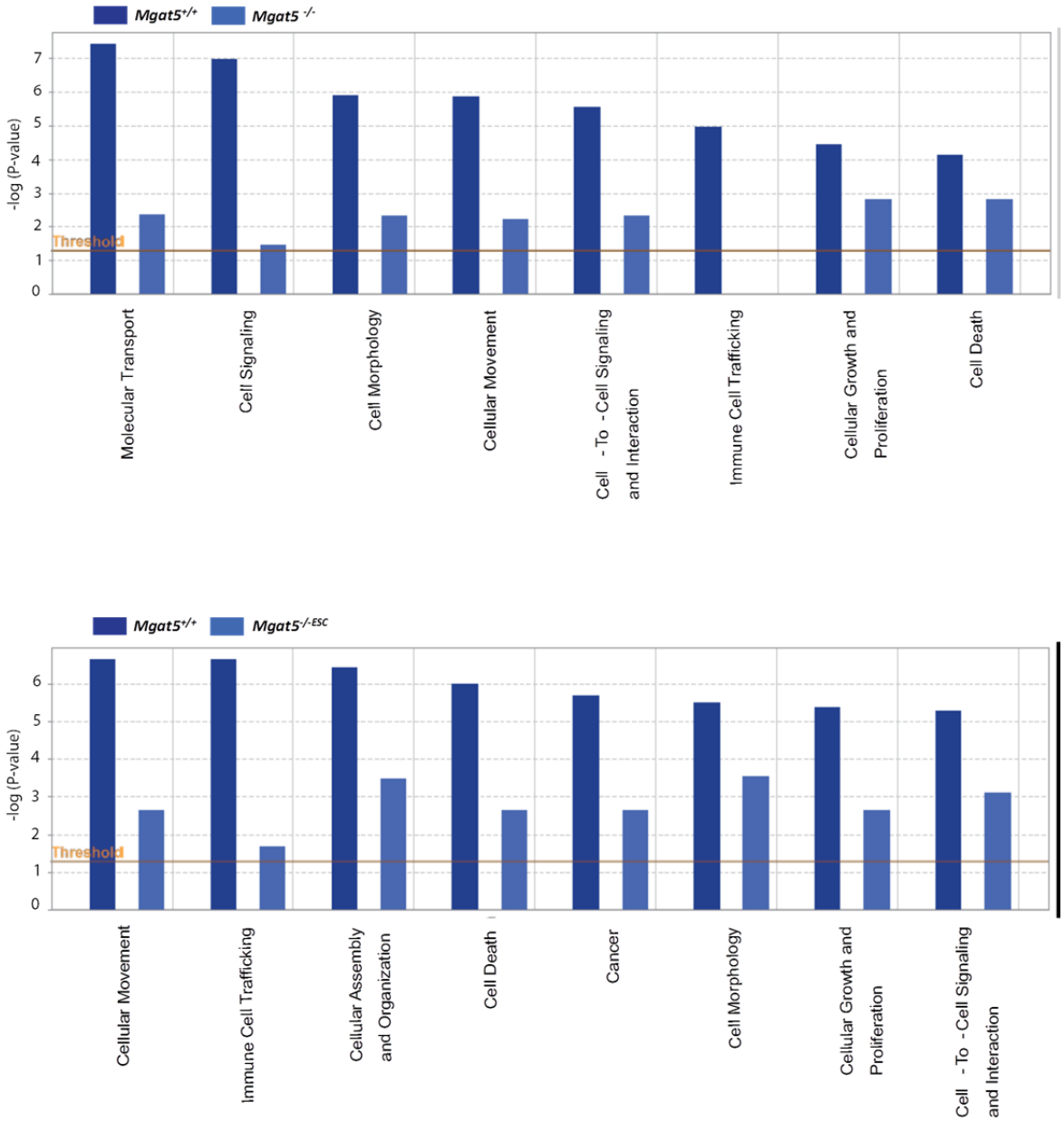

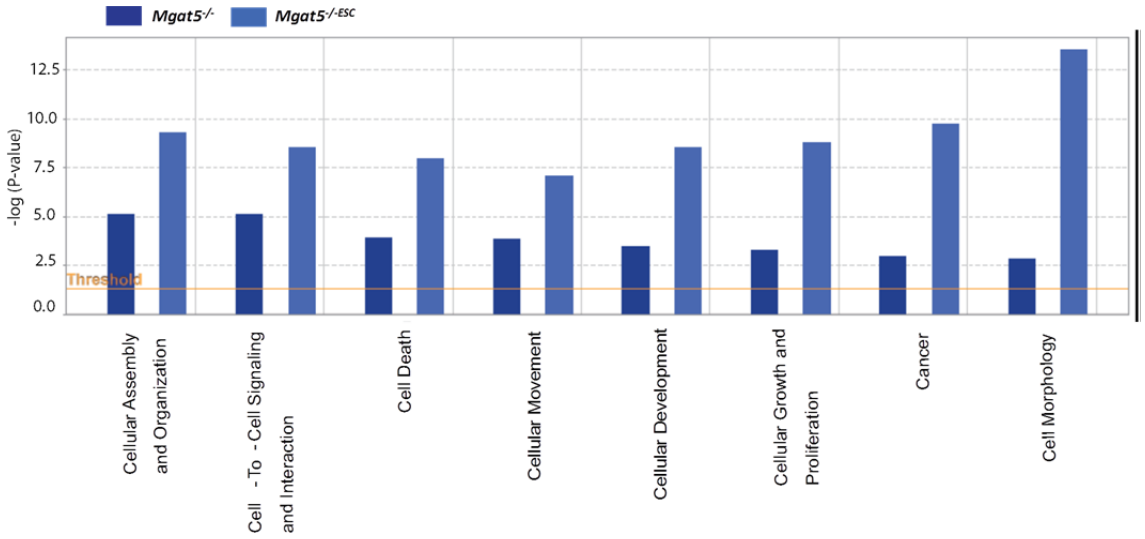

Proteins enriched in each of the two cell lines (above cut off values) compared for all the three comparisons: *Mgat5*$^{+/+}$ vs. *Mgat5*$^{-/-}$, *Mgat5*$^{+/+}$ vs. *Mgat5*$^{-/-ESC}$ and *Mgat5*$^{-/-}$ vs. *Mgat5*$^{-/-ESC}$ were searched through Ingenuity Pathway Analysis.

Figure A. 4 Triple label lactose treatment for SILAC

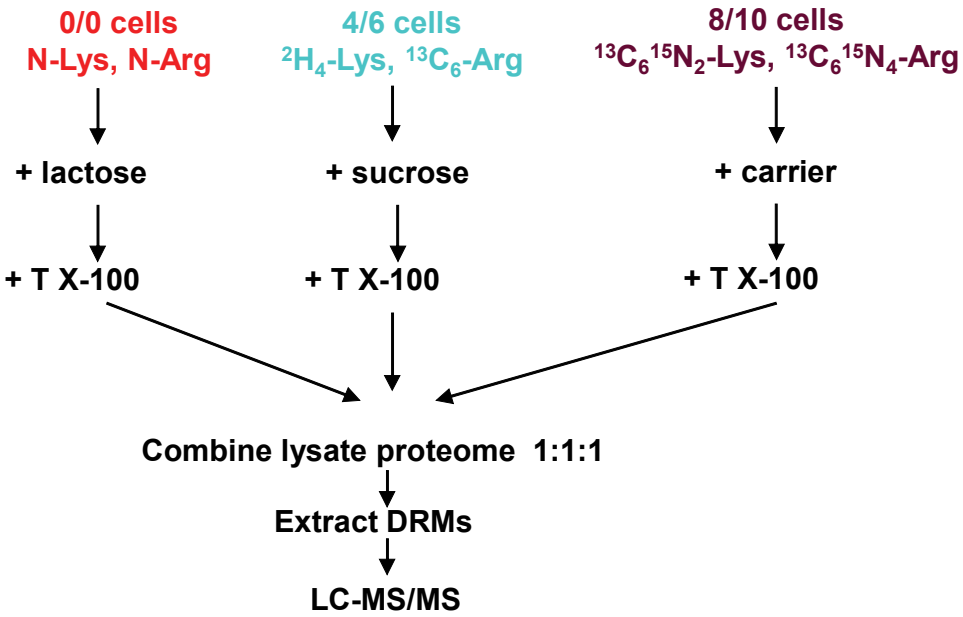

0/0 lactose treated *Mgat5*$^{+/+}$ cells were combined 1:1:1 with 4/6 sucrose treated and 8/10 control cells. DRMs of the combined sample were extracted using Triton X-100 followed by protein digestion and LC-MS/MS analysis.